TRIUMF **Document-######**

Magnetic Field Probe

Document Type:	**Project Record**		
Release:	**1**	**Release Date:**	**2026-11-03**
Author(s):	**G. Marcoux**		

	Name:	
Authors:	**G. Marcoux**	
Reviewed By:	**A. Surname**	**Approval Record**
	A. Surname	
Approved By:	**A. Surname**	

History of Changes

Release Number	Date	Description of Changes	Author(s)
1	YYYY-MM-DD	Initial release	G. Marcoux

Keywords: Magnetic Field Mapping, HAICU, Magnetic Trap, COMSOL, Hall Sensor Array, TMAG5173, Linear Stage, Laplace Reconstruction, Error Budget

Distribution List: HAICU Team

Contents

1 Introduction 4

1.1 Purpose 4

1.2 Scope 5

2 Measurement System 6

2.1 Equipment 6

2.2 Magnetic field data and field reconstruction 9

3 Electronics 11

3.1 System Architecture 11

3.2 I²C Addressing 12

3.3 Chip Settings 13

4 Data 13

4.1 Raw Chip Data 13

4.2 Magnetic Field Plots 14

5 Initial Testing 16

5.1 Chip Response 16

5.2 Scanning GUI 18

5.3 Scan Repeatability 19

5.4 Stage Oscillation 21

6 Error Budget 22

6.1 A. Chip Error 22

6.2 B. Chip Position Offsets 23

6.3 C. Field Reconstruction 24

6.4 Chip position offset B and field reconstruction C errors combined 25

6.5 D. Probe Insertion 26

6.6 B, C and D Combined 26

7 Python Tools 27

Appendix A: Schematics 28

Appendix B: Installation Steps 29

Appendix C: Chip Response Plots 34

Appendix D: Scan Repeatability Plots 50

Appendix E: Magnetic Field Map Reconstruction 54

1 Introduction

The HAICU experiment is designed to confine atoms in a magnetic trap formed by quadrupole packs, gate coils and boost coils (Figure 1). This document describes the system designed to map the magnetic field inside the trap bore.

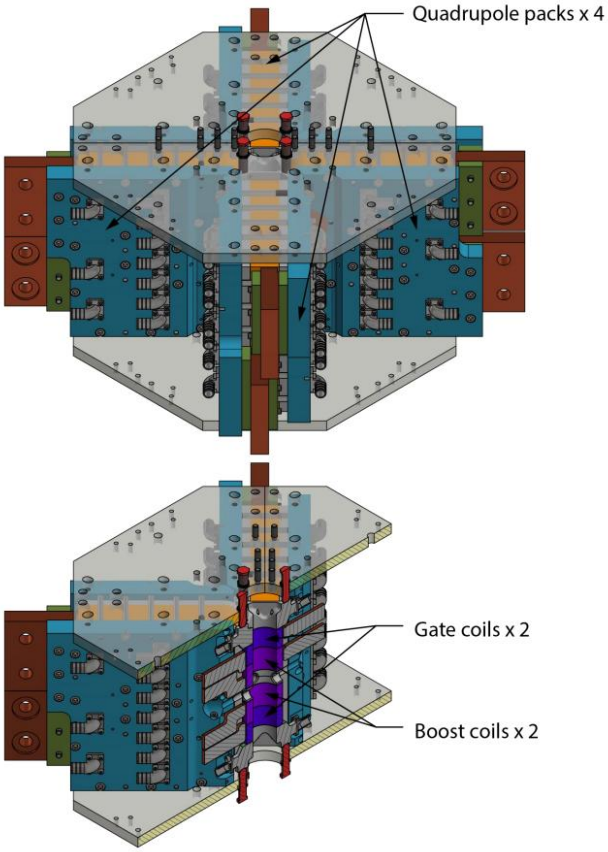

Fig. 4 Mechanical model of the magnetic trap

Figure 1: *Mechanical model of the HAICU magnetic trap (quadrupole packs ×4, gate coils ×2, boost coils ×2).*

1.1 Purpose

The purpose of the field mapping is to confirm that the magnetic field in the trap matches the COMSOL simulation of the quadrupole and coil fields for DC operation. A probe carrying an array of 3-axis Hall sensors is designed to scan along the trap axis, and the discrete readings reconstruct a full 3D field map that can be compared directly with the COMSOL field data. A contour plot of the COMSOL data is shown in Figure 2 showing fields up to 500mT at full power(7.87V @2160A).

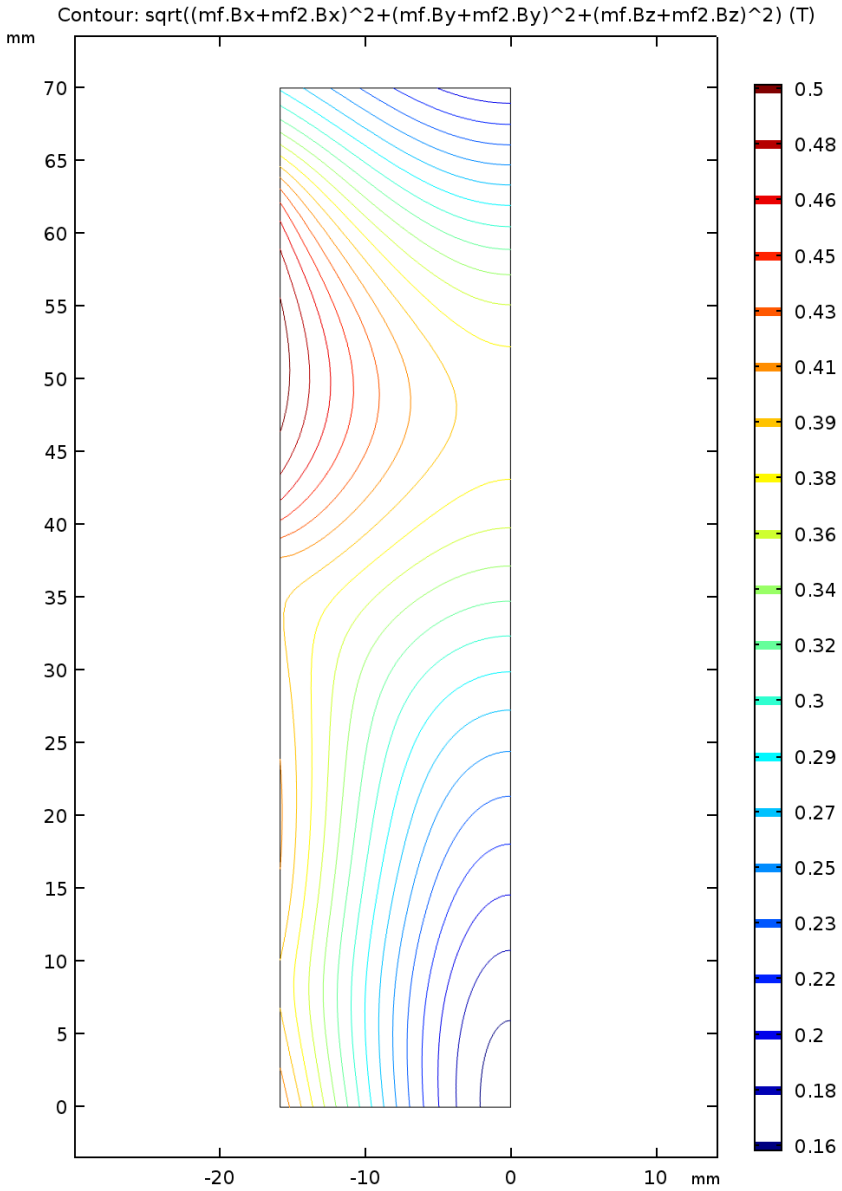

Figure 2: *COMSOL |B| contour, sqrt((mf.Bx+mf2.Bx)² + (mf.By+mf2.By)² + (mf.Bz+mf2.Bz)²) in T*

1.2 Scope

This document covers the measurement system including the sensor and motor control electronics, the field reconstruction method, the probe integration and installation, test scans, and the error budget.

2 Measurement System

The probe design consists of a simple single axis linear stage with a PCB on the end with Hall-effect sensors that provide Bx, By and Bz data for a user defined number of steps. This then provides a cylindrical volume of discrete points that can be compared to COMSOL data.

2.1 Equipment

The magnetic probe assembly, as shown in Figure 3-7, is inserted from the top of the 6-way cross and comprises a linear actuator holding a PCB assembly of an array of Hall sensors:

- Linear actuator: Accu-Glass HTL-275-4 with Option 11, DC stepper motor, 100 mm travel.
- Sensor array: 23 × TMAG5173-A2,B2,D2, 3-axis Hall sensors.
- Motor control PCB: ESP32-S3-DEVKITC-1-N8R8 and TMC2209 stepper driver.
- All probe materials used are non-magnetic.

The magnetic trap bore radius of the measurement volume is 15.73mm, and the sensor PCB radius is 12.7mm to allow for adequate clearance from the bore walls. The assembly pressure under normal operating conditions is 10^{-11} Torr therefore it is critical to avoid any contamination caused by contact of the probe to any surface that will be pumped down. There is a shaft below the Sensor PCB to guide the probe through a dry PEEK bearing to ensure straightness. Appendix B shows probe installation steps.

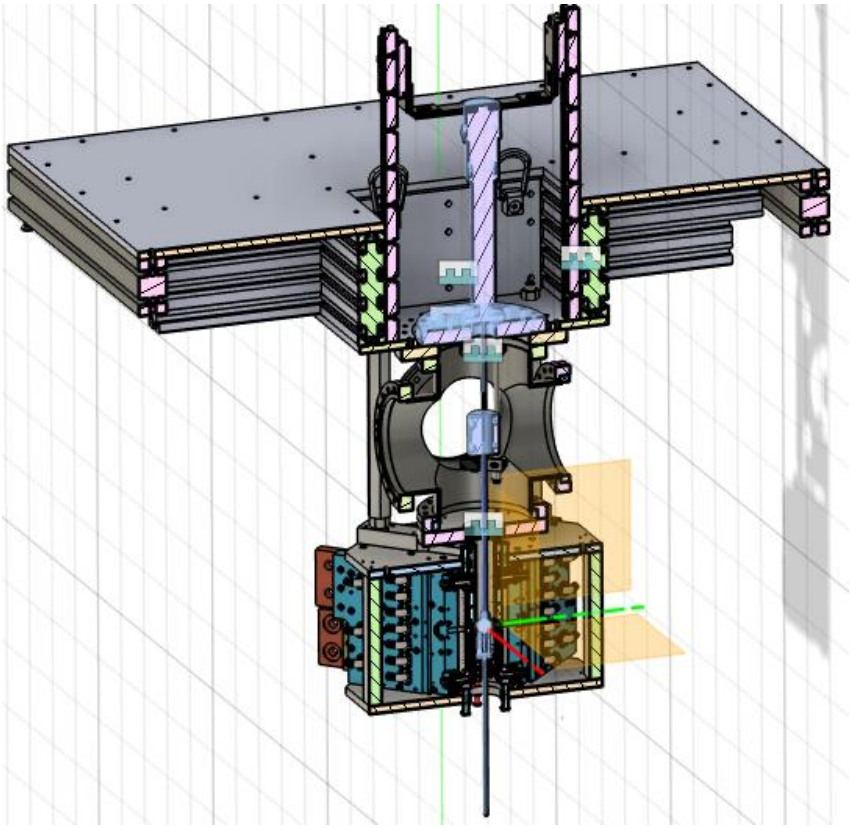

Figure 3: *Magnetic Probe assembly installed in HAICU trap model*

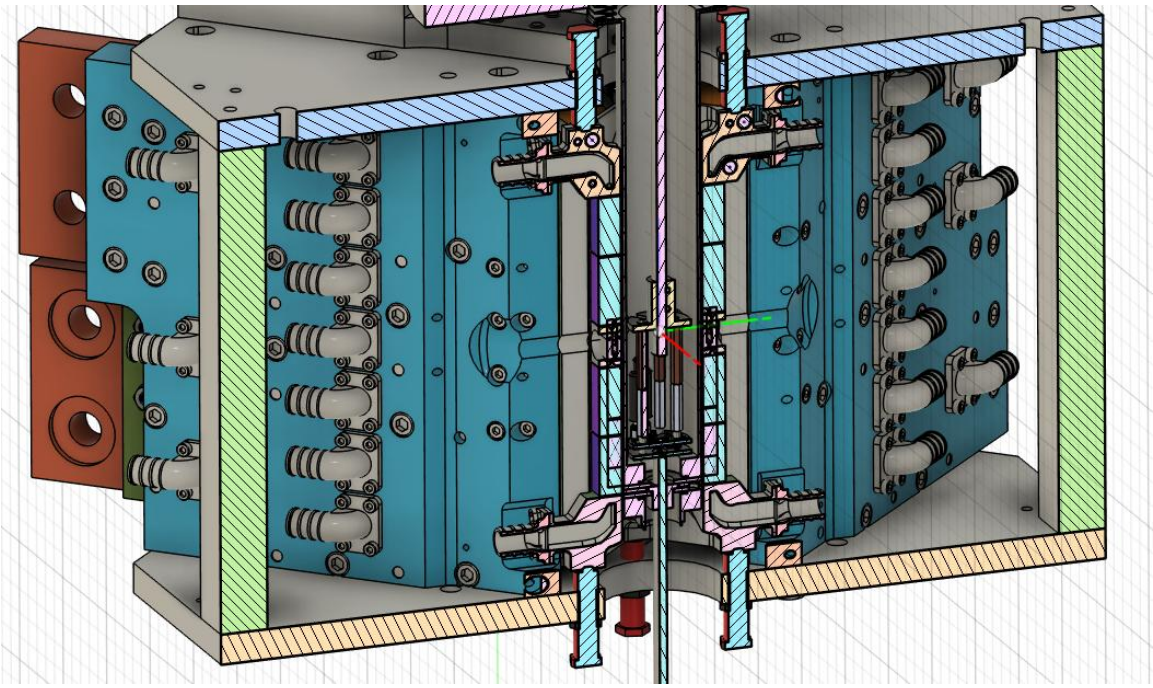

Figure 4: *Sensor PCB assembly inserted in trap model*

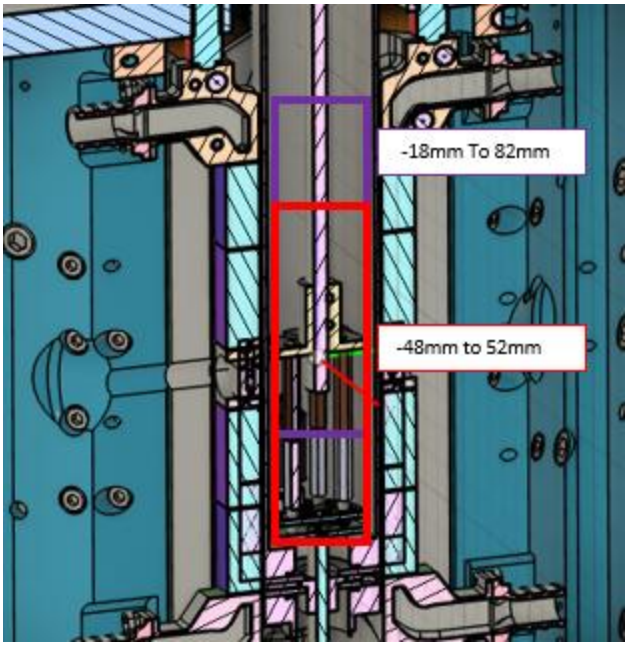

Figure 5: *Probe travel in the trap bore: 100 mm stage travel. Red and purple boxes show two scan ranges for two probe shaft positions. The red box is the default scan range. The upper shaft needs to be physically adjusted to scan a new "box".*

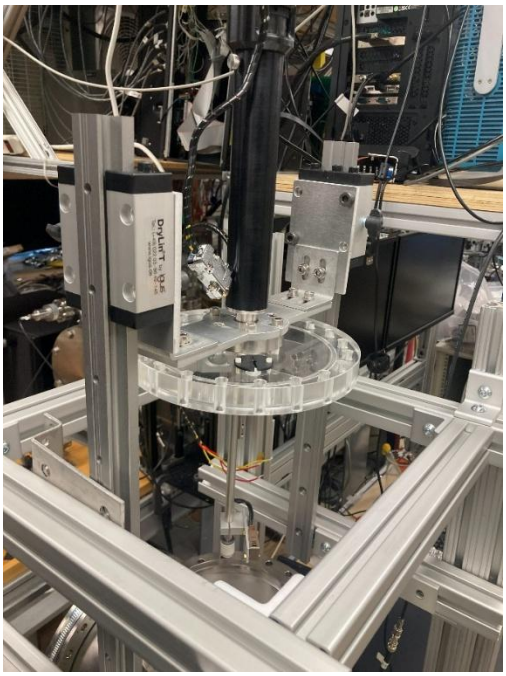

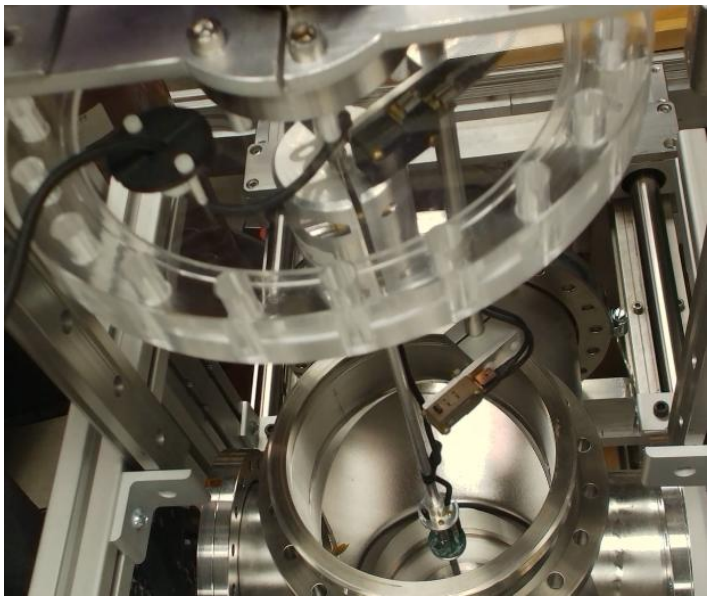

Figure 6: *Linear stage and probe retracted*



Figure 7: *Sensor PCB assembly*

2.2 Magnetic field data and field reconstruction

Inside the bore there are no magnets or current. The field therefore satisfies Maxwell's equations in their source-free form ($\nabla \cdot B = 0$ and $\nabla \times B = 0$), and it can be written as $B = -\nabla \Phi$, where Φ is a harmonic function that satisfies Laplace's equation. A limited set of 3-axis readings is enough to determine a Laplace solution that is valid throughout the volume. More details about the theory behind the field reconstruction can be found in Appendix F.

Different chip array configurations were compared *(comsol_field_validate.py)* by sampling the COMSOL data and reconstructing the field based on discrete chip locations (Figure 8). The reconstructed field was then compared with the full COMSOL field. The results confirmed that increasing chip density within the max radius does not prove valuable to field reconstruction errors. The critical part is to have a minimum of 7 chips at the max radius to keep field prediction within the PCB diameter below 1% error. Beyond 7 chips at the max radius benefits only the error imposed by extrapolating the field beyond the max PCB array radius.

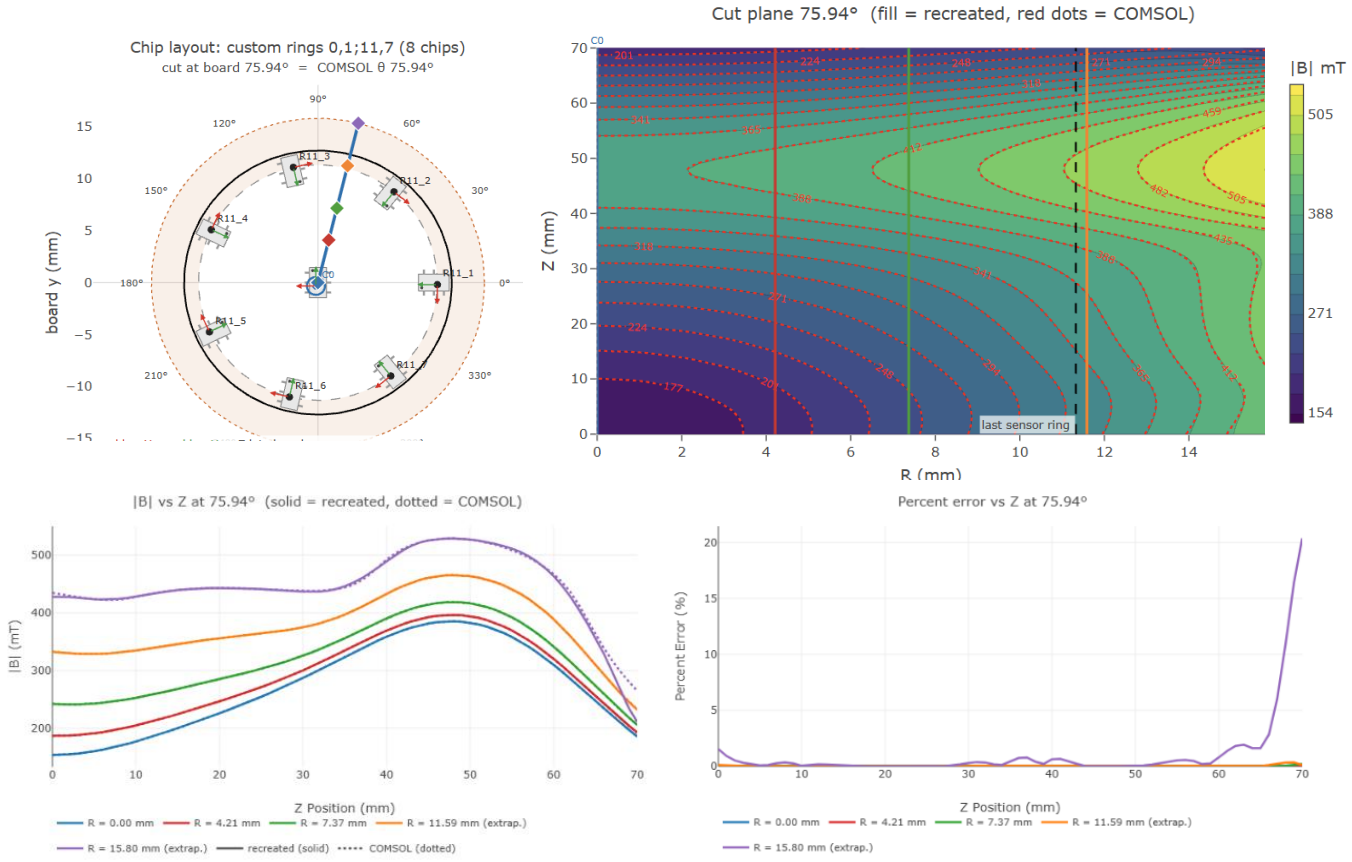

Figure 8: *Sensor density comparison tool: reconstructed field on cut planes*

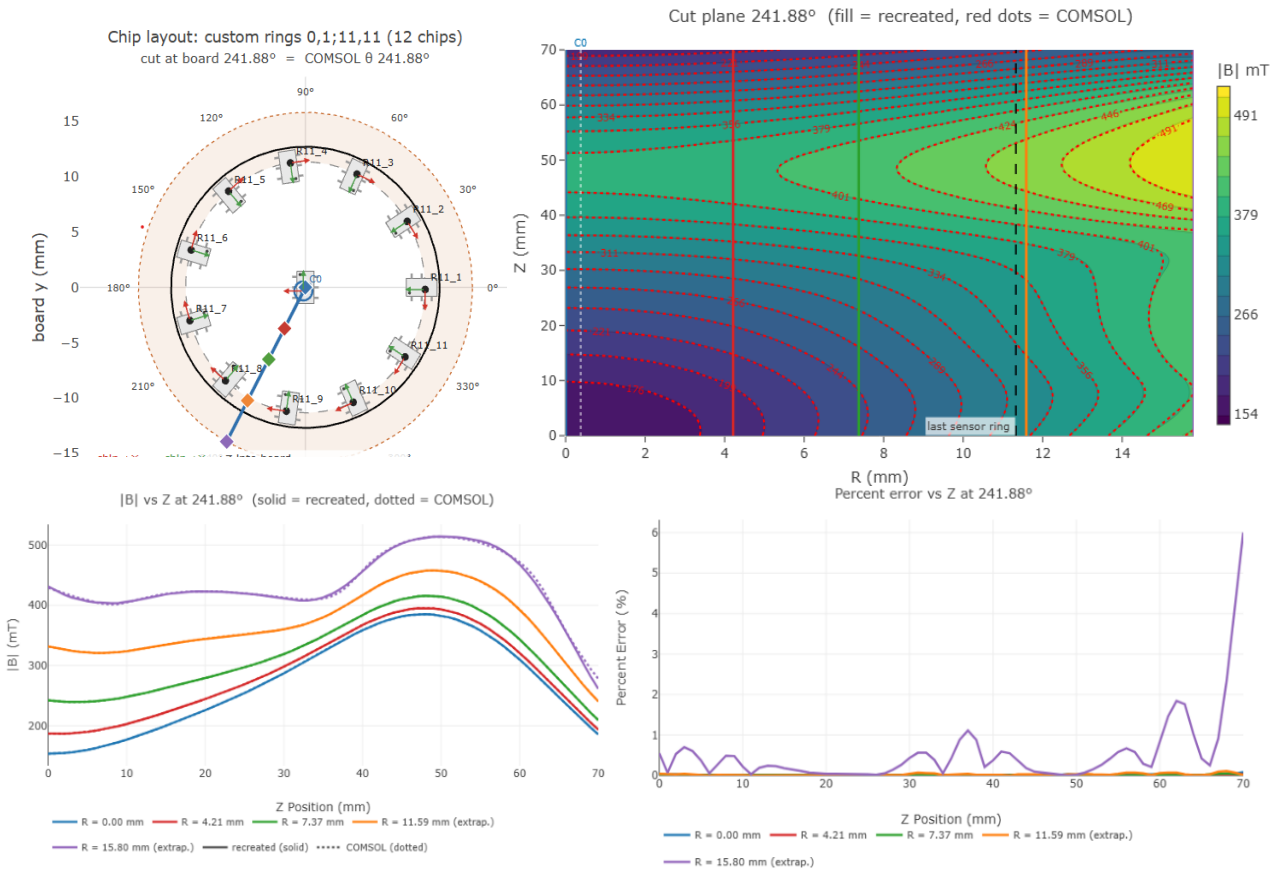

Figure 9: *Reconstructed field and the error relative to COMSOL for two chip layouts (Figure 8).*

Although the reconstruction does not require a heavily dense board to reach errors below 1% with ideal data, when chip errors are introduced, more chips allow for error averaging. The chip number was then chosen to provide as much information as possible while allowing reasonable electronic design complexity. The selected layout is shown in Figure 10 with 23 chips; centre (U1), r ≈ 4 mm (U2–U6, 5 chips), r = 7.5 mm (U7–U12, 6 chips) and r ≈ 11.3 mm (U13–U23, 11 chips). The PCB design is further explored in section 3.

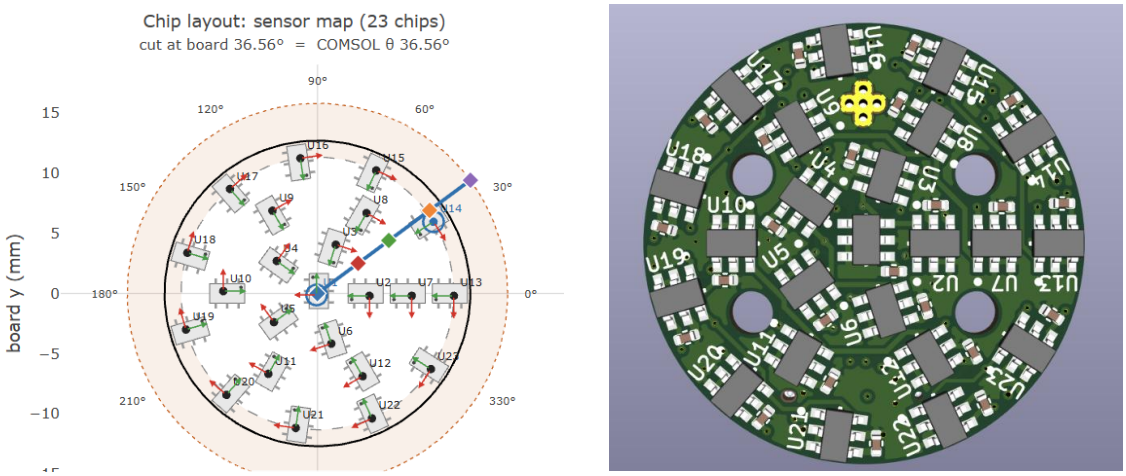

Figure 10: *Chosen chip configuration simulation (left) KiCad design (right).*

3 Electronics

3.1 System Architecture

The electronics are split across two PCBs (Figure 11). The detailed schematics are in Appendix A.

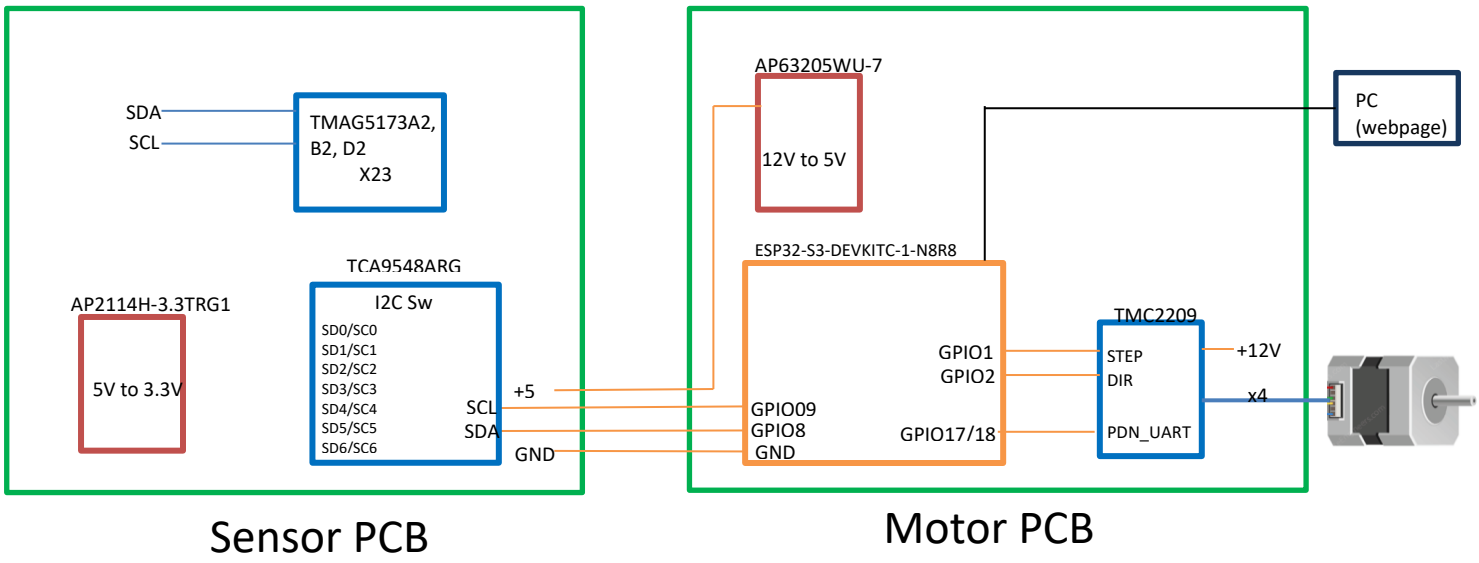

Figure 11: *System architecture: Sensor PCB (left) and Motor PCB (right).*

- **Sensor PCB:** 23 × TMAG5173 3-axis linear Hall-effect sensors (266 mT range on x, y and z), a TCA9548A 8-channel I²C switch

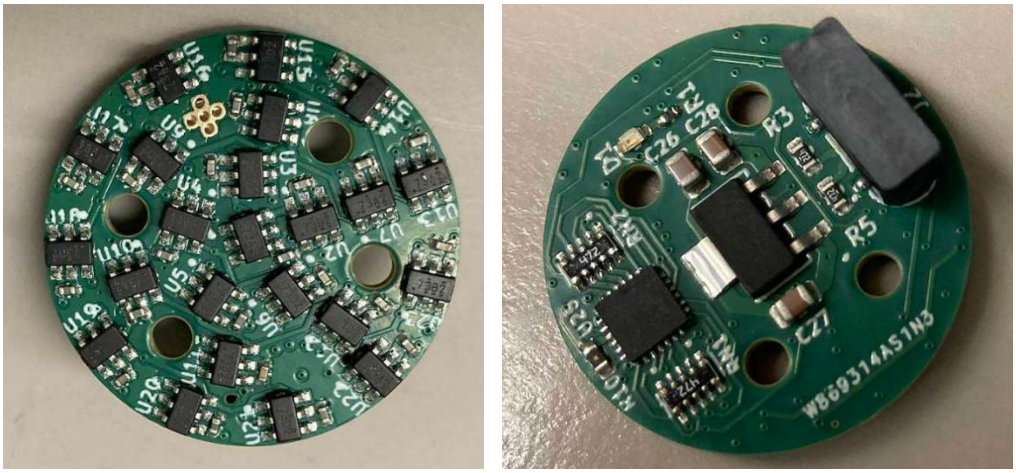

Figure 12: *Sensor PCB front and back*

- **Motor PCB:** ESP32-S3-DEVKITC-1-N8R8 microcontroller, TMC2209 stepper driver. The motor PCB box can be connected to a laptop or Pi to run the webpage GUI (*fieldmap_gui_web.py*).

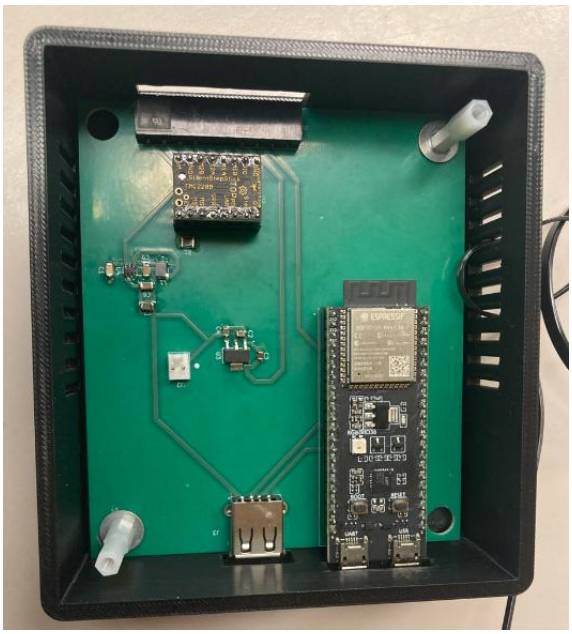

Figure 13: *Motor PCB*

- **Sensor PCB–Motor PCB:** +5 V, I²C SDA, I²C SCL and GND, carried on a USB-C cable between both PCBs that runs along the probe shaft.

3.2 I²C Addressing

The ESP32-S3 uses a single I²C bus. The TCA9548A switch splits it into 8 channels (SD0/SC0 to SD7/SC7). Each channel connects to three TMAG5173 variants, A2, B2 and D2, which have different factory I²C addresses (0x22, 0x35 and 0x44). The same three addresses are reused on every channel without conflict, so no address programming is needed at start-up.

Table 1: *Sensor map: I²C switch channel, factory address, part number and Hall-element position and rotation in the PCB frame.*

Ref	MUX CH	Address	Part	Hall x (mm)	Hall y (mm)	Rot (°)
U1	0	0x22	TMAG5173A2QDBVRQ1	-0.075	-0.125	0
U2	0	0x35	TMAG5173B2QDBVRQ1	4.325	-0.195	90
U3	0	0x44	TMAG5173D2QDBVRQ1	1.522	4.053	162
U4	1	0x22	TMAG5173A2QDBVRQ1	-3.384	2.700	-126
U5	1	0x35	TMAG5173B2QDBVRQ1	-3.614	-2.384	-54
U6	1	0x44	TMAG5173D2QDBVRQ1	1.151	-4.174	18
U7	2	0x22	TMAG5173A2QDBVRQ1	7.825	-0.195	90
U8	2	0x35	TMAG5173B2QDBVRQ1	4.081	6.679	150
U9	2	0x44	TMAG5173D2QDBVRQ1	-3.744	6.874	-150
U10	3	0x22	TMAG5173A2QDBVRQ1	-7.825	0.195	-90
U11	3	0x35	TMAG5173B2QDBVRQ1	-4.081	-6.679	-30
U12	3	0x44	TMAG5173D2QDBVRQ1	3.744	-6.874	30
U13	4	0x22	TMAG5173A2QDBVRQ1	11.325	-0.195	90
U14	4	0x35	TMAG5173B2QDBVRQ1	9.633	5.959	122.727
U15	4	0x44	TMAG5173D2QDBVRQ1	4.882	10.221	155.454
U16	5	0x22	TMAG5173A2QDBVRQ1	-1.419	11.238	-171.819
U17	5	0x35	TMAG5173B2QDBVRQ1	-7.269	8.687	-139.092
U18	5	0x44	TMAG5173D2QDBVRQ1	-10.811	3.378	-106.365
U19	6	0x22	TMAG5173A2QDBVRQ1	-10.921	-3.003	-73.638
U20	6	0x35	TMAG5173B2QDBVRQ1	-7.564	-8.431	-40.911
U21	6	0x44	TMAG5173D2QDBVRQ1	-1.805	-11.182	-8.183
U22	7	0x22	TMAG5173A2QDBVRQ1	4.527	-10.383	24.542
U23	7	0x35	TMAG5173B2QDBVRQ1	9.421	-6.287	57.269

3.3 Chip Settings

Each Bx, By and Bz value returned by a sensor is the average of 32 conversions (32× averaging). At this setting, the TMAG5173 RMS magnetic noise is 18.6 µT. The chip was also set to a selectable full range of ±266mT. This range allows the field to be measured up to half power operation of the magnet before the sensor saturates. Hall effect chips to be integrated into an array for field mapping are not available for measuring fields >300mT. Since the goal of the measurement is to confirm the magnet is matching the COMSOL data, the chip range is adequate.

4 Data

4.1 Raw Chip Data

The component data is a 4-hex digit word read as a signed 16-bit two's-complement number then multiplied by 266/32758 to arrive to a mT as per the datasheet formula $B = \text{code} \times 2 \cdot |\text{range}| / 2^{16}$. The csv data from a scan is supplied in the chip's local frame in mT as per Figure 14. The columns are: Step, Position_mm, Scan_mm, Step_mm, Sensor, X_mT, Y_mT, Z_mT and Avg (32×).

Step	Position_mm	Scan_mm	Step_mm	Sensor	X_mT	Y_mT	Z_mT	Avg
0	0	0	0	U1	0.121765	-0.42212	-0.65753	32x
0	0	0	0	U2	0.381531	-0.07306	-0.56012	32x
0	0	0	0	U3	0.008118	0.300354	-0.77118	32x
0	0	0	0	U4	-0.38153	0.316589	-0.62506	32x
0	0	0	0	U5	-0.21106	-0.25165	-0.58447	32x
0	0	0	0	U6	0.194824	-0.30847	-0.81177	32x
0	0	0	0	U7	0.332825	-0.21918	-0.59259	32x
0	0	0	0	U8	0.073059	0.45459	-0.56012	32x
0	0	0	0	U9	-0.17859	0.194824	-0.56012	32x
0	0	0	0	U10	-0.38965	-0.04871	-0.47894	32x
0	0	0	0	U11	-0.16235	-0.22729	-0.85236	32x
0	0	0	0	U12	0.259766	-0.12988	-0.92542	32x
0	0	0	0	U13	0.373413	0.032471	-0.70624	32x
0	0	0	0	U14	0.503296	0.276001	-0.58447	32x
0	0	0	0	U15	-0.04059	0.45459	-0.57635	32x
0	0	0	0	U16	-0.33282	0.405884	-0.43024	32x
0	0	0	0	U17	-0.34906	0.259766	-0.61694	32x
0	0	0	0	U18	-0.38965	-0.03247	-0.60071	32x
0	0	0	0	U19	-0.35718	0.113647	-0.44647	32x
0	0	0	0	U20	-0.23541	-0.11365	-0.71436	32x
0	0	0	0	U21	0.162354	-0.37341	-0.86047	32x
0	0	0	0	U22	0.202942	-0.21918	-0.73871	32x
0	0	0	0	U23	0.340942	-0.14612	-0.59259	32x
1	1.0001	1.0001	1.0001	U1	0.162354	-0.39777	-0.70624	32x
1	1.0001	1.0001	1.0001	U2	0.414001	-0.08118	-0.59259	32x
1	1.0001	1.0001	1.0001	U3	0.10553	0.308472	-0.78741	32x
1	1.0001	1.0001	1.0001	U4	-0.43024	0.332825	-0.64941	32x
...								

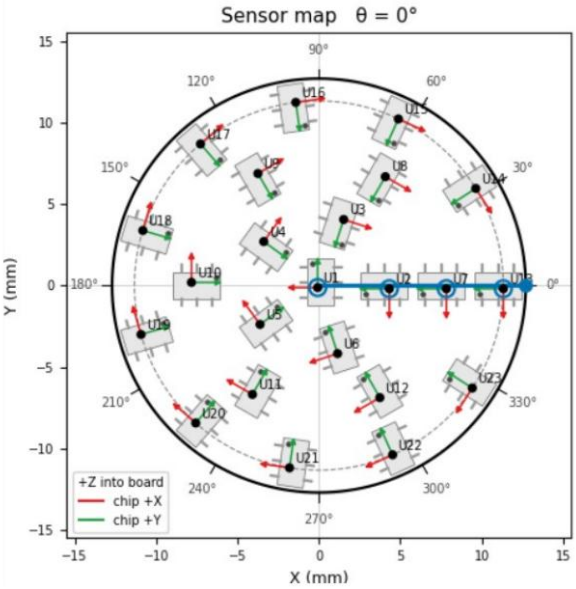

Figure 14: *Raw data format (left) and the sensor map showing each chip's local X/Y axes on the board (right).*

4.2 Magnetic Field Plots

Python script, *Scan_viewer.py,* can be used to view the scan data. The individual measured field components are plotted B vs. z position, Figure 15 shows Bx components of a test scan. Figure 15 also shows the green trace using the Avg(1x) acquisition setting and associated quantization error around 0.5mT. Appendix C shows data for all three B components.

The script also generates a magnetic field contour plot for a specified angle that can be exported as a CSV and a plot of |B| vs axial position for a specified radius as shown in Figure 16. The script also allows the user to specify a z offset and rotation offset to match the PCB frame to the trap frame.

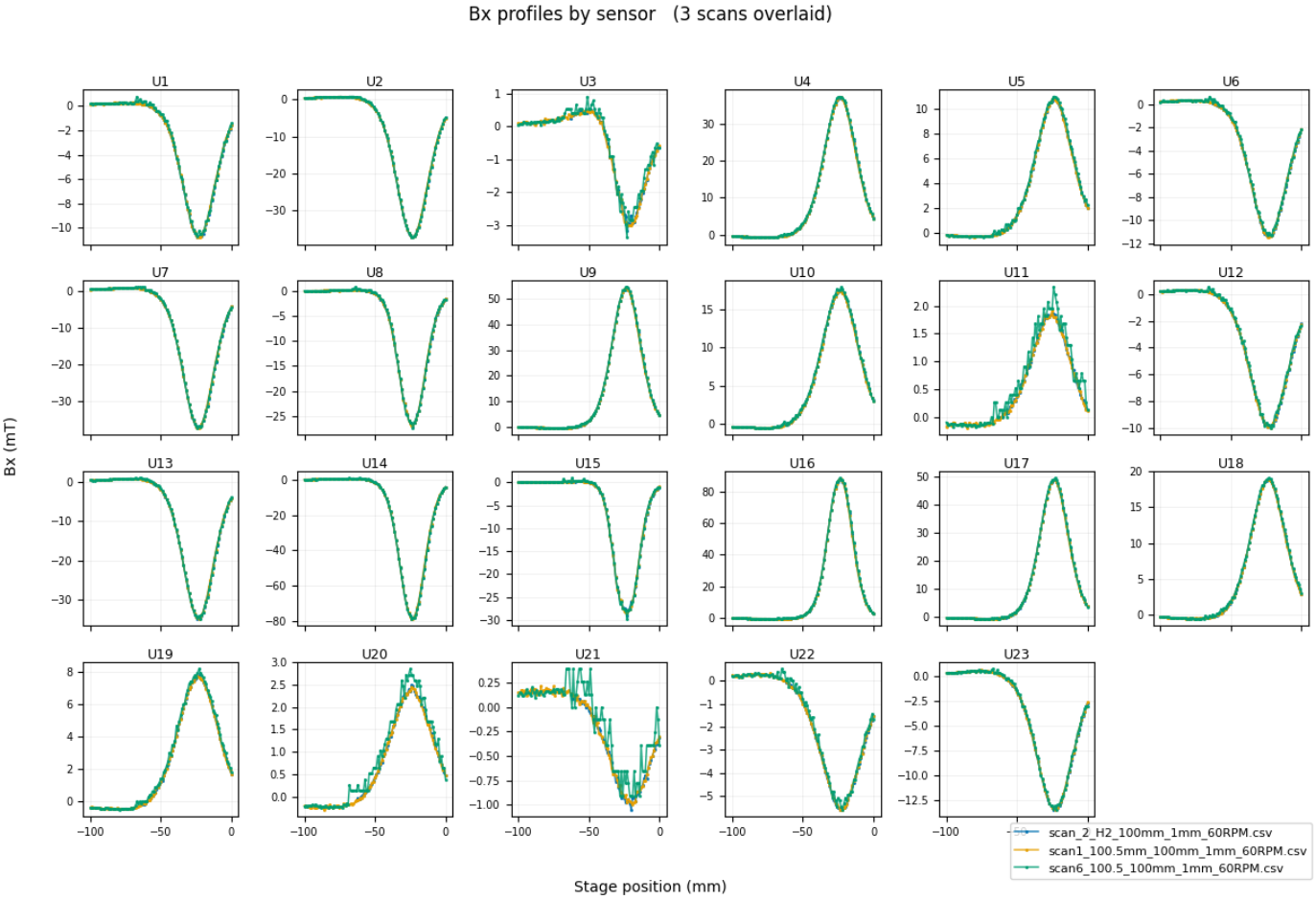

Figure 15: *Bx vs. axial position scanning data for each chip.*

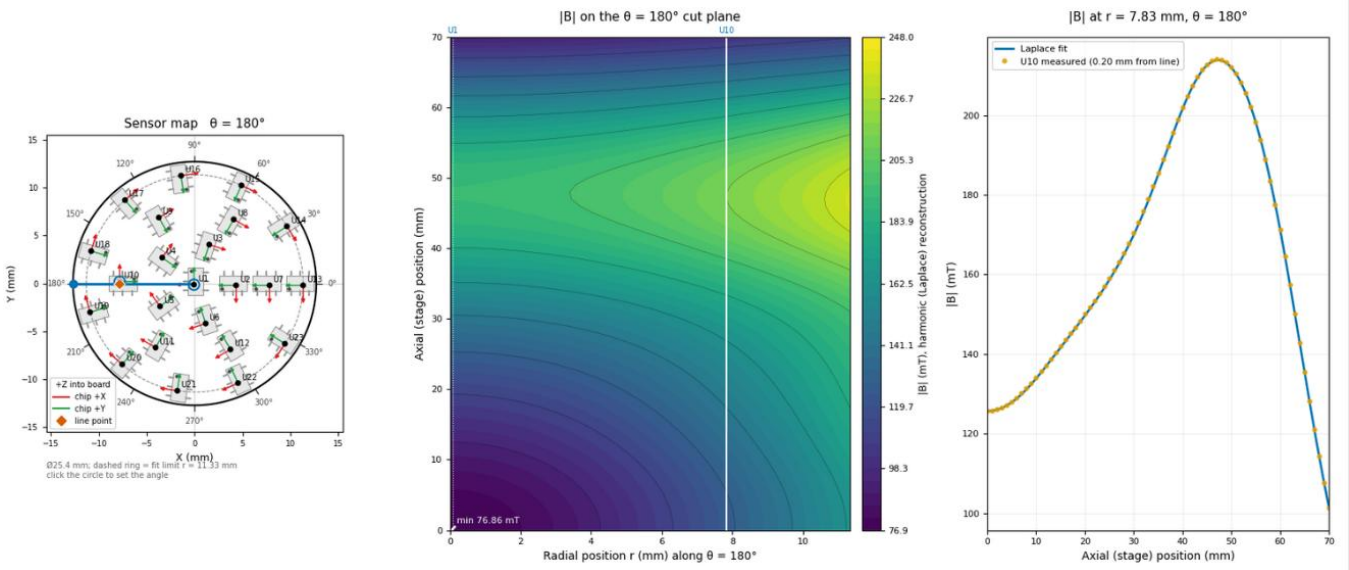

Figure 16: *Field map outputs: sensor map (left), |B| on the ϑ = 180° cut plane (centre) and axial |B| profile at r = 7.83 mm (right).*

The script also has a fit diagnostic feature where it leaves a chip out for the fit then compares the value predicted by the fit at the chip location with its measured value. It plots the RMS error value across the scan as shown in Figure 17. This feature was used to determine multipole order n and knot spacing for field reconstruction described in Appendix E.

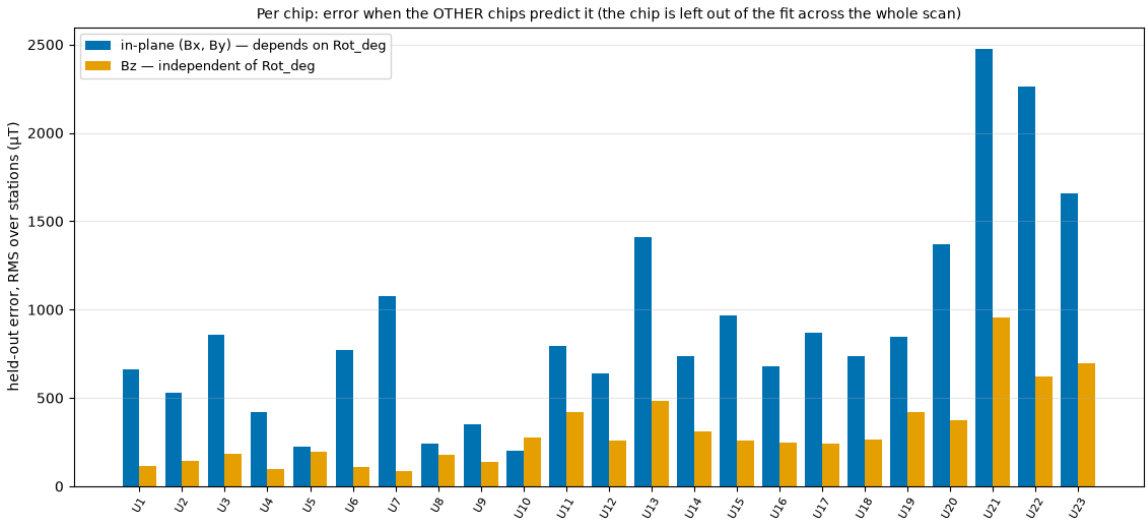

Figure 17: *Leave-one-out fit diagnostic: RMS error at each chip, predicted from the other chips, across the scan.*

5 Initial Testing

5.1 Chip Response

The goal of the chip response test is to confirm that every chip responds independently to a test magnet. A test magnet (Honeywell 102MG11) was placed centered in front of each chip using 3D-printed test discs as per Figure 18.

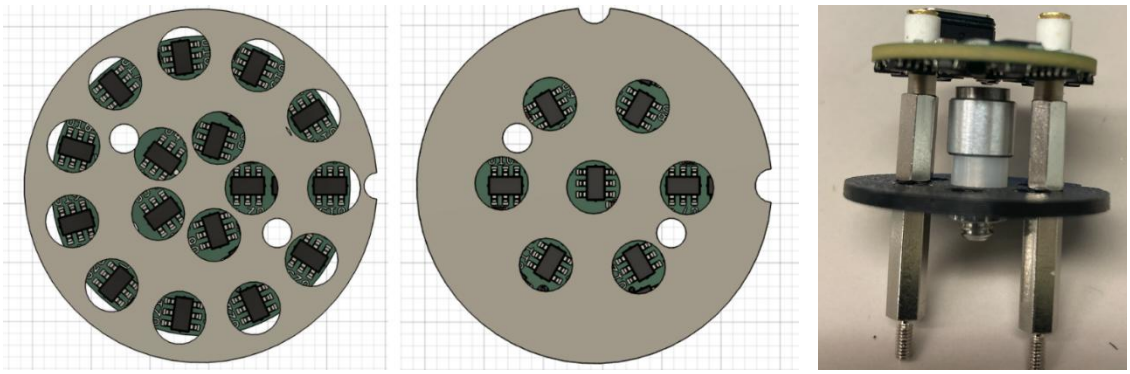

Figure 18: *Printed discs for chip response testing (left), testing assembly (right).*

Figure 19 shows the reconstructed |B| map with the magnet placed in front of each chip. The Bx, By and Bz maps for each chip are found in Appendix C along with the acquired raw data. This test confirmed that all chip channels, addresses and position mapping is correct.

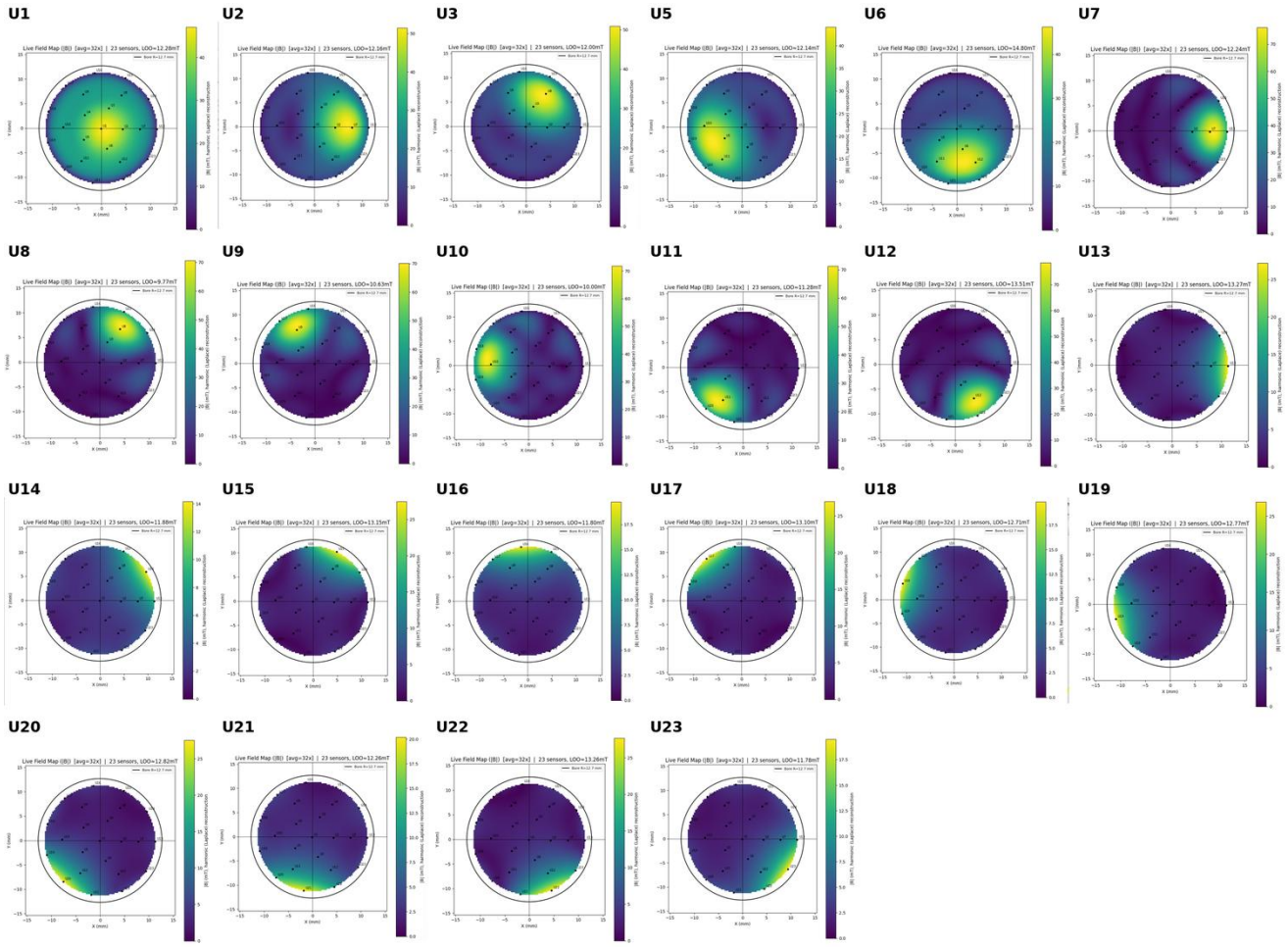

Figure 19: *|B| maps (32× average) with the test magnet in front of each chip.*

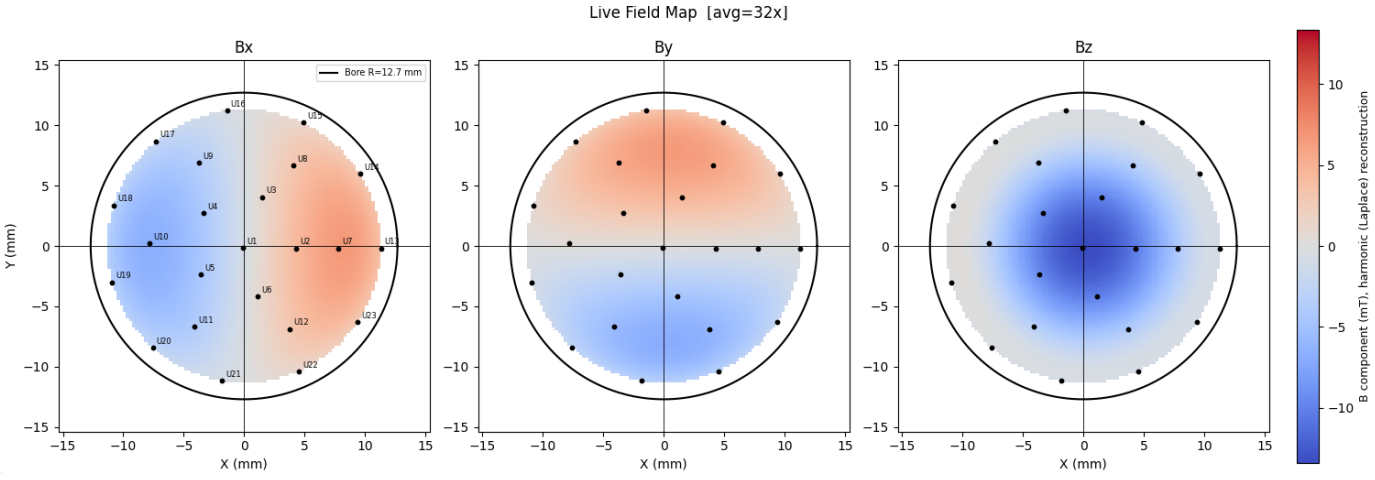

Figure 20: *Example component response data in Appendix C, U1: Bx, By and Bz maps.*

5.2 Scanning GUI

Scans are conducted using python script, *fieldmap_gui_web.py*, which is a webpage that can be accessed by any PC on the same network. The scan is set by its distance, step size and motor speed (for example, 100 mm, 1 mm steps, 60 RPM). At each step the stage stops, all 23 sensors are read with specified averaging, and the data is written to CSV in the raw format of Section 4.1. The GUI also shows a live field map of the current readings.

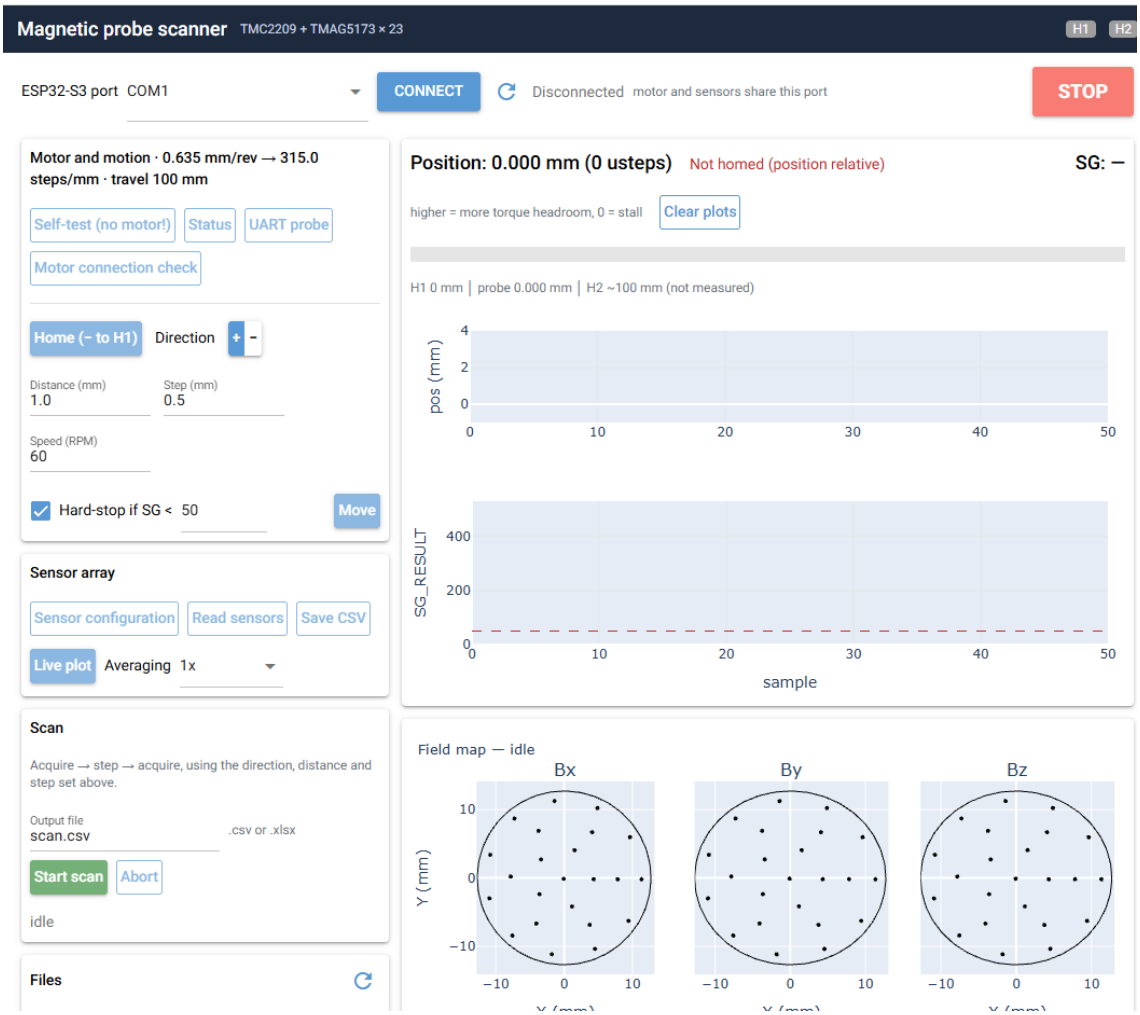

Figure 21: *Scanning GUI webpage.*

Scan testing data was acquired with the probe installed in the mock setup at UBC as shown in Figure 22. The results are described in section 5.3.

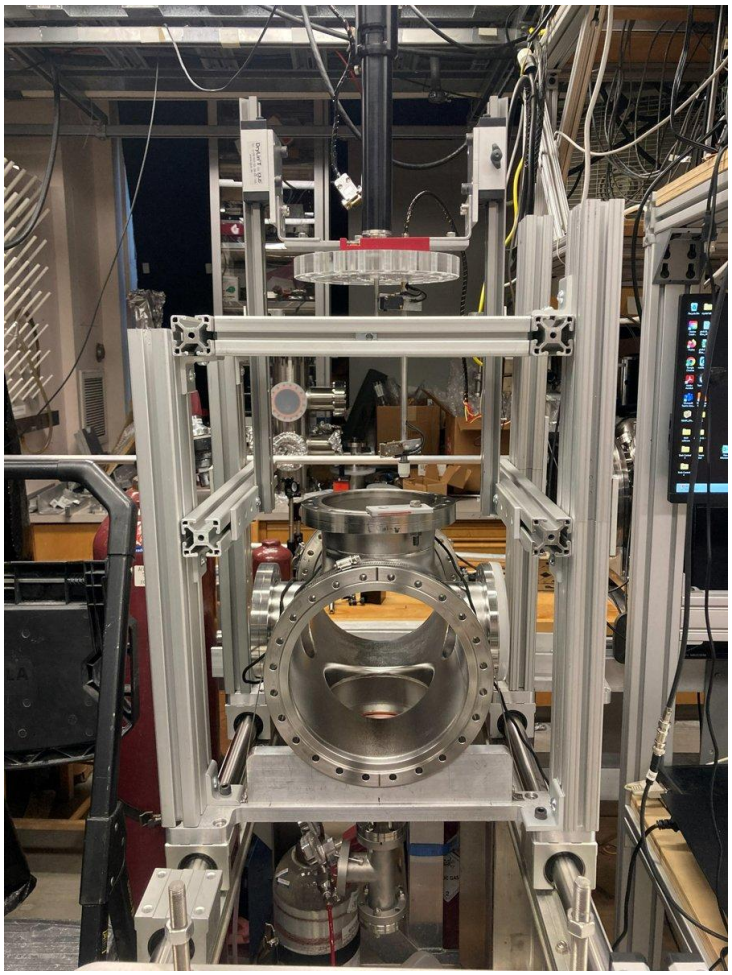

Figure 22: *UBC setup for initial testing.*

5.3 Scan Repeatability

A test magnet was fixed at a constant location on the vacuum chamber and the probe was scanned repeatedly over its 100 mm range, acquiring Bx, By and Bz every 1 mm (each value a 32-sample average). Figure 23 shows Bx of the test data of Appendix D, where the plots compare three scan runs. The scans in this case are acquired from fully retracted to fully extended: start at home (H1), scan/acquire to 100 mm, retract to H1, repeat.

- The overlaid scans show that the extend/retract cycle does not lose steps and positional accuracy is kept within the quantization error of the sensors.
- The green trace is 1× (no averaging) and the yellow and blue traces are 32× averaged. With no averaging the quantization error becomes visible at fields <5mT.
- The By, Bz and |B| profiles and deviations are in Appendix D.
- Linear stage precision holds despite oscillation described in 5.4.

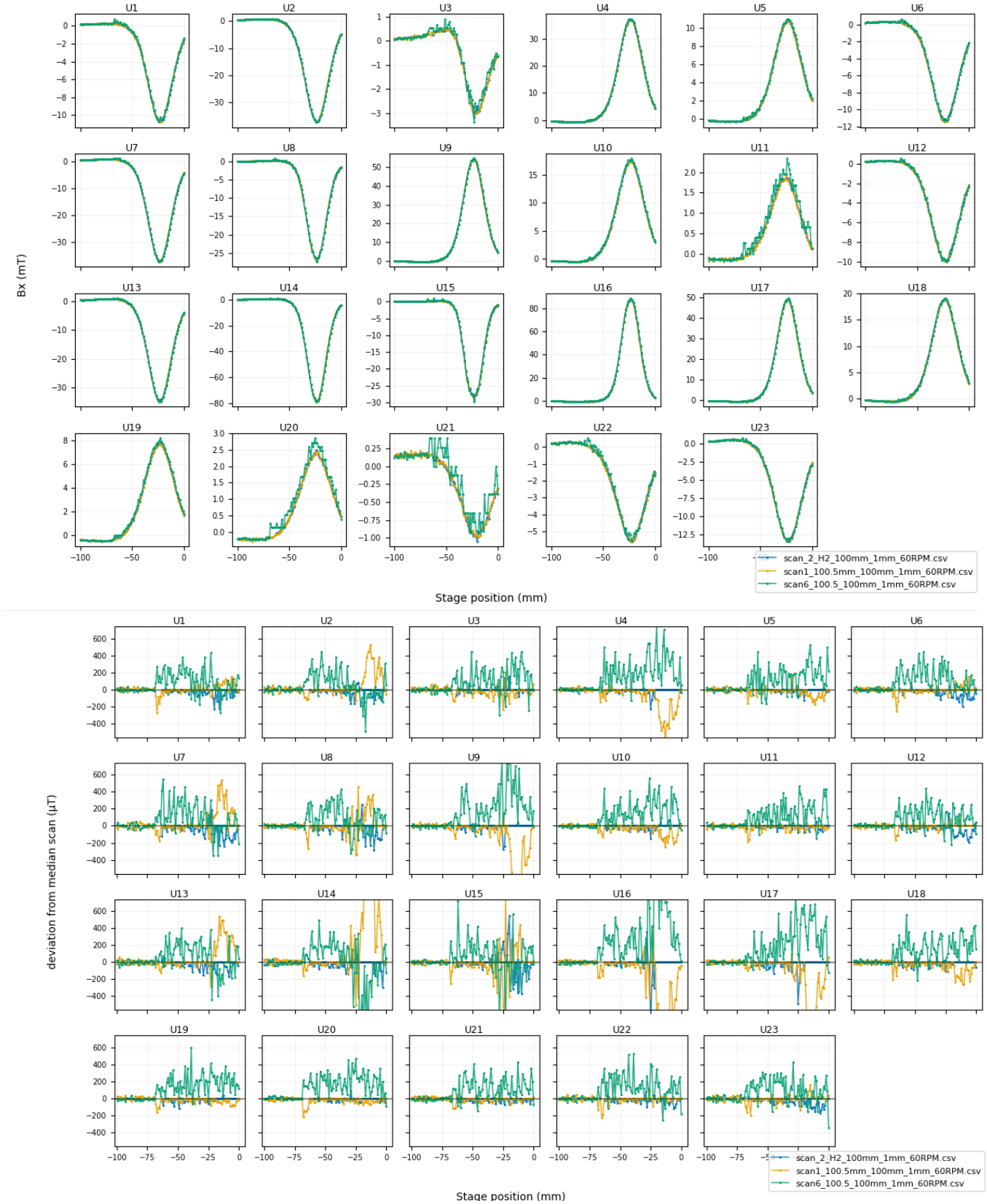

Figure 23: *Bx profiles by sensor, scans overlaid.*

5.4 Stage Oscillation

The TMC2209 StallGuard result (SG_RESULT), which is based on the motor back-EMF, shows a periodic oscillation during linear stage movement. Accu-Glass confirmed that this behavior is normal for the HTL-275-4. The oscillations are present at all RPMs. Figures 24-26 show the oscillation via the back EMF reading for 50 RPM and 60 RPM, and at both ends of the travel.

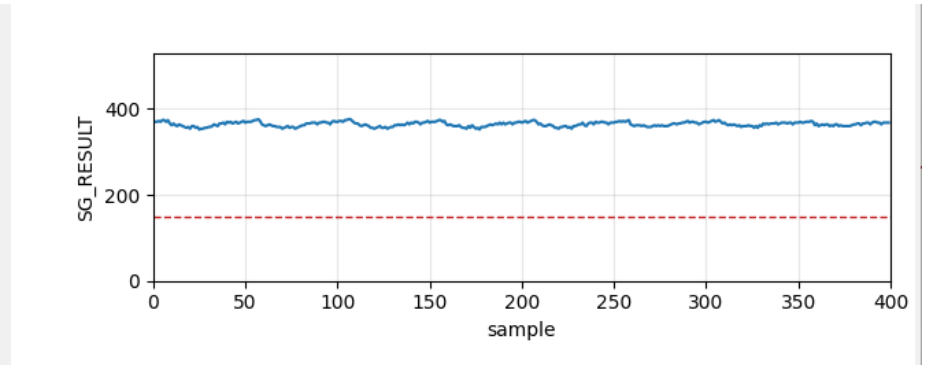

Figure 24: *SG_RESULT at 50 RPM, stage position < 20 mm.*

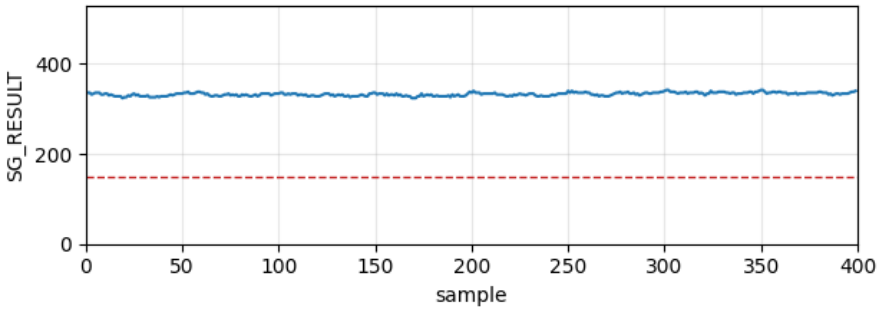

Figure 25: *SG_RESULT at 50 RPM, stage position > 80 mm.*

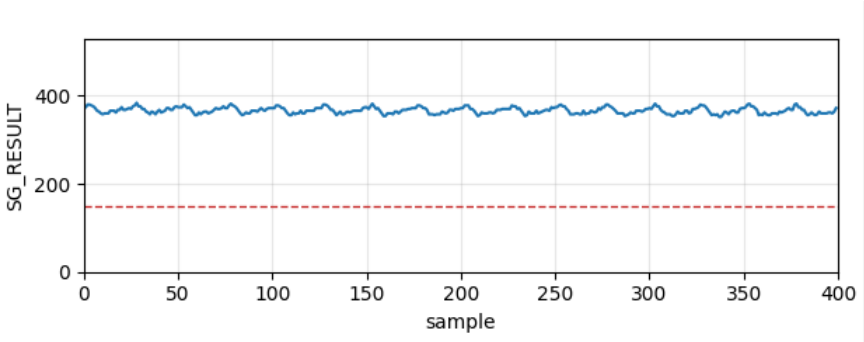

Figure 26: *SG_RESULT at 60 RPM.*

Although there is oscillation in the stage, the repeatability scan testing confirmed that the results are repeatable: positional accuracy within 13 µm/1 mm is kept after multiple extend/retract cycles.

6 Error Budget

Four error sources are considered: A. the sensor chip, B. chip position accuracy, C. field reconstruction from discrete points, and D. probe insertion into the trap. Table 2 shows the error budget summary described in section 6.1 to 6.4.

Table 2: *Error budget summary (% of local |B|).*

Error source	Typical	Worst case
A. Chip: gain, linearity, offset, noise	0.8% (25 °C), 1.1% (50 °C)	3.3% (25 °C), 3.58% (50 °C)
B. Chip placement: x, y, z	≤0.31% X/Y, ≤0.18% Z, ≤0.21% |B| (RMS)	≤1.0% X/Y, ≤0.49% Z, ≤0.63% |B|
C. Field reconstruction	0.19%	0.19%
D. Probe insertion (1 mm, 1°), incl.	X 1.0–2.0%, Y 1.2–2.2% (RMS)	Z and |B| up to 5.8% (RMS)
B + C + D combined	Median 1.71%; 95% of points < 5.77%	6.76%

Adding the worst-case chip error (A, 3.58% at 50 °C) to the worst-case B + C + D result gives 7.6% as a root-sum-square. Typical error 5.8%.

6.1 A. Chip Error

The chip error is calculated from the TMAG5173 datasheet equations: Eq. 14 at room temperature, Eq. 15 with room-temperature calibration, and Eq. 16 across temperature without calibration.

$$\text{Error}_{\text{LM_25C}} = \frac{\sqrt{(B \times \text{SENS}_{\text{ER}})^2 + B_{\text{off}}^2 + N_{\text{RMS_25}}^2}}{B} \times 100\% \quad (14)$$

where

- $\text{Error}_{\text{LM_25C}}$ is total error in % during linear measurement at 25°C.
- B is input magnetic field.
- SENS_{ER} is sensitivity error in decimal number at 25°C. As an example, enter 0.05 for sensitivity error of 5%.
- B_{off} is offset error at 25°C.
- $N_{\text{RMS_25}}$ is RMS noise at 25°C.

$$\text{Error}_{\text{LM_Temp}} = \frac{\sqrt{(B \times \text{SENS}_{\text{DR}})^2 + B_{\text{off_DR}}^2 + N_{\text{RMS_Temp}}^2}}{B} \times 100\% \quad (15)$$

where

- $\text{Error}_{\text{LM_Temp}}$ is total error in % during linear measurement across temperature after room temperature calibration.
- B is input magnetic field.
- SENS_{DR} is sensitivity drift in decimal number from value at 25°C. As an example, enter 0.05 for sensitivity drift of 5%.
- $B_{\text{off_DR}}$ is offset drift from value at 25°C.
- $N_{\text{RMS_Temp}}$ is RMS noise across temperature.

$$\text{Error}_{\text{LM_Temp_NCal}} = \frac{\sqrt{(B \times \text{SENS}_{\text{ER}})^2 + (B \times \text{SENS}_{\text{DR}})^2 + B_{\text{off}}^2 + B_{\text{off_DR}}^2 + N_{\text{RMS_Temp}}^2}}{B} \times 100\% \quad (16)$$

where

- $\text{Error}_{\text{LM_Temp_NCal}}$ is total error in % during linear measurement across temperature without room temperature calibration.

The budget uses Eq. 16 with offset compensation. Tables 3 and 4 show the datasheet parameters used and the resulting chip error vs field strength.

Table 3: *TMAG5173A2-Q1 parameters from datasheet.*

PARAMETER	MAX	TYP
SENS,ER, 25°C	3.30%	0.80%
Boff	0.7mT	0.1mT
Boff_DR	6.8uT/°C*(ABS(T-25)/1000)	1.2uT/°C*(ABS(T-25)/1000)
NRMS (x32 AVG)	18.6uT	18.6uT
SENS,DR	(T-25)/(125-25)*5.5%	(T-25)/(125-25)*3%

Table 4: *Chip error vs field strength (Eq. 16 uses offset compensation).*

B (mT)	Eq 14 (25 °C) w off	Eq 15 (at T, cal)	Eq 15 (at 25 °C, cal)	Eq 16 (at T, no cal)	Eq 16 (at 25, no cal), same as 14	A. Eq16, Off comp, 25°C, MAX	B. Eq16, Off comp, 50°C, MAX	Eq16, Off comp, 25°C, TYP	C. Eq16, Off comp, 50°C, TYP
10	7.74%	2.19%	0.19%	8.04%	7.74%	3.31%	3.96%	0.82%	1.15%
20	4.81%	1.62%	0.09%	5.08%	4.81%	3.30%	3.68%	0.81%	1.11%
30	4.04%	1.49%	0.06%	4.31%	4.04%	3.30%	3.62%	0.80%	1.10%
50	3.58%	1.42%	0.04%	3.85%	3.58%	3.30%	3.59%	0.80%	1.10%
75	3.43%	1.39%	0.02%	3.70%	3.43%	3.30%	3.58%	0.80%	1.10%
100	3.37%	1.39%	0.02%	3.65%	3.37%	3.30%	3.58%	0.80%	1.10%
125	3.35%	1.38%	0.01%	3.62%	3.35%	3.30%	3.58%	0.80%	1.10%
150	3.33%	1.38%	0.01%	3.61%	3.33%	3.30%	3.58%	0.80%	1.10%
175	3.32%	1.38%	0.01%	3.60%	3.32%	3.30%	3.58%	0.80%	1.10%
200	3.32%	1.38%	0.01%	3.59%	3.32%	3.30%	3.58%	0.80%	1.10%
225	3.31%	1.38%	0.01%	3.59%	3.31%	3.30%	3.58%	0.80%	1.10%
239.4	3.31%	1.38%	0.01%	3.59%	3.31%	3.30%	3.58%	0.80%	1.10%

6.2 B. Chip Position Offsets

To get a % error due to chip position, a position offset was applied to each chip and the field at the offset position of the COMSOL data was compared to an ideal position reading.

- %error = (field reading at offset position − reading at design position) as a % of local |B|, using the COMSOL quad + coil field data (polarB.txt).
- Pick-and-place tolerance: x, y and z offsets up to ±0.05 mm.

- Command: python position_error_spec.py polarB.txt --tol 0.05 --boards 2000. For each of 2,000 simulated boards a random offset within ±0.05 mm is applied and the error is read at every scan position.
- Worst case is the largest error over all 23 chips, all z positions and every corner of the tolerance box. Typical is the RMS over the 2,000 boards.

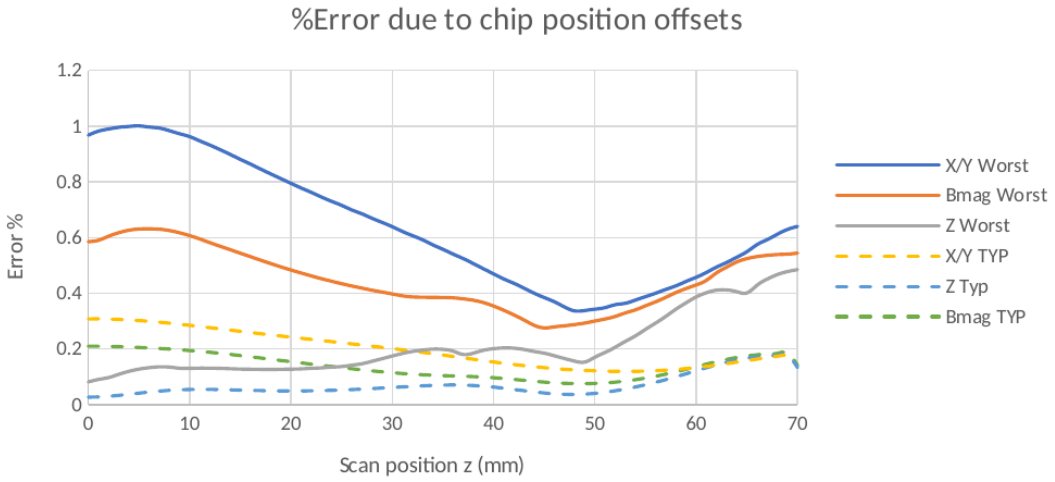

Figure 27: *% error due to chip position offsets vs scan position z.*

6.3 C. Field Reconstruction

COMSOL field values were taken at the chip locations as discrete data points, the field was reconstructed from those points only, and the reconstruction was compared with the full COMSOL field using python script *comsol_validate_data.py.* Inside the outer sensor ring (r ≤ 11.33 mm) the maximum error is 0.19%.

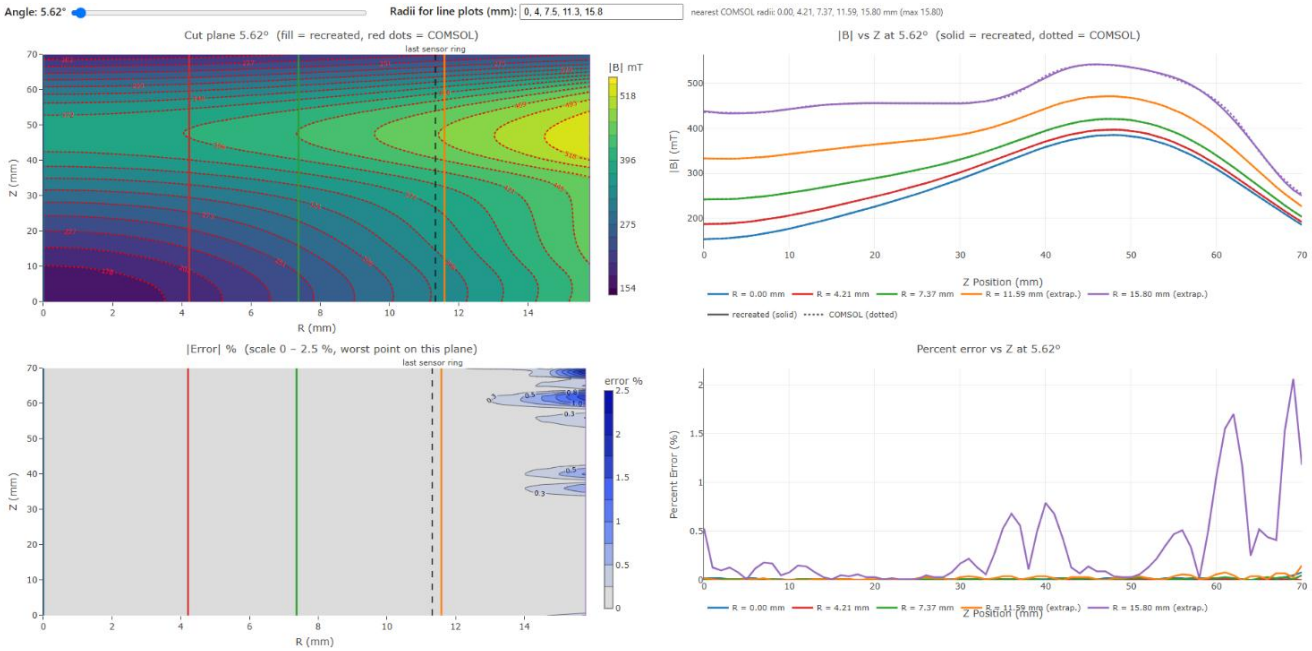

Figure 28: *Reconstructed field vs COMSOL.*

6.4 Chip position offset B and field reconstruction C errors combined

The chip map leading to worst-case and typical errors from section 6.3 were used to reproduce a field map and compare with the COMSOL data. Figures 29 and 30 show combined error of B and C of <1% for worst-case chip placement and <0.6% for typical placement. The errors are proportional to the local field strength and the local gradient.

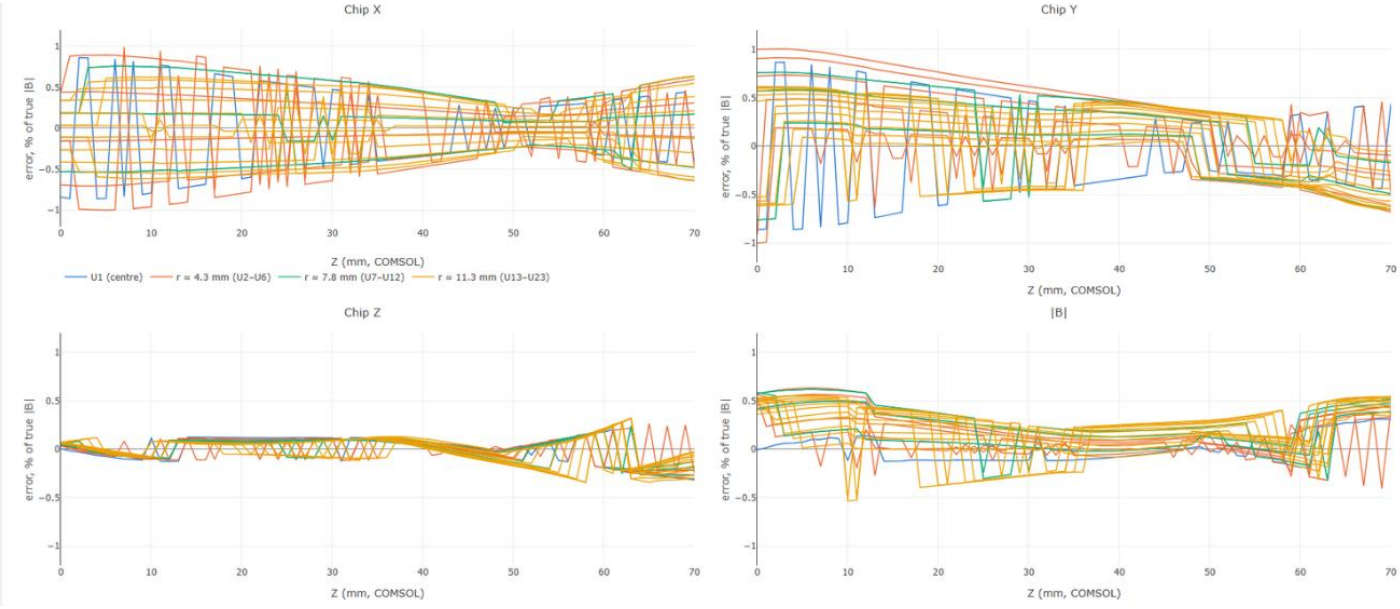

Figure 29: *B + C combined, worst-case offsets.*

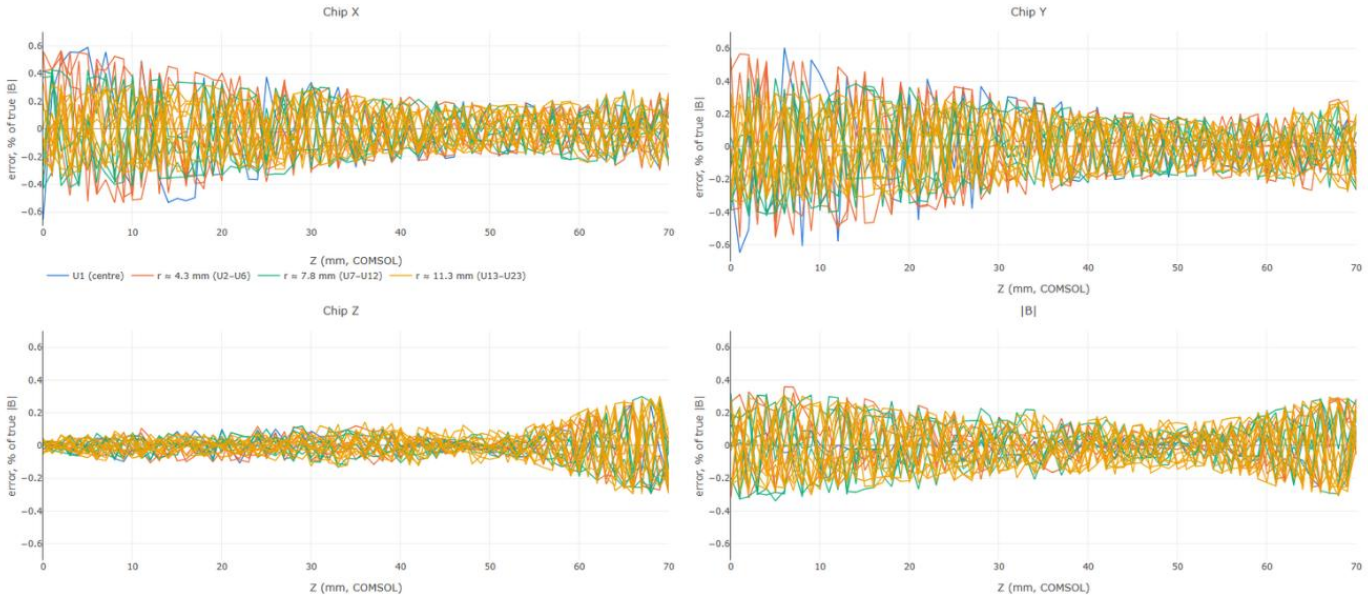

Figure 30: *B + C combined, typical offsets.*

6.5 D. Probe Insertion

The trap region is connected to the 6-way cross vacuum flange via a bellows and assembly stack up leads to probe position uncertainty after insertion. The probe position therefore needs to be measured after insertion which will introduce a measurement and rotation error.

- Probe z insertion error: 1mm, probe rotation error (set by fixture): 1°
- Bz changes by up to about 16 mT for every 1 mm of axial movement, while the in-plane field changes by only about 2 mT per mm, so the X and Y readings move much less than Z for the same 1 mm shift.

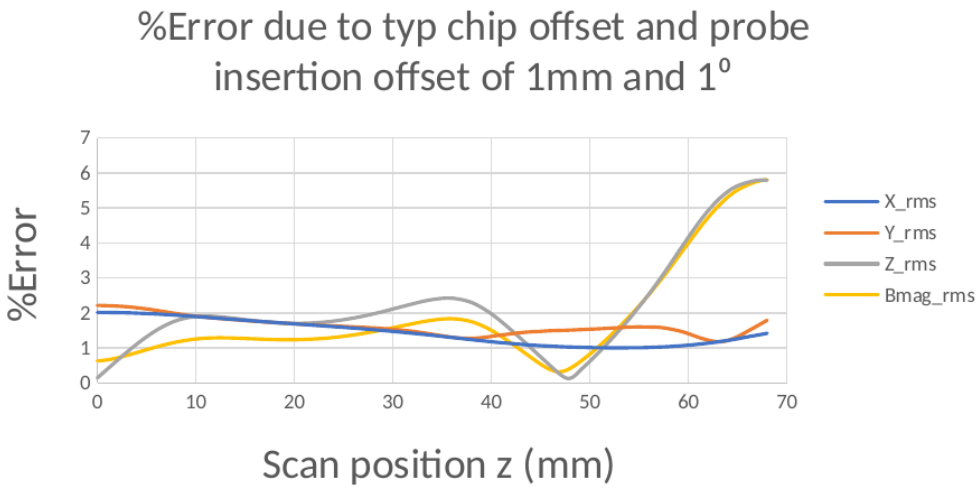

Figure 31: *% error due to typical chip offset and a probe insertion offset of 1 mm and 1°.*

6.6 B, C and D Combined

With chip placement, reconstruction and insertion errors combined, the median error is 1.71%, 95% of points are below 5.77%, and the worst case is 6.76%.

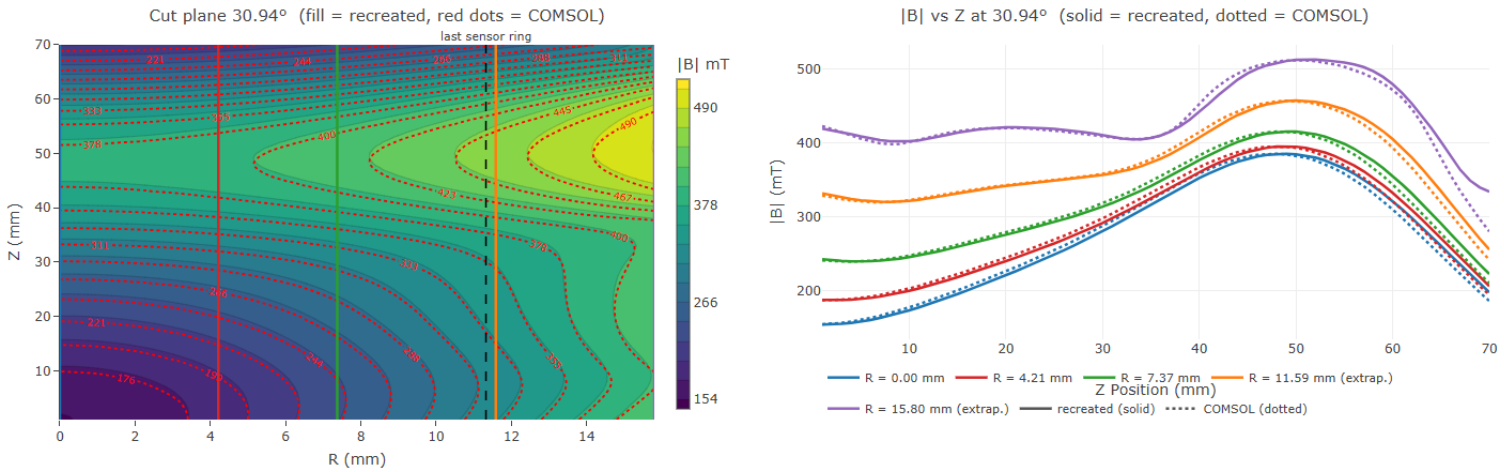

Figure 32: *B + C + D combined: reconstructed vs COMSOL cut plane and axial profile.*

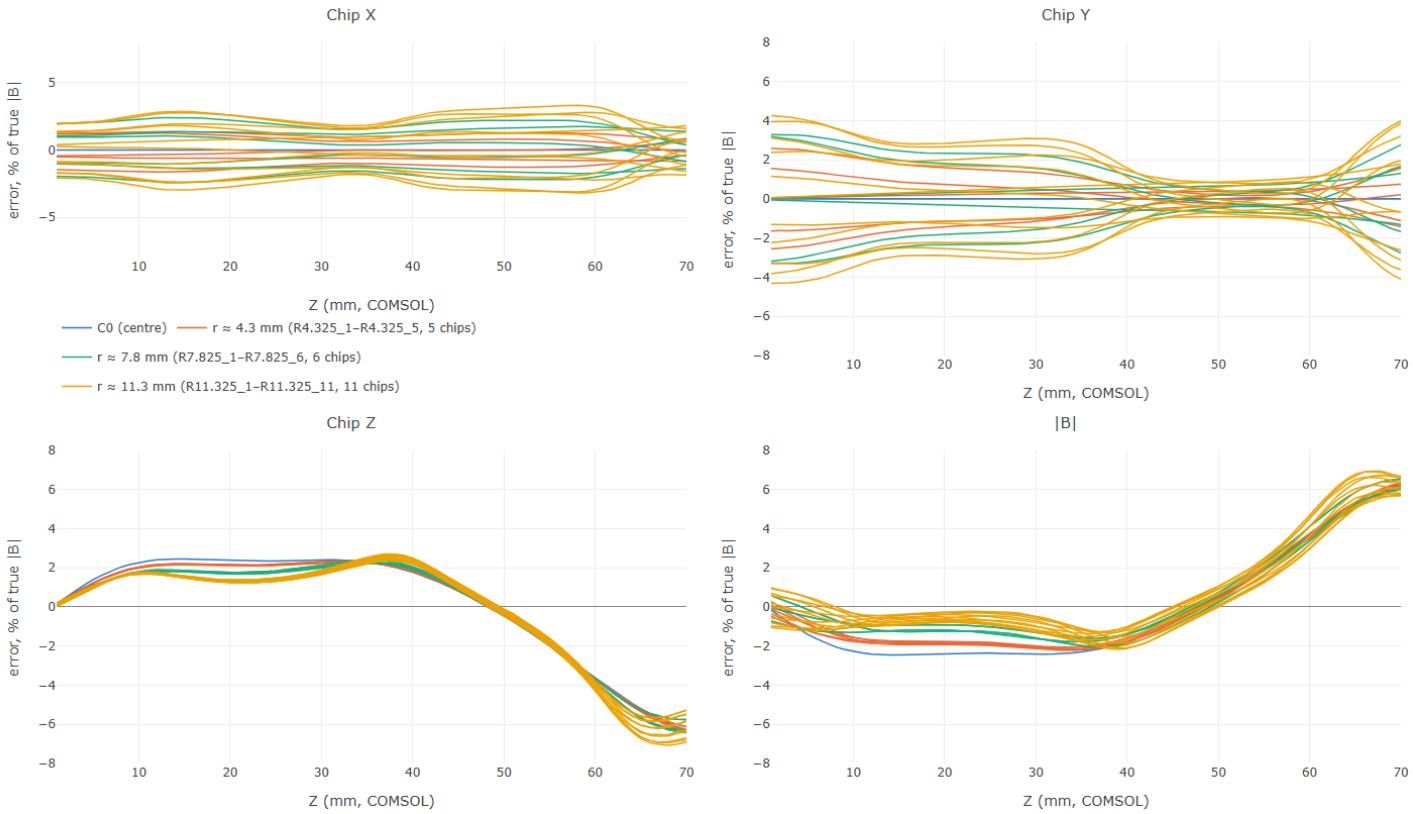

Figure 33: *B + C + D combined: % error for chip X, Y, Z and |B| vs z.*

7 Python Tools

1. **Scanning script:** *fieldmap_gui_web.py,* depicted in Figure 21.
2. **Scan results:** *scan_viewer.py,* depicted in Figures 15 and 16, import csv data acquired with scanning script and view plots/maps.
3. **Results compare to COMSOL:** *comsol_validate_data.py*, Figure 8, etc. import scan results and compare to COMSOL data, or create a synthetic chip array and compare to COMSOL.
4. **Chip position error:** *position_error_spec.py*, used to apply positional offsets to chip locations and allocate COMSOL data to those locations/ compare to ideal.

Appendix A: Schematics

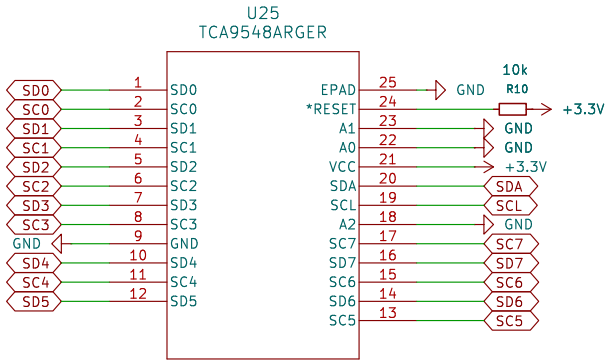

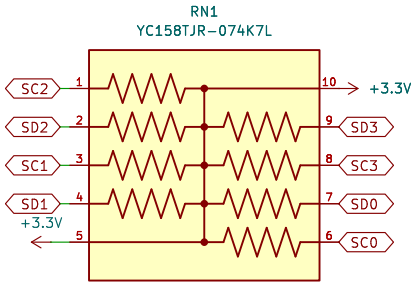

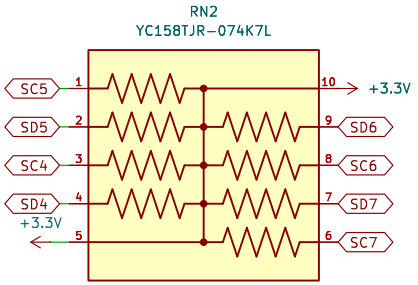

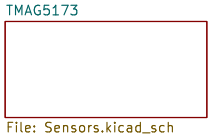

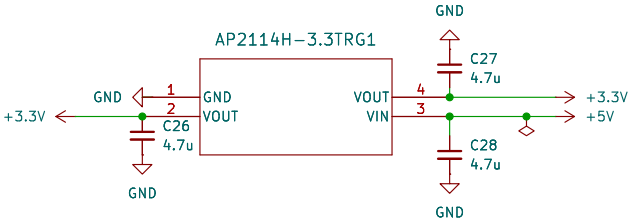

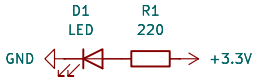

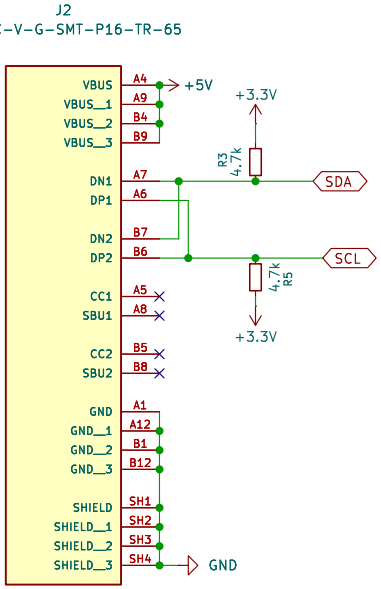

Drawing By: G.Marcoux

Sheet: /
File: Magnetic Trap Mapping Rev C.kicad_sch

Title: Magnetic Field Sensor Array

Size: A4	Date: 2026-04-21	**Rev: A**
KiCad E.D.A. 9.0.6		Id: 1/2

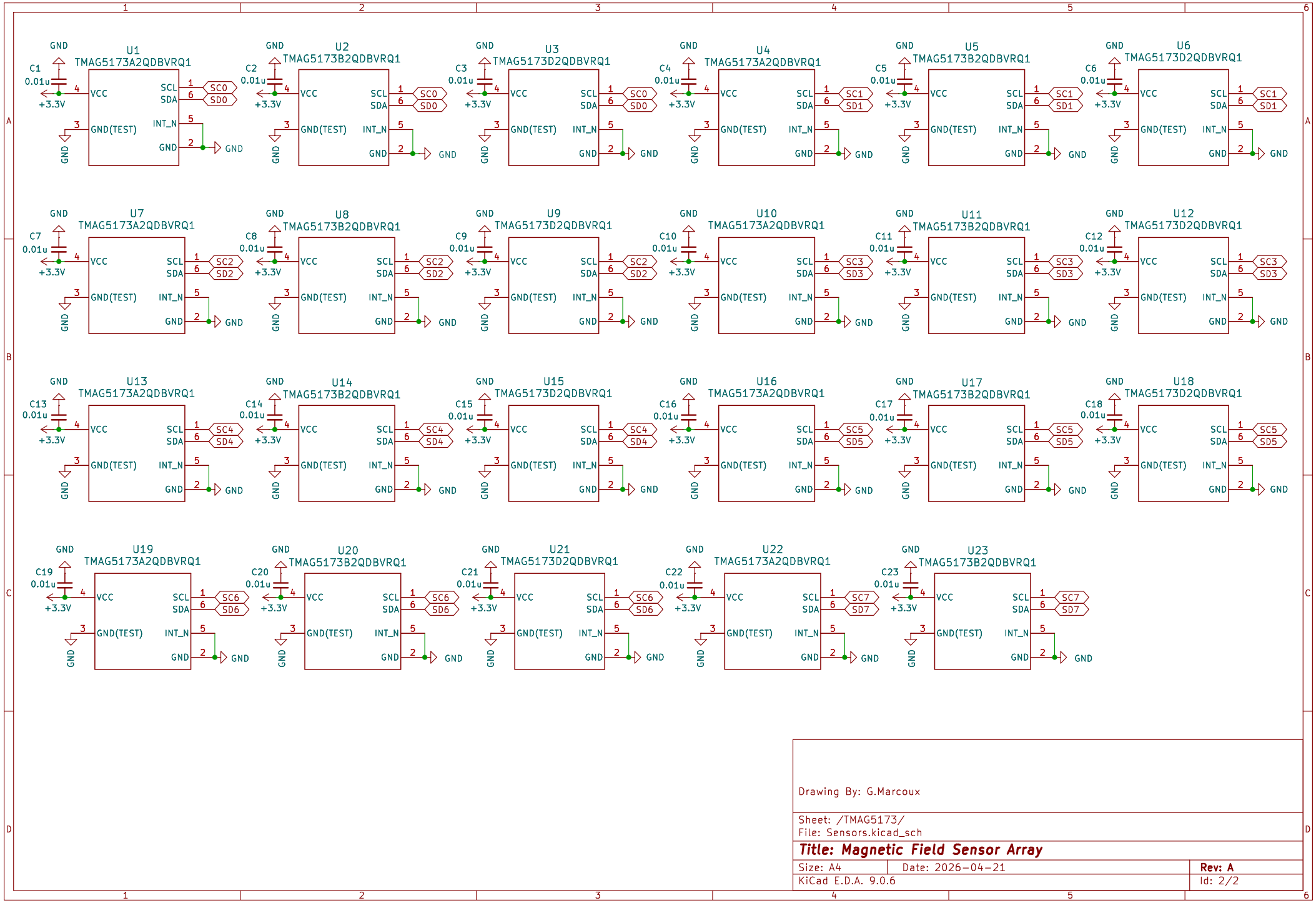

Drawing By: G.Marcoux

Sheet: /TMAG5173/
File: Sensors.kicad_sch

Title: Magnetic Field Sensor Array

Size: A4	Date: 2026-04-21	**Rev: A**
KiCad E.D.A. 9.0.6		Id: 2/2

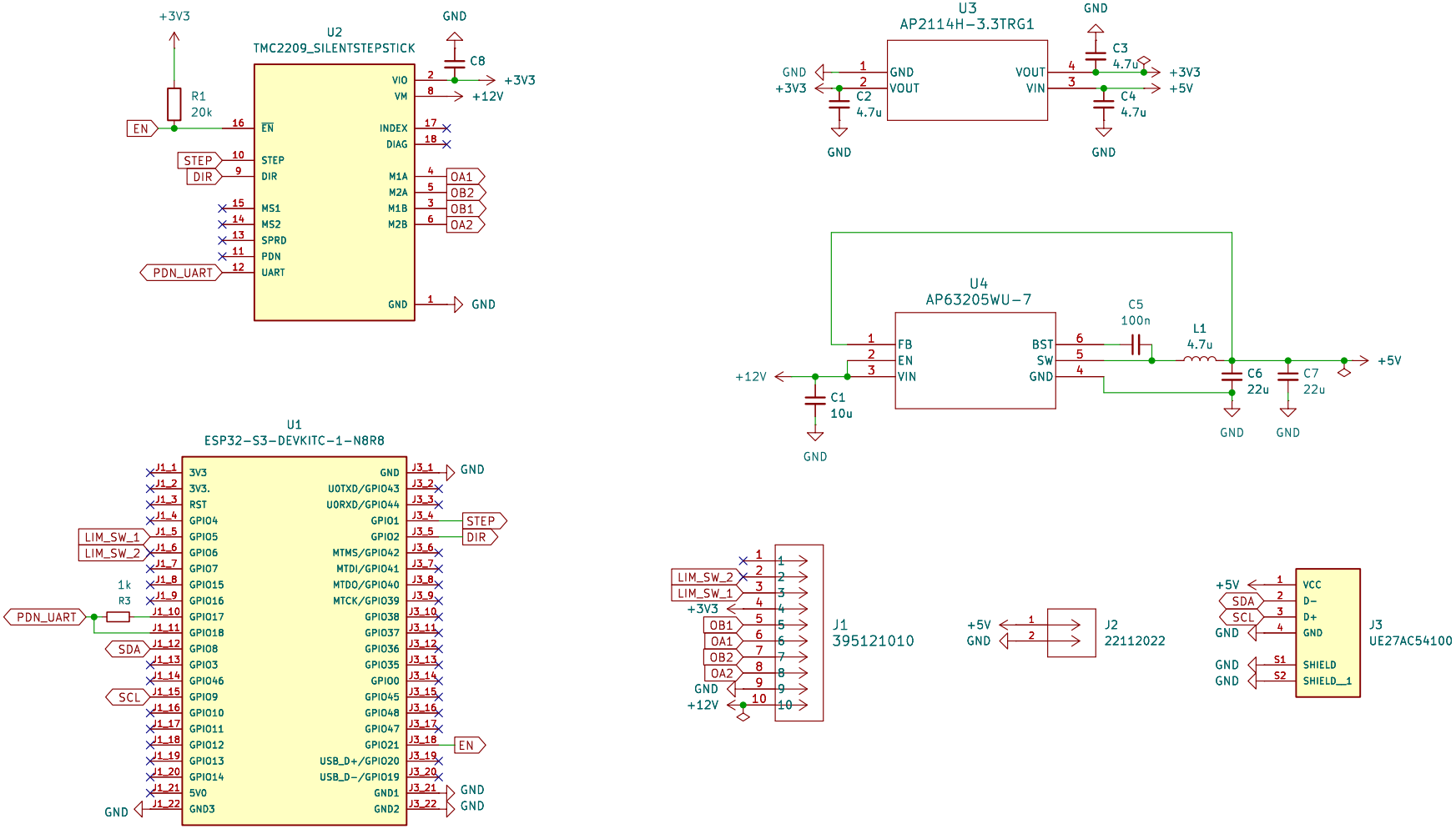

Drawing By: G.Marcoux

Sheet: /
File: Motor_HUB_RevC.kicad_sch

Title: Magnetic Field Probe Motor Control

Size: A4	Date: 2026-04-21	**Rev: A**
KiCad E.D.A. 9.0.6		Id: 1/1

Appendix B: Installation Steps

Installation was tested on a mock setup at UBC that recreates the 32 cm × 32 cm access hole. An installation power point includes videos to aid in probe installation. Please refer to slides for further explanation which includes videos.

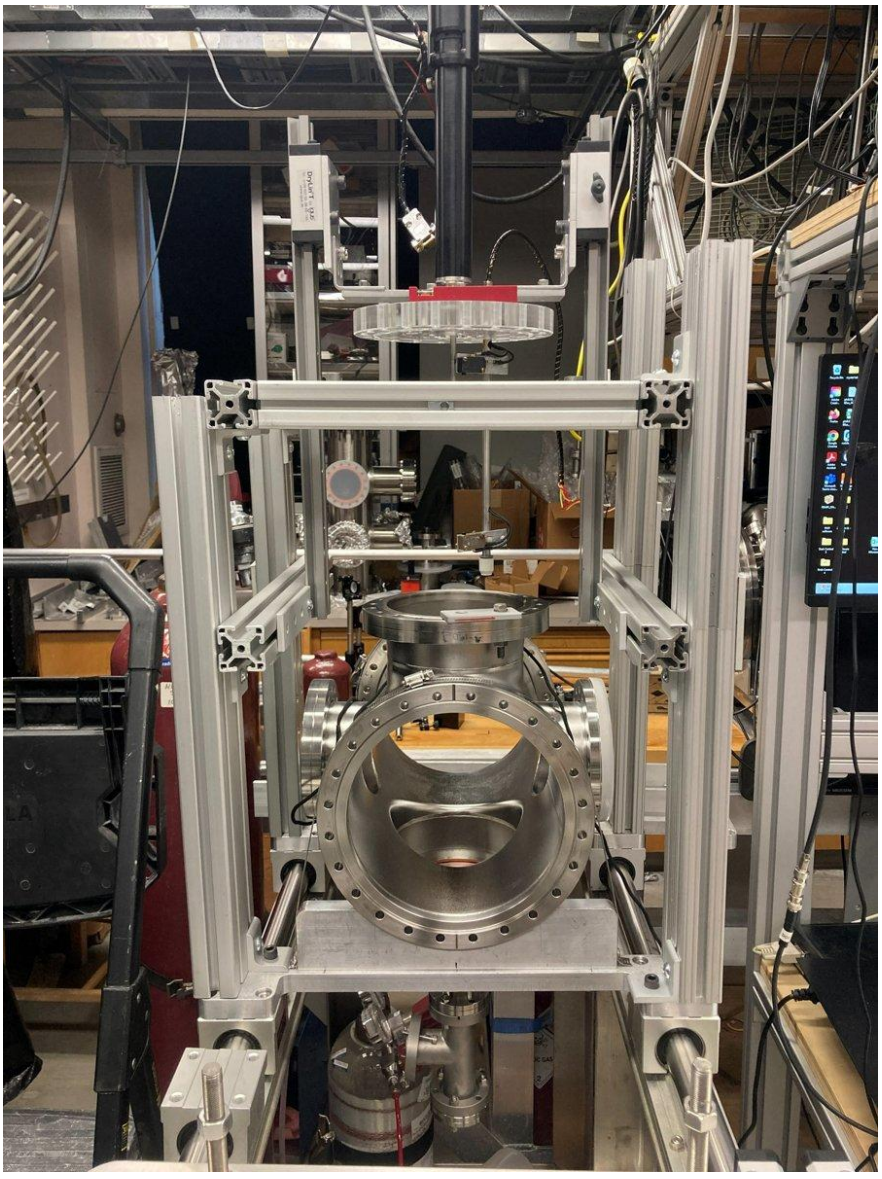

Figure 34: *Mock setup at UBC.*

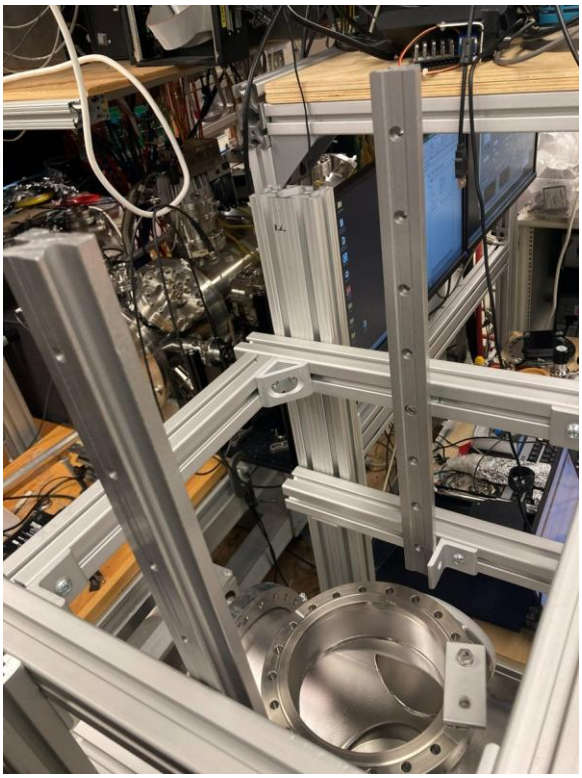

Figure 35: *Step 1: fasten linear rail and add angle bracket. Step 2: lower probe flange onto the vacuum box with insertion brackets installed.*

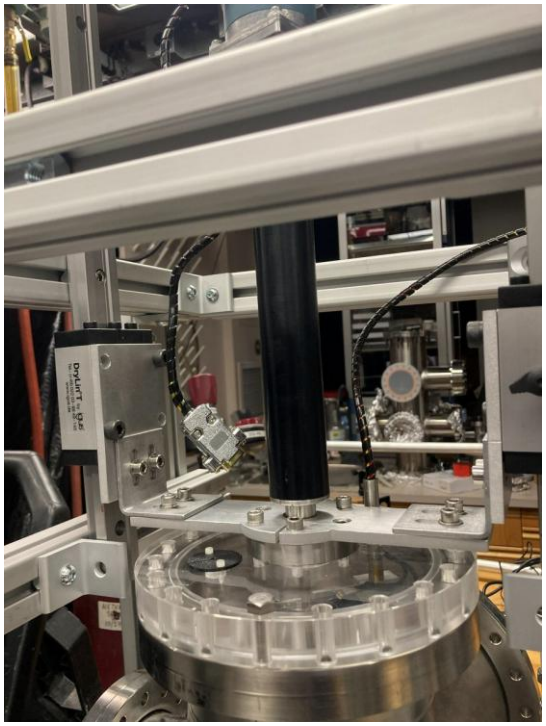

Figure 36: *Step 3: put carriages and lock as needed, fasten angle brackets;*

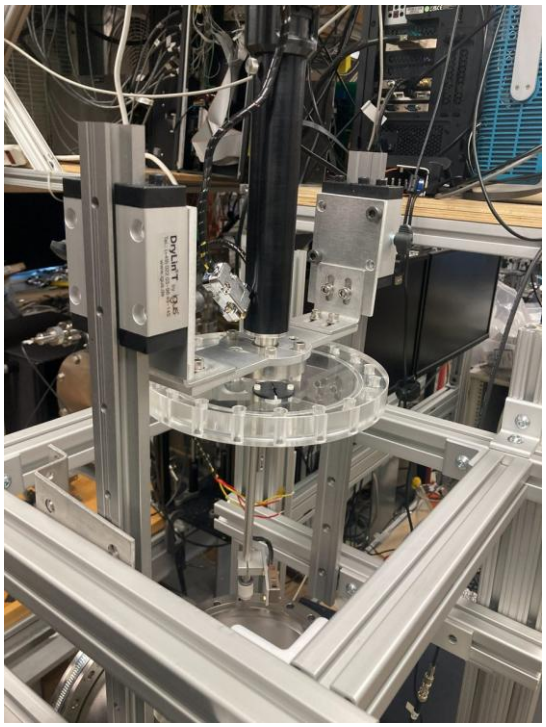

Figure 37: *Step 4: raise probe assembly and shim linear rails to ensure straightness for smooth travel.*

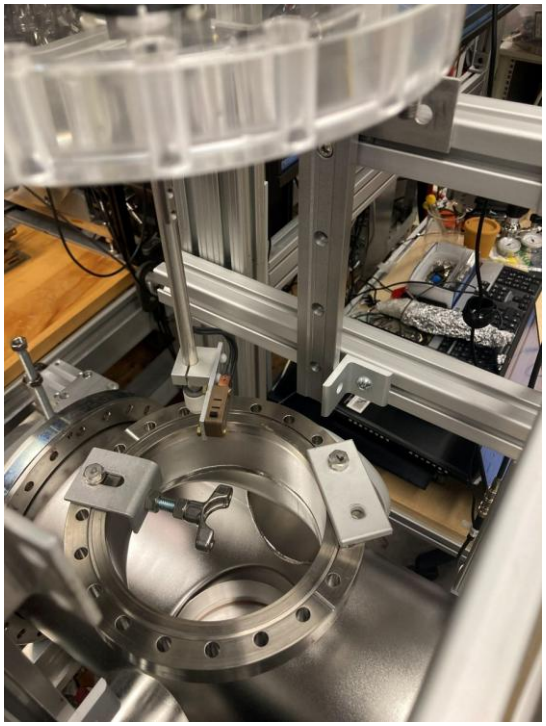

Figure 38: *Step 5: install probe holder (requires the double-nut rods).*

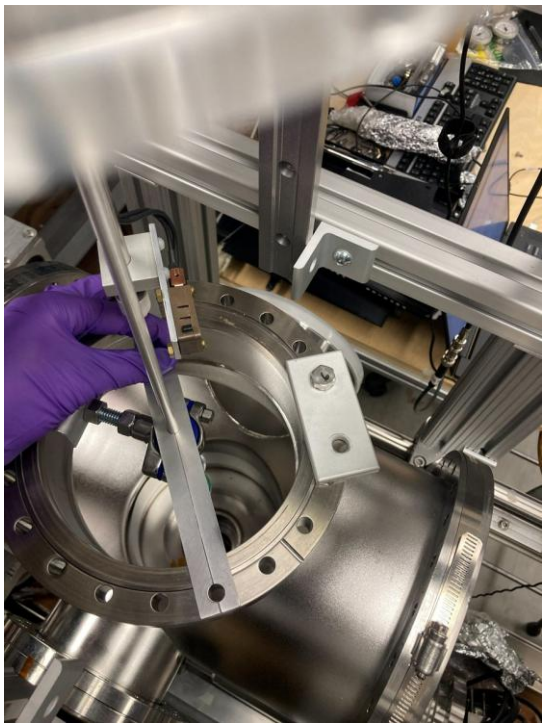

Figure 39: *Step 7: insert probe and align probe shaft to the correct angle using the alignment plates.*

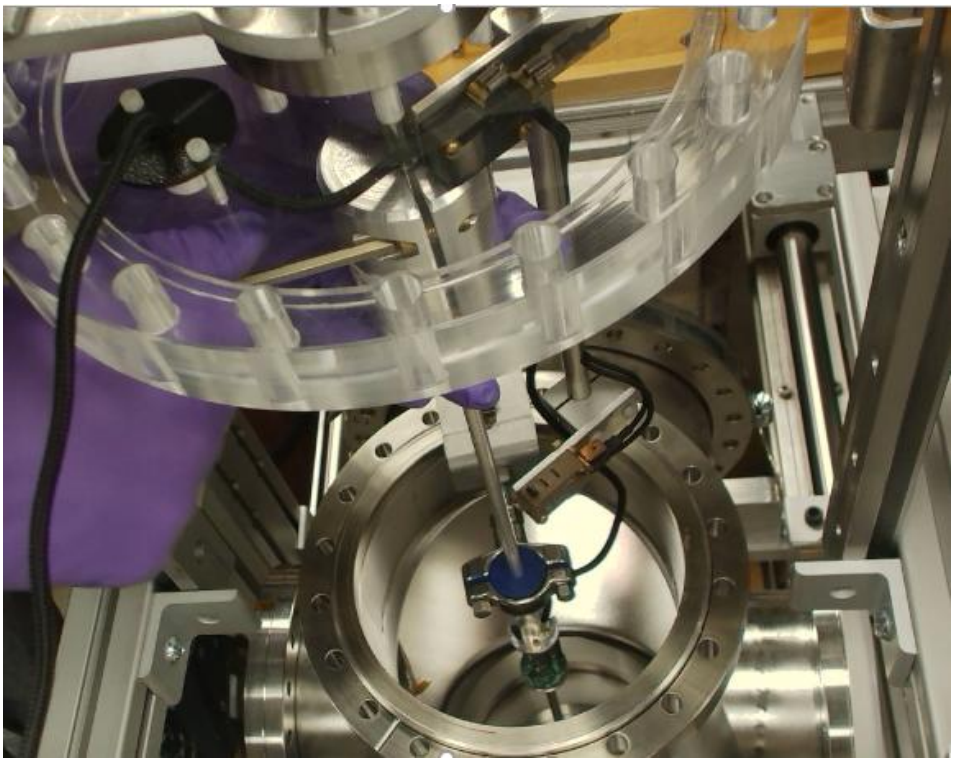

Figure 40: *Step 8-9: couple probe shaft to linear rail shaft; remove probe holder*

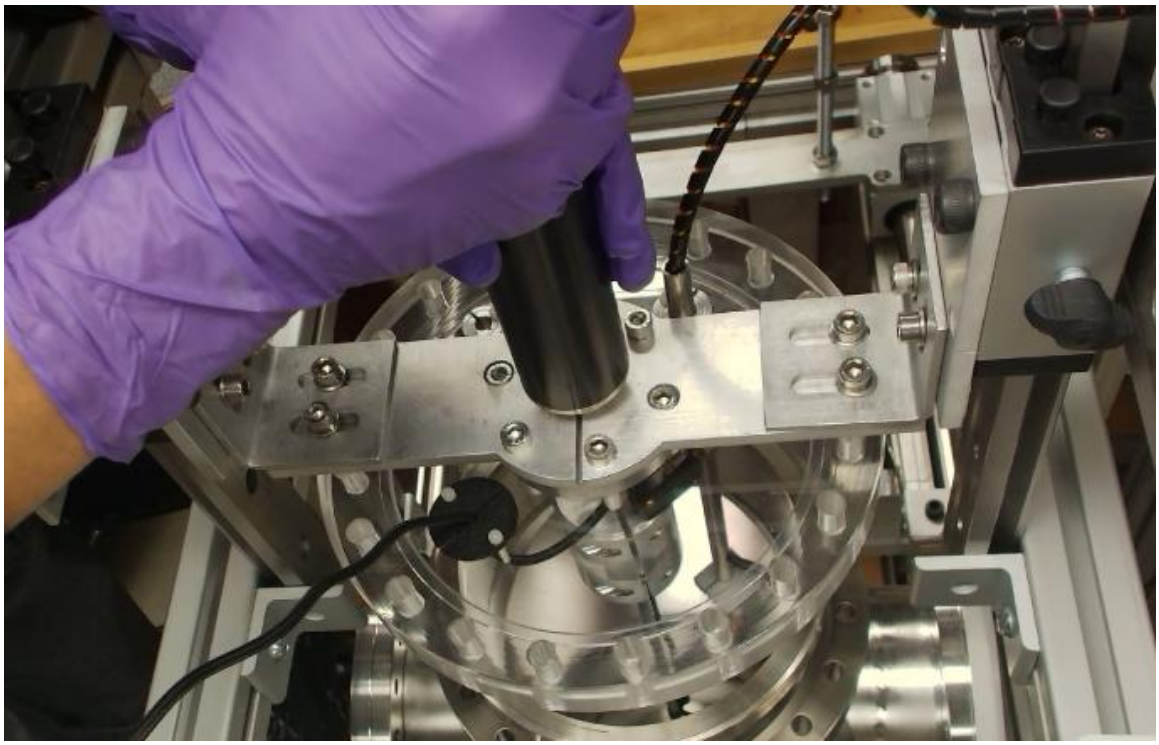

Figure 41: *Step 10: unlock rails and slowly lower assembly by ensuring the bottom shaft is guided into the dry PEEK bearing below the trap (Figure 42).*

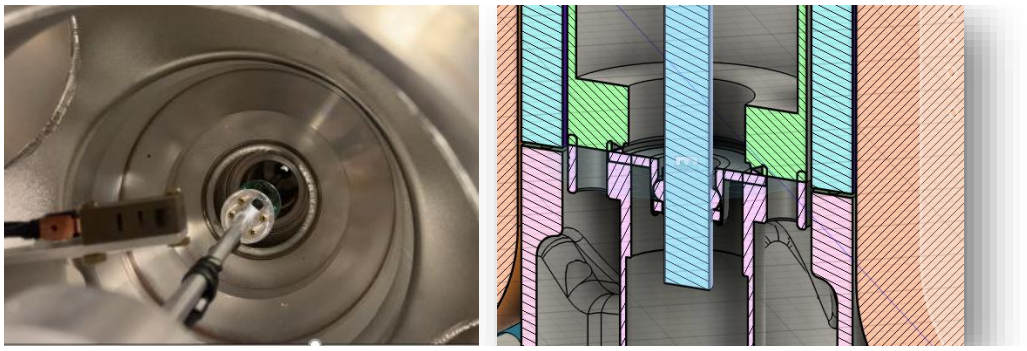

Figure 42: *Dry PEEK bearing for shaft guiding below the trap.*

Appendix C: Chip Response Plots

Bx, By and Bz maps (32× average) with test magnet 102MG11 centred in front of each chip.

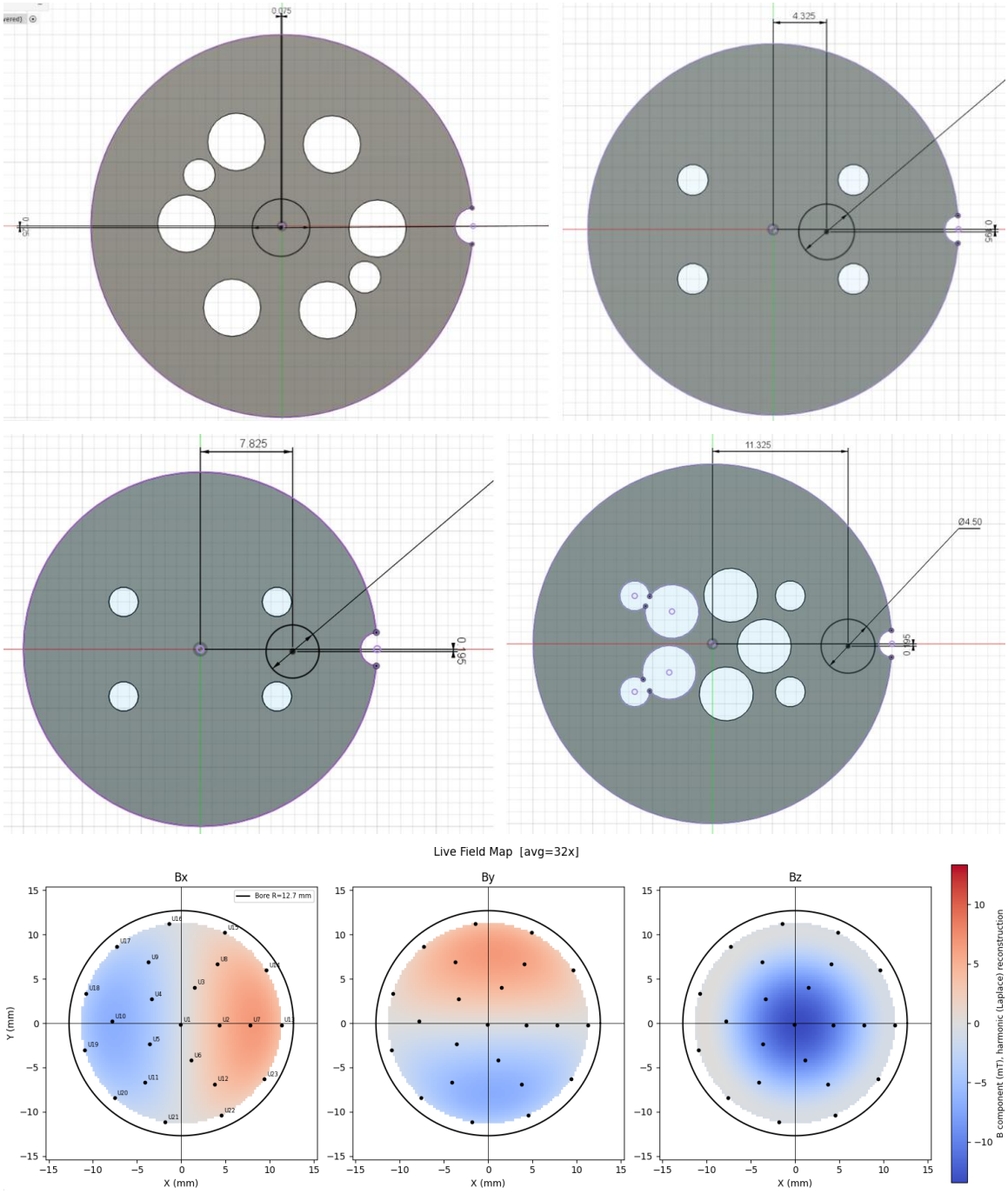

Figure 43: *U1: Bx, By and Bz response.*

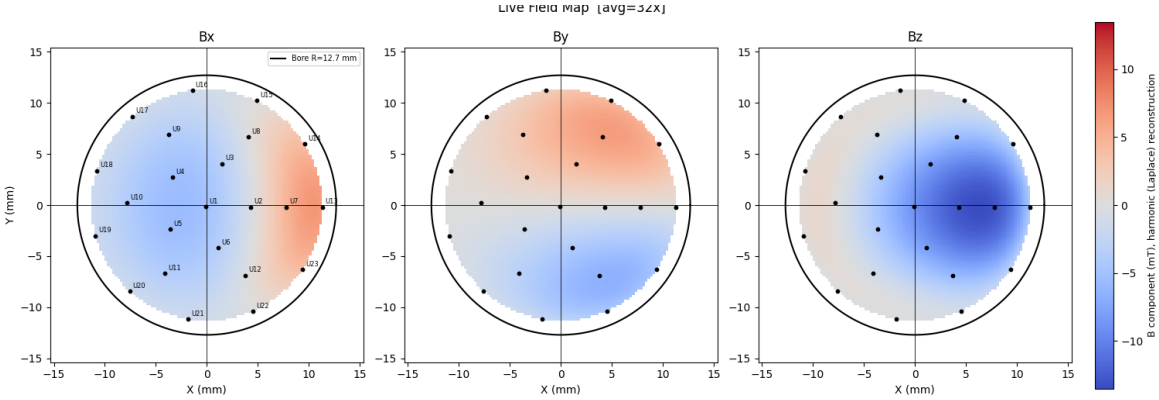

Figure 44: *U2: Bx, By and Bz response.*

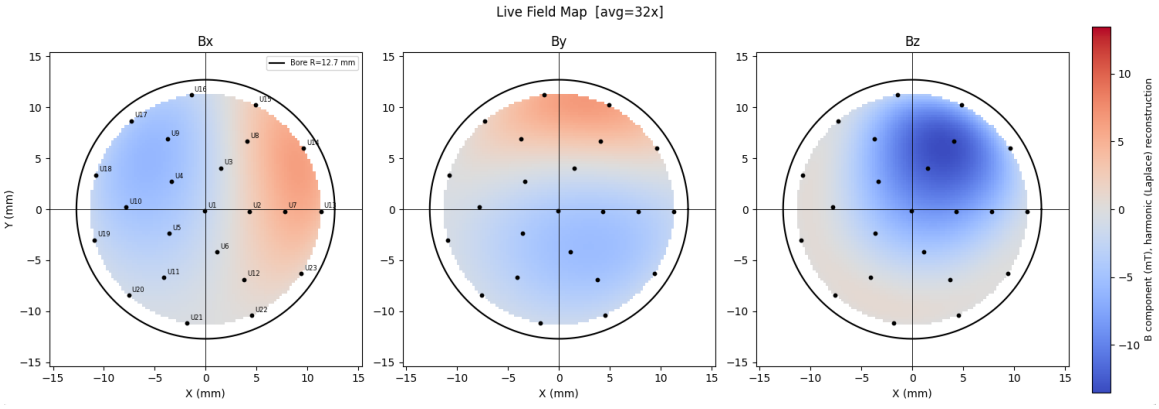

Figure 45: *U3: Bx, By and Bz response.*

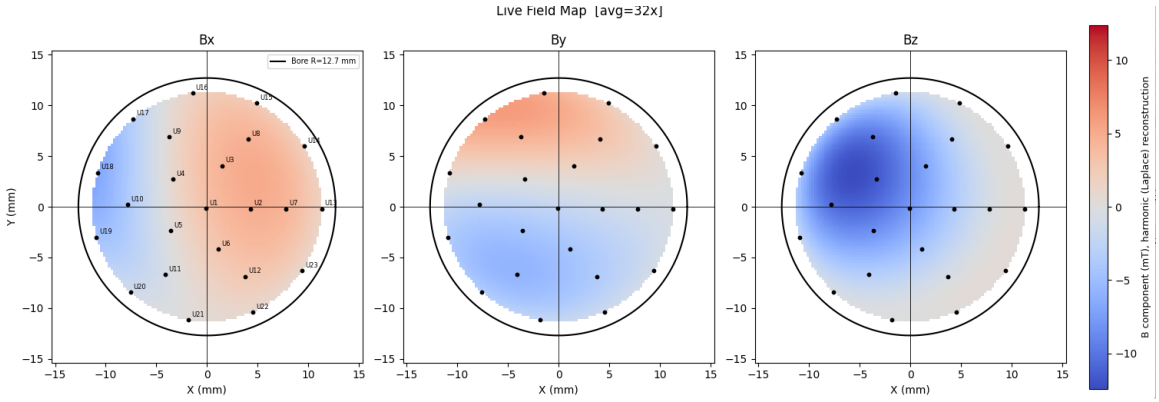

Figure 46: *U4: Bx, By and Bz response.*

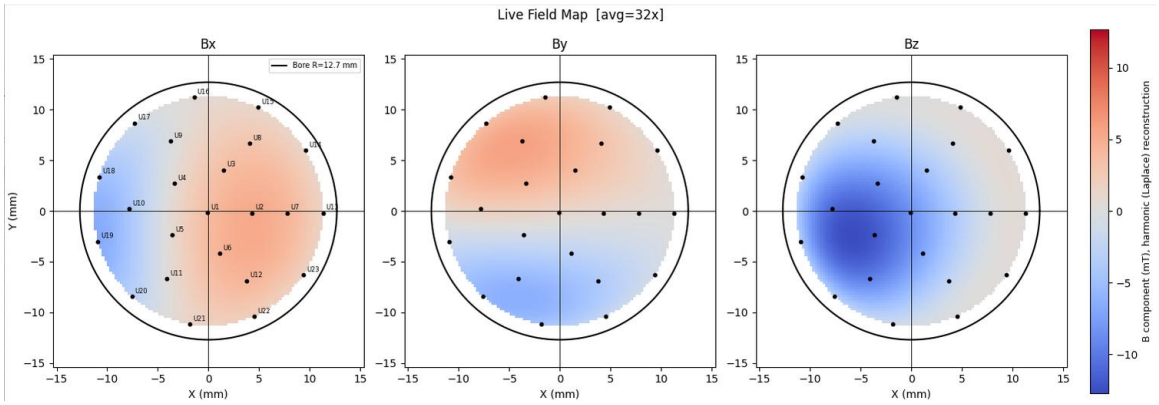

Figure 47: *U5: Bx, By and Bz response.*

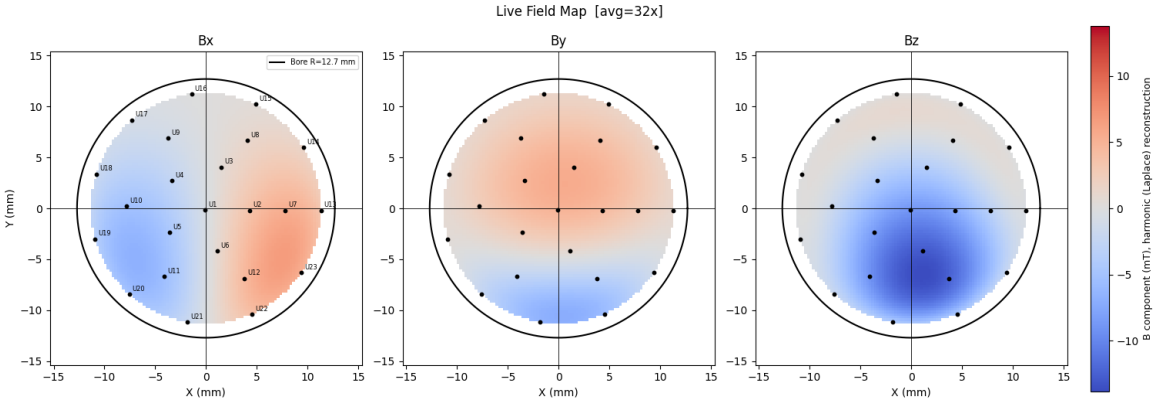

Figure 48: *U6: Bx, By and Bz response.*

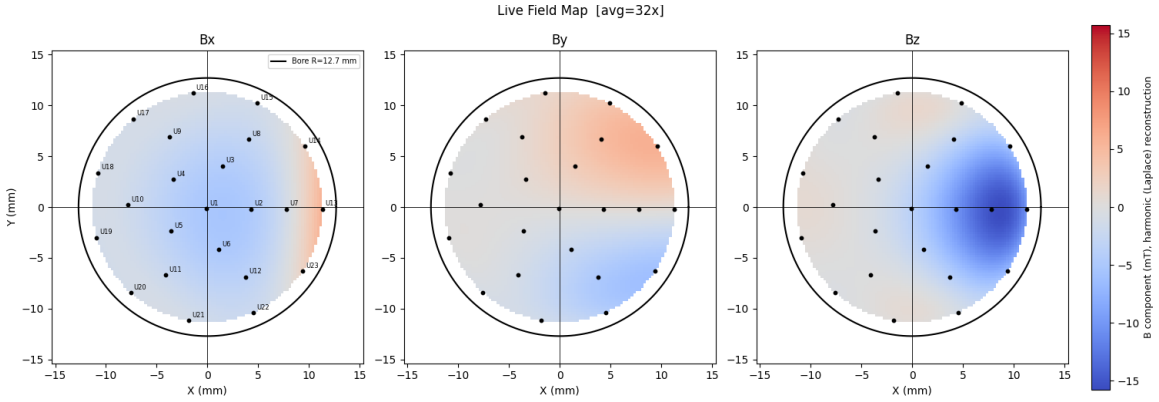

Figure 49: *U7: Bx, By and Bz response.*

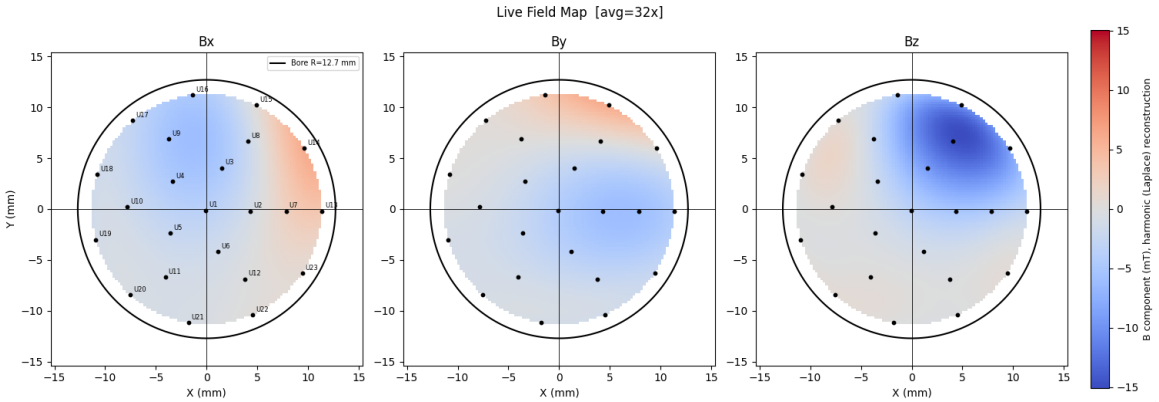

Figure 50: *U8: Bx, By and Bz response.*

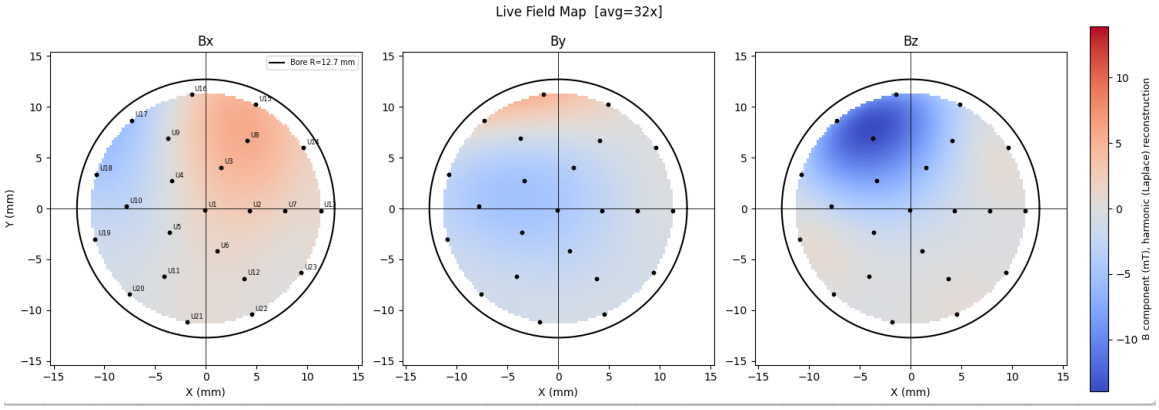

Figure 51: *U9: Bx, By and Bz response.*

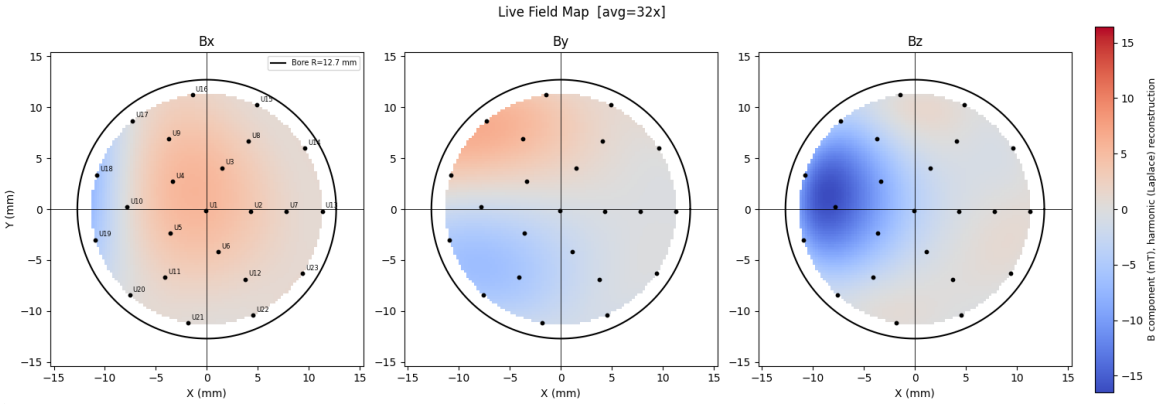

Figure 52: *U10: Bx, By and Bz response.*

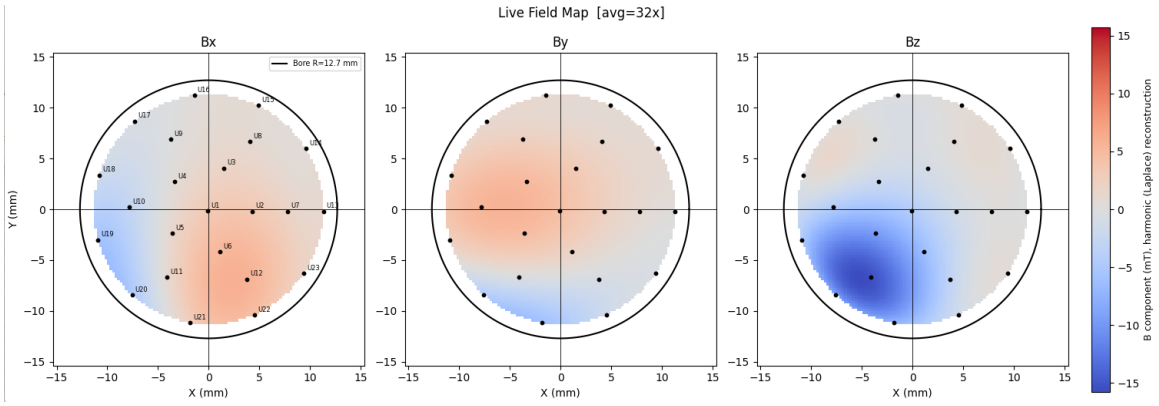

Figure 53: *U11: Bx, By and Bz response.*

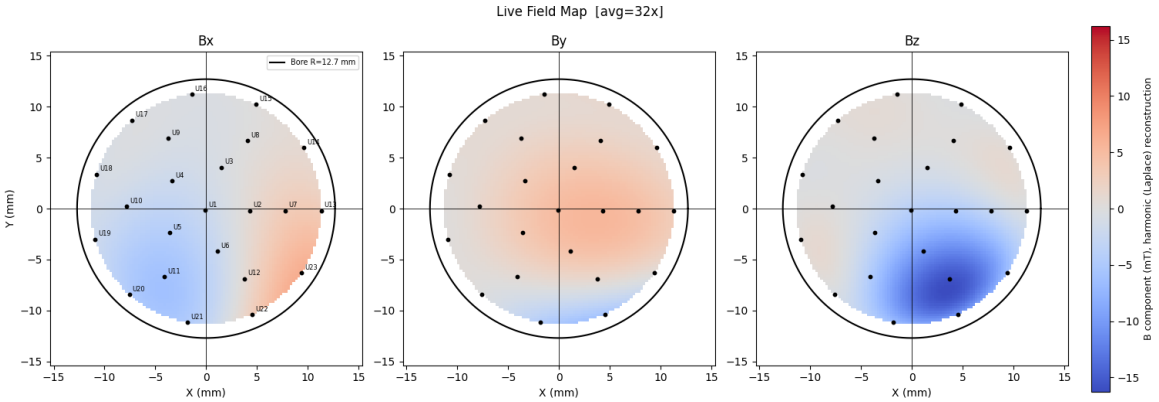

Figure 54: *U12: Bx, By and Bz response.*

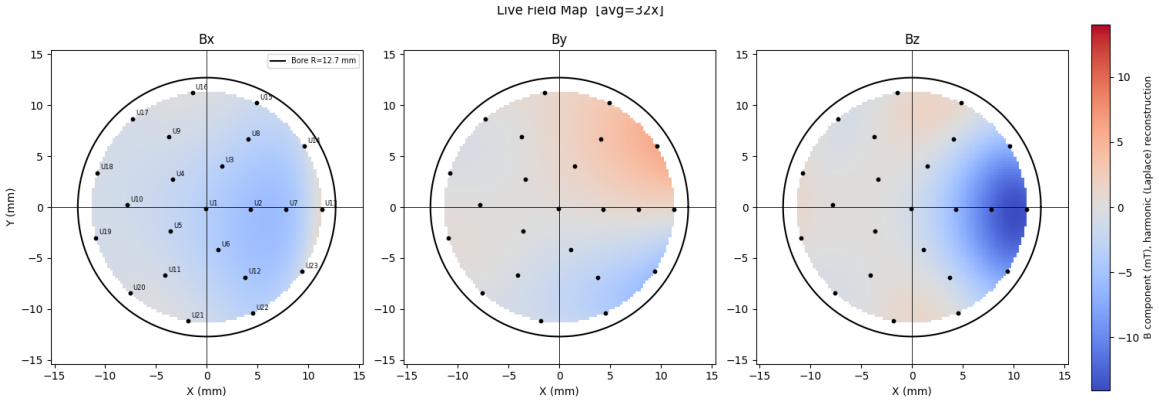

Figure 55: *U13: Bx, By and Bz response.*

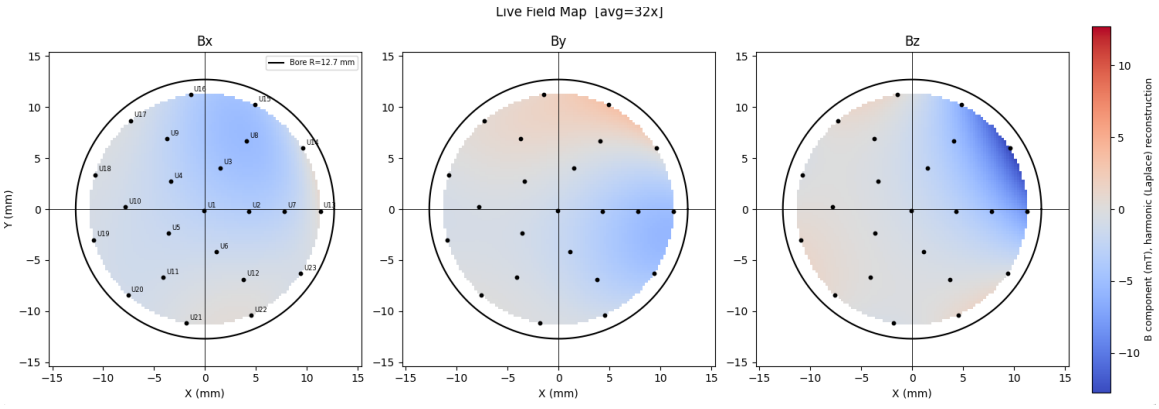

Figure 56: *U14: Bx, By and Bz response.*

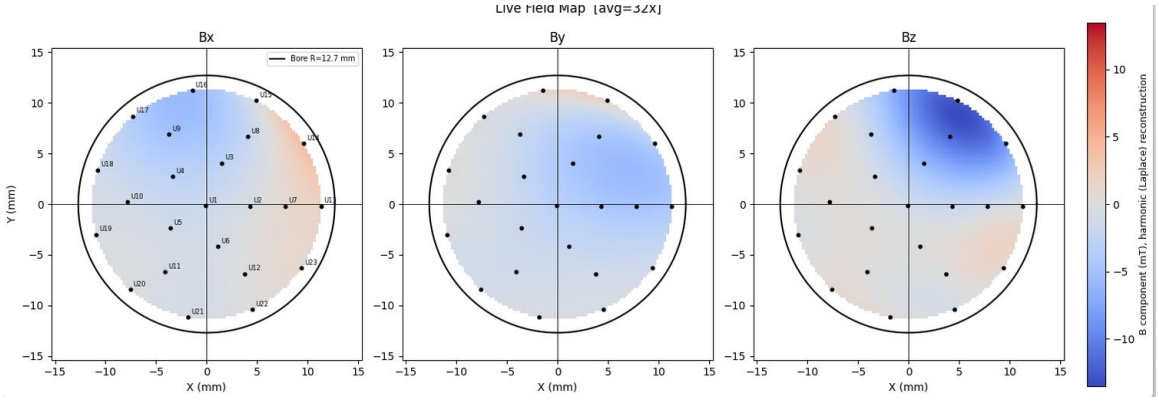

Figure 57: *U15: Bx, By and Bz response.*

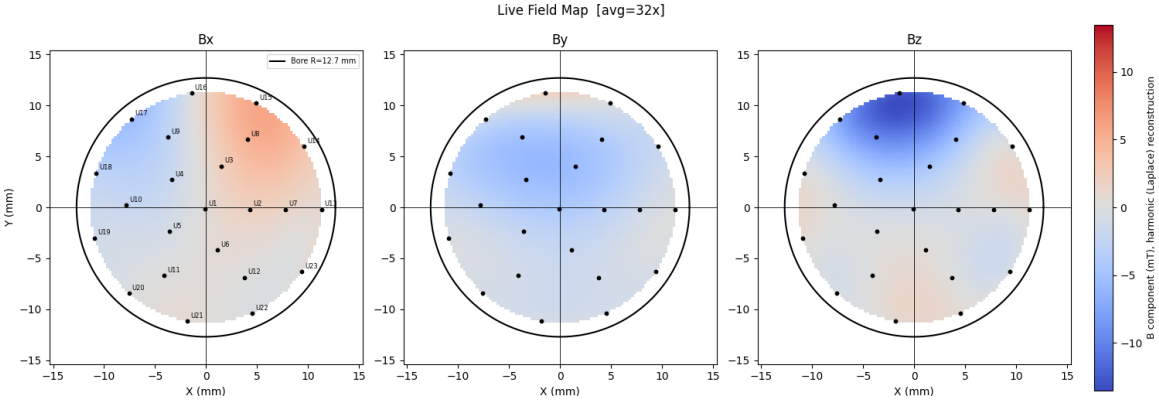

Figure 58: *U16: Bx, By and Bz response.*

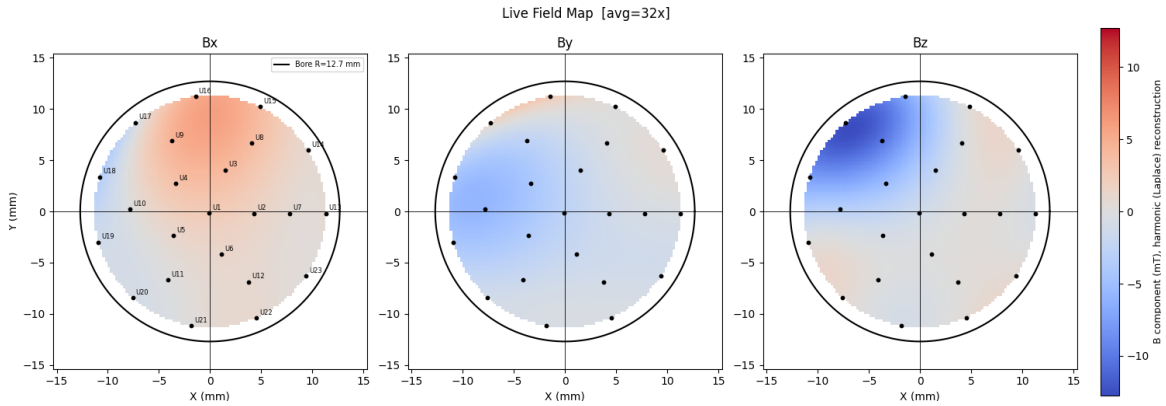

Figure 59: *U17: Bx, By and Bz response.*

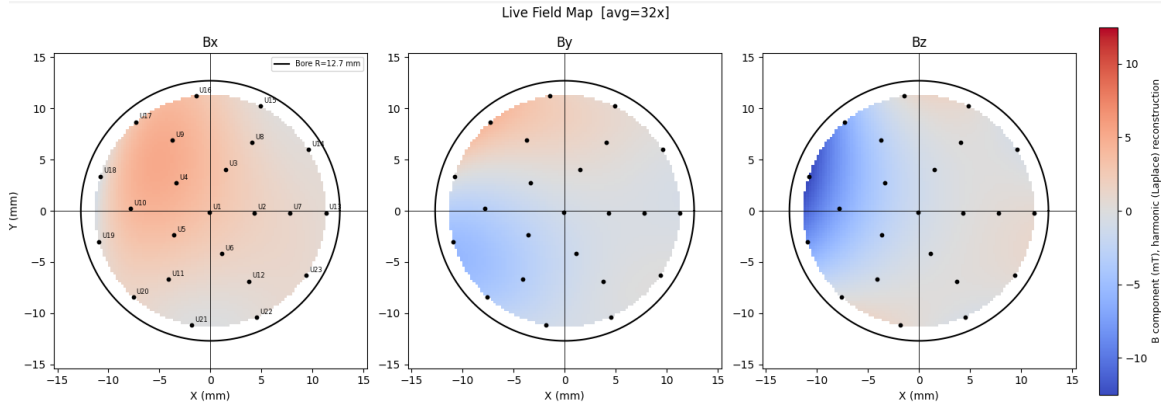

Figure 60: *U18: Bx, By and Bz response.*

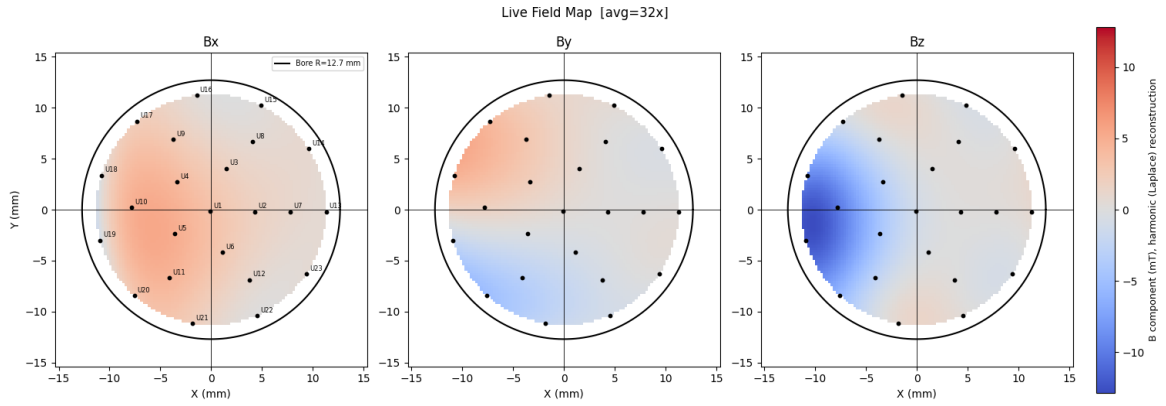

Figure 61: *U19: Bx, By and Bz response.*

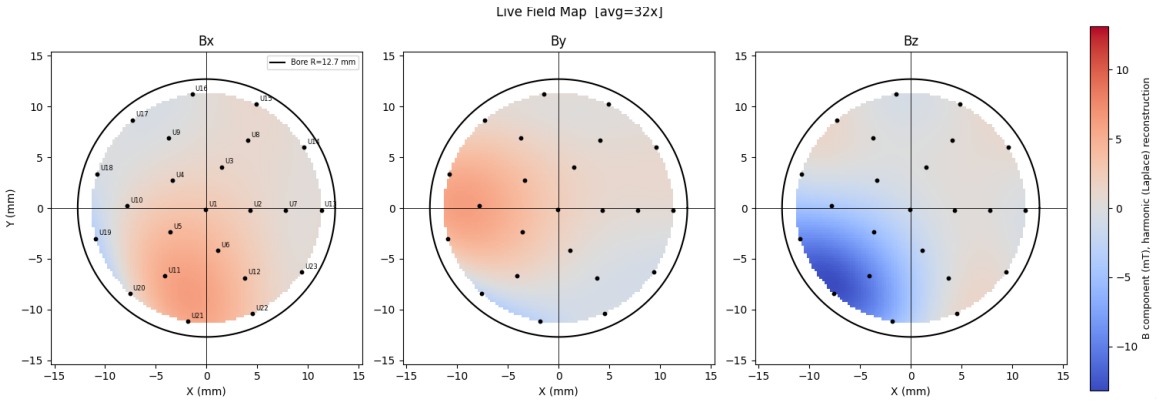

Figure 62: *U20: Bx, By and Bz response.*

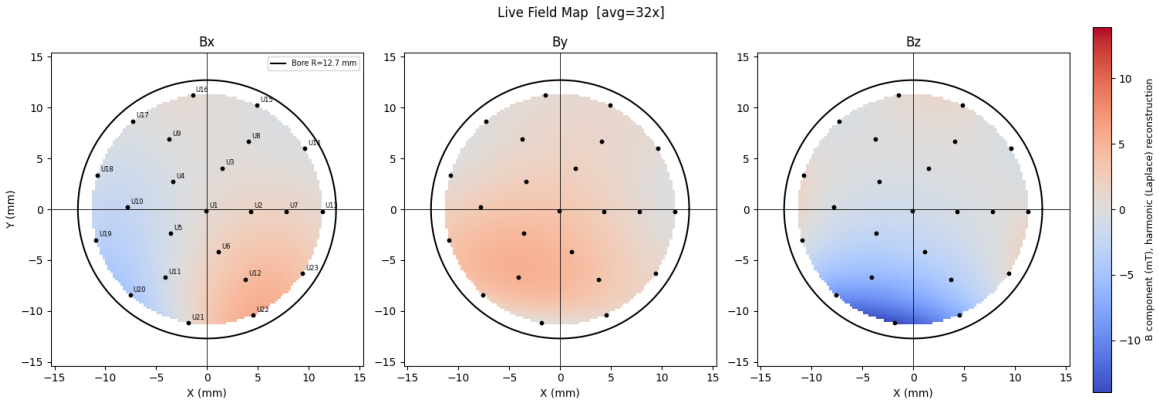

Figure 63: *U21: Bx, By and Bz response.*

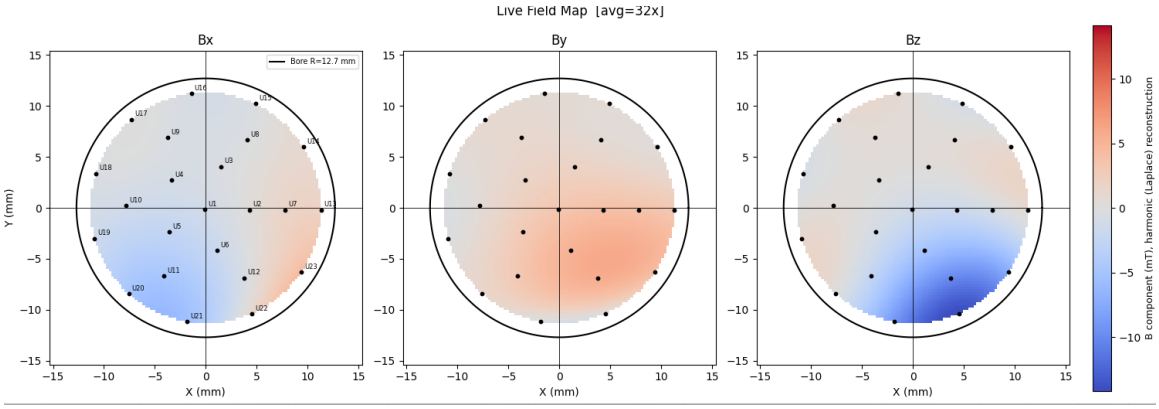

Figure 64: *U22: Bx, By and Bz response.*

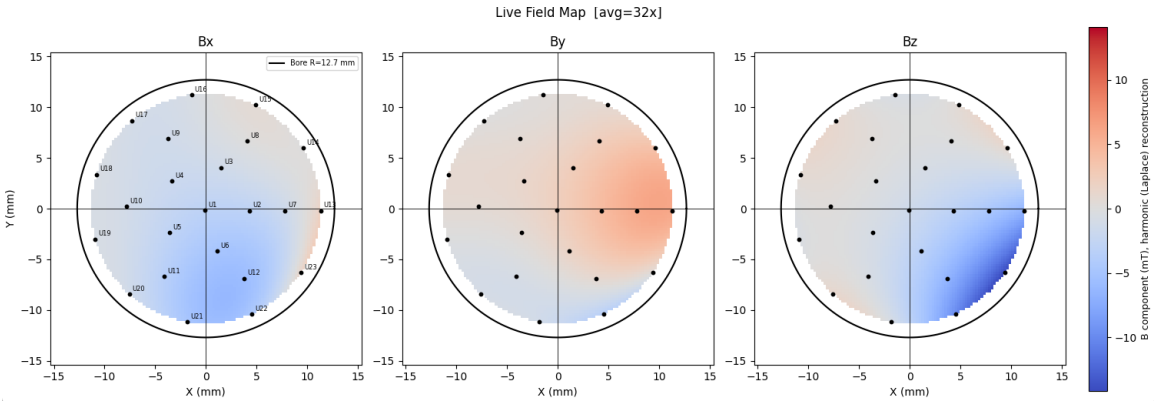

Figure 65: *U23: Bx, By and Bz response.*

Table 5 Chip data for when the magnet is placed 2 mm above the highlighted component.

Ref	X_mT	Y_mT	Z_mT	X_mT	Y_mT	Z_mT	X_mT	Y_mT	Z_mT	X_mT	Y_mT	Z_mT	X_mT	Y_mT	Z_mT	X_mT	Y_mT	Z_mT
U1	2.516	-6.518	-78.433	-42.447	4.116	-30.36	-17.25	37.017	-20.067	29.646	28.452	-20.034	36.781	-18.882	-24.71	-6.957	-40.84	-21.788
U2	4.205	43.227	-29.524	-7.2	0.536	-78.23	-33.916	18.378	-17.136	-4.668	11.657	1.307	2.663	11.811	1.185	24.361	19.052	-8.329
U3	5.942	38.884	-19.077	35.182	21.763	-20.01	12.063	-3.125	-78.222	-31.31	22.169	-15.732	-3.856	12.591	1.023	3.572	10.537	1.956
U4	0.357	38.746	-15.57	4.505	13.313	1.023	21.699	18.216	-6.007	10.358	-2.127	-80.389	-31.156	21.853	-17.136	-3.815	11.316	1.818
U5	-4.781	44.258	-21.642	-3.271	11.876	0.998	2.249	10.65	1.916	22.835	20.237	-7.947	7.858	1.559	-77.832	-30.725	18.906	-11.56
U6	-0.982	47.561	-34.07	-22.689	19.426	-9.847	-4.773	11.397	1.348	2.719	11.267	1.526	22.51	20.383	-9.141	8.215	-3.393	-81.526
U7	0.844	14.539	0.86	-5.423	46.855	-34.427	-9.116	13.954	0.414	-1.031	4.091	2.013	0.666	3.97	1.851	6.746	10.553	1.826
U8	0.487	12.72	1.015	10.829	20.481	-0.909	-3.474	45.605	-44.785	-6.137	10.366	1.9	-0.739	4.31	1.843	0.917	4.319	2.111
U9	-0.114	11.641	1.486	1.9	6.405	2.387	11.657	19.458	-1.794	-19.401	43.194	-30.855	-4.457	7.842	2.062	-0.373	3.377	1.948
U10	-0.276	12.647	2.265	-0.049	4.27	1.973	1.9	5.536	2.427	16.812	27.275	-7.306	-16.828	35.442	-16.56	-2.955	6.445	2.549
U11	-0.747	14.847	1.656	-1.77	5.569	1.518	-0.106	3.799	1.64	2.849	7.054	2.005	17.396	34.938	-16.901	-17.209	25.847	-6.941
U12	-0.714	16.308	1.031	-8.11	13.719	-0.455	-1.77	4.976	1.908	0.276	3.937	1.778	4.083	8.994	1.835	17.145	47.927	-40.751
U13	-0.26	5.13	2.021	-0.958	16.804	1.445	-2.728	5.893	2.167	-0.479	1.77	1.331	0.041	1.77	1.226	1.469	4.595	2.257
U14	0.032	4.765	1.826	2.687	13.483	2.744	-4.091	13.151	1.534	-0.812	2.565	1.721	-0.032	1.599	1.226	0.698	2.411	1.737
U15	-0.041	4.448	1.688	1.835	6.494	2.866	0.219	19.296	0.097	-2.038	4.814	2.249	-0.438	1.786	1.226	0.13	1.697	1.274
U16	-0.008	4.27	1.762	0.812	3.62	2.135	3.645	12.599	2.021	-3.482	10.342	2.46	-0.706	2.516	1.583	-0.024	1.518	1.193
U17	0.057	4.051	1.859	0.325	2.208	1.615	2.054	5.496	2.419	-1.388	18.598	0.934	-1.534	4.416	2.054	-0.235	1.575	1.307
U18	-0.122	4.132	2.135	-0.057	1.867	1.412	0.796	2.922	1.94	2.922	15.066	1.826	-3.401	8.783	2.322	-0.584	2.151	1.672
U19	-0.081	4.546	2.419	-0.235	2.135	1.356	0.26	2.159	1.542	2.395	7.168	2.598	-2.021	17.071	1.128	-1.315	3.961	2.192
U20	-0.203	4.66	2.435	-0.528	2.257	1.274	-0.024	1.713	1.218	1.072	3.791	1.94	2.687	15.911	1.072	-3.036	7.704	2.476
U21	-0.065	4.611	2.443	-0.771	2.874	1.445	-0.057	1.502	1.128	0.552	2.07	1.388	2.63	7.687	2.192	-3.426	15.886	1.421
U22	-0.308	5.138	2.516	-1.835	5.252	1.867	-0.584	2.07	1.437	0	1.762	1.339	1.112	4.172	2.127	1.94	19.369	0.95
U23	-0.162	5.203	2.281	-2.744	10.147	1.867	-1.031	3.109	1.729	-0.097	1.599	1.21	0.544	2.338	1.534	3.434	10.171	2.492
	X_mT	Y_mT	Z_mT	X_mT	Y_mT	Z_mT	X_mT	Y_mT	Z_mT	X_mT	Y_mT	Z_mT	X_mT	Y_mT	Z_mT	X_mT	Y_mT	Z_mT
U1	-14.068	-0.739	0.698	-8.199	11.146	1.063	5.179	11.568	0.99	11.446	0.292	1.429	8.069	-11.543	0.739	-6.04	-11.259	1.169
U2	5.91	-44.063	-39.314	-22.746	-1.583	-2.176	-4.189	4.181	1.94	-0.114	3.353	1.762	3.369	4.741	2.038	17.615	0.576	-0.56

U3	12.599	2.557	1.023	26.837	-38.267	-31.846	-27.008	-5.869	-6.965	-4.4	4.246	1.964	-0.446	4.059	1.753	2.598	3.718	1.932
U4	1.607	4.213	1.851	8.174	4.895	2.013	29.962	-21.114	-18.175	-29.289	-12.152	-9.189	-7.671	5.171	1.981	-0.95	3.791	1.794
U5	-1.77	4.108	1.835	0.641	4.124	1.826	5.723	4.708	1.924	29.427	-14.458	-11.803	-31.967	-29.354	-29.483	-9.1	3.953	1.94
U6	-14.725	2.792	0.511	-3.166	4.319	1.859	0.219	3.767	1.656	4.481	4.319	2.038	25.384	-2.711	-5.252	-17.299	-41.579	-32.032
U7	5.958	-2.492	-76.972	-14.799	7.687	0.536	-1.348	2.078	1.518	-0.016	1.193	1.128	1.136	2.029	1.55	11.3	5.82	1.38
U8	9.676	6.437	1.404	12.826	-0.544	-78.189	-14.19	7.265	0.235	-1.201	2.07	1.559	-0.13	1.713	1.242	1.088	2.265	1.567
U9	1.307	2.143	1.567	9.254	6.746	1.932	9.027	-2.029	-74.739	-10.277	4.944	1.705	-1.283	2.159	1.656	-0.008	1.388	1.234
U10	0.032	1.745	1.323	1.007	2.289	1.68	8.824	5.885	1.567	2.427	-4.854	-78.758	-12.883	7.59	1.023	-1.258	2.24	1.721
U11	-1.461	2.468	1.429	-0.203	1.867	0.982	0.901	2.249	1.21	10.772	6.632	1.112	7.42	0.836	-78.279	-11.982	6.405	1.274
U12	-12.582	6.673	0.714	-1.624	2.5	1.51	-0.065	1.632	1.055	1.12	2.305	1.534	10.813	7.671	1.274	3.515	-4.676	-80.966
U13	4.603	46.384	-44.014	-6.048	6.031	2.208	-0.609	1.242	1.055	-0.106	0.706	0.731	0.317	1.161	1.031	4.172	5.106	2.257
U14	12.867	15.586	-1.161	-21.901	29.67	-12.688	-1.713	2.322	1.697	-0.089	0.763	0.86	0.203	0.942	0.836	1.242	1.948	1.486
U15	2.882	3.872	1.916	18.752	45.256	-30.969	-7.29	7.2	1.826	-0.641	1.136	1.007	-0.179	0.917	0.714	0.244	1.063	0.877
U16	0.844	1.664	1.307	8.913	10.464	1.688	-21.228	33.55	-19.823	-1.745	2.24	1.64	-0.373	1.015	0.869	0	0.893	0.771
U17	0.333	0.974	0.942	2.029	2.809	1.997	20.692	35.182	-23.72	-7.33	7.176	1.9	-0.771	1.461	1.25	-0.114	0.796	0.796
U18	0.138	0.885	0.877	0.601	1.494	1.283	7.192	8.304	1.607	-24.41	33.656	-23.403	-2.598	3.004	2.021	-0.308	0.917	0.966
U19	-0.138	1.177	0.917	0.122	1.242	0.99	1.64	2.768	1.786	23.817	37.487	-25.904	-9.993	11.462	1.258	-0.893	1.737	1.404
U20	-0.463	1.299	0.99	-0.089	1.039	0.747	0.479	1.445	1.063	7.468	8.174	1.81	-14.035	43.754	-30.92	-2.874	3.418	2.029
U21	-0.958	1.721	1.315	-0.122	0.796	0.698	0.244	0.722	0.698	1.745	2.289	1.648	18.76	26.853	-9.279	-12.315	12.607	0.446
U22	-4.01	4.53	2.192	-0.609	1.348	1.072	-0.073	0.877	0.779	0.406	1.331	1.201	4.879	6.186	2.378	-9.538	49.153	-49.355
U23	-16.073	18.192	-2.922	-1.64	2.159	1.583	-0.114	0.877	0.771	0.138	0.763	0.82	1.307	2.192	1.583	19.905	24.174	-6.592
	X_mT	**Y_mT**	**Z_mT**	**X_mT**	**Y_mT**	**Z_mT**	**X_mT**	**Y_mT**	**Z_mT**	**X_mT**	**Y_mT**	**Z_mT**	**X_mT**	**Y_mT**	**Z_mT**	**X_mT**	**Y_mT**	**Z_mT**
U1	-5.041	-0.187	1.778	-4.286	2.224	1.94	-2.378	4.148	1.883	0.219	5.025	1.883	3.077	3.978	1.973	4.237	1.323	2.078
U2	1.169	-17.404	-0.576	-9.36	-9.197	1.388	-7.103	-1.128	2.086	-3.572	1.307	1.778	-1.453	1.68	1.453	-0.43	1.534	1.299
U3	5.13	0.097	1.924	8.751	-5.577	2.021	4.522	-16.739	-0.073	-9.741	-12.241	0.17	-8.142	-0.869	1.948	-3.247	1.445	1.908
U4	0.739	1.973	1.201	1.794	1.932	1.583	4.132	1.38	2.046	8.686	-2.76	1.973	7.103	-16.958	-0.471	-8.767	-12.542	1.201
U5	-0.877	1.826	1.185	-0.244	1.729	1.218	0.503	1.843	1.242	1.429	2.005	1.534	4.148	1.494	2.135	8.191	-2.452	2.314
U6	-5.853	0.235	1.762	-2.792	1.486	1.615	-1.242	1.697	1.258	-0.365	1.729	1.169	0.487	1.77	1.234	1.38	1.672	1.437
U7	3.856	-47.204	-45.037	-24.515	-7.631	-3.239	-6.372	1.477	2.111	-1.721	1.177	1.437	-0.601	0.779	0.909	-0.203	0.463	0.812

U8	5.796	1.721	2.062	23.395	-7.842	-3.255	-0.544	-48.211	-47.083	-22.194	-4.871	-2.37	-4.595	1.867	2.094	-1.153	1.201	1.437
U9	0.877	0.998	1.055	2.086	1.486	1.721	7.33	1.721	2.378	30.271	-13.873	-11.211	-26.042	-39.062	-36.578	-12.201	-0.787	2.297
U10	-0.016	0.95	0.836	0.227	0.982	0.974	0.804	1.21	1.177	2.167	1.762	1.818	10.659	1.055	2.111	32.471	-31.651	-23.695
U11	-0.942	1.291	0.82	-0.398	1.072	0.698	-0.122	1.039	0.544	0.146	1.12	0.706	0.893	1.412	1.177	3.133	1.891	1.762
U12	-7.03	1.477	1.737	-2.046	1.526	1.412	-0.836	1.234	0.901	-0.349	1.023	0.755	0.065	1.063	0.714	0.422	1.08	0.893
U13	8.069	-1.461	-81.169	-27.162	6.096	-4.083	-3.978	2.151	1.924	-0.982	0.934	1.047	-0.325	0.576	0.658	-0.154	0.414	0.52
U14	18.143	6.746	-0.658	10.813	-2.703	-82.021	-30.23	6.421	-6.786	-3.823	2.208	2.021	-0.674	0.934	1.08	-0.106	0.43	0.698
U15	2.492	1.973	1.688	16.422	6.283	0.487	14.661	0.268	-81.721	-29.394	7.59	-7.087	-3.361	2.111	1.908	-0.714	0.796	0.998
U16	0.568	0.958	0.877	2.452	1.908	1.867	16.243	6.251	0.593	11.6	1.072	-79.147	-22.462	7.484	-1.518	-2.825	1.851	2.046
U17	0.252	0.584	0.584	0.633	0.852	1.031	2.362	1.835	1.826	15.156	6.291	0.682	6.624	3.271	-81.761	-22.226	6.194	-0.893
U18	0.073	0.536	0.56	0.211	0.584	0.796	0.658	0.852	1.055	2.273	2.029	1.908	20.7	8.248	-1.721	1.762	0.049	-83.06
U19	-0.187	0.844	0.633	-0.032	0.812	0.674	0.146	0.836	0.755	0.422	1.201	1.096	2.695	2.37	2.078	20.976	6.786	-1.778
U20	-0.373	0.804	0.593	-0.17	0.682	0.568	-0.041	0.617	0.365	0.049	0.779	0.593	0.641	1.128	1.047	3.028	2.249	1.851
U21	-0.682	0.917	0.836	-0.235	0.511	0.584	-0.073	0.349	0.333	0.073	0.365	0.446	0.325	0.52	0.625	0.698	0.869	0.958
U22	-3.353	2.346	1.745	-0.917	1.031	1.096	-0.398	0.771	0.698	-0.203	0.528	0.625	0.041	0.609	0.544	0.13	0.674	0.69
U23	-24.134	6.835	-3.109	-3.499	2.135	1.908	-0.877	0.934	1.015	-0.292	0.576	0.698	-0.032	0.528	0.544	0.032	0.438	0.56
	X_mT	**Y_mT**	**Z_mT**	**X_mT**	**Y_mT**	**Z_mT**	**X_mT**	**Y_mT**	**Z_mT**	**X_mT**	**Y_mT**	**Z_mT**	**X_mT**	**Y_mT**	**Z_mT**			
U1	4.846	-0.917	1.875	3.661	-3.515	1.867	1.283	-4.822	1.867	-1.948	-4.189	2.224	-4.14	-2.963	2.265			
U2	0.154	1.688	1.226	1.015	1.737	1.396	2.646	1.68	1.664	5.983	-0.349	2.403	10.309	-7.996	1.794			
U3	-1.591	1.794	1.412	-0.52	1.672	1.201	0.276	1.518	1.177	0.99	1.323	1.461	2.281	1.364	1.932			
U4	-9.709	-2.663	1.932	-4.757	1.567	1.997	-1.908	1.973	1.494	-0.568	1.778	1.437	-0.008	1.81	1.372			
U5	10.245	-13.711	-0.341	-5.699	-18.127	-1.429	-9.895	-4.733	1.526	-4.7	0.95	2.281	-2.314	1.672	1.835			
U6	3.304	1.713	1.737	7.241	-0.463	1.981	10.504	-10.017	0.536	-2.752	-18.013	-0.073	-10.334	-7.184	1.753			
U7	0.073	0.617	0.747	0.341	0.722	0.934	1.356	1.063	1.307	4.992	1.145	2.33	21.203	-5.666	-1.818			
U8	-0.544	1.088	0.966	-0.179	0.917	0.828	0.049	0.804	0.86	0.511	0.909	1.153	1.494	1.396	1.729			
U9	-3.637	1.445	1.932	-1.031	1.08	1.291	-0.308	0.747	0.958	0.146	0.56	0.942	0.308	0.658	1.007			
U10	-30.246	-34.914	-35.085	-13.581	0.633	1.372	-3.117	1.81	1.908	-0.804	1.12	1.421	-0.349	0.901	1.063			
U11	12.112	0.99	1.21	33.266	-32.787	-33.948	-32.519	-25.425	-22.218	-9.238	1.161	2.281	-2.76	1.55	1.77			
U12	1.096	1.494	1.21	3.718	2.143	1.989	16.17	-0.804	0.146	17.421	-44.55	-45.922	-29.768	-14.076	-9.806			

U13	-0.032	0.479	0.511	0.081	0.56	0.601	0.568	0.844	0.934	2.801	1.908	1.948	18.289	6.932	-0.52			
U14	0.008	0.463	0.584	0.114	0.3	0.576	0.276	0.446	0.649	0.714	0.804	1.096	2.622	1.891	2.078			
U15	-0.317	0.658	0.617	-0.195	0.463	0.487	-0.081	0.292	0.349	0.146	0.43	0.641	0.528	0.828	1.039			
U16	-0.893	1.088	1.055	-0.333	0.625	0.633	-0.154	0.398	0.487	0	0.414	0.576	0.154	0.56	0.714			
U17	-3.718	2.297	1.932	-0.852	1.072	1.055	-0.235	0.601	0.682	-0.008	0.398	0.576	0.073	0.455	0.617			
U18	-26.447	7.403	-4.595	-3.694	2.297	2.046	-0.804	0.974	1.112	-0.195	0.552	0.804	-0.097	0.446	0.706			
U19	11.795	3.466	-79.261	-27.925	9.384	-5.528	-3.718	2.695	2.094	-0.787	1.161	1.299	-0.308	0.869	0.909			
U20	17.396	7.144	-0.69	9.222	3.775	-79.91	-26.447	8.118	-5.009	-3.239	2.102	2.119	-0.917	1.047	1.185			
U21	2.508	1.883	1.713	17.193	6.892	-0.325	11.681	2.232	-79.967	-23.241	6.786	-2.622	-3.556	1.932	1.981			
U22	0.584	1.031	1.063	2.346	2.184	1.932	16.982	7.014	-0.187	2.955	0.268	-80.552	-25.749	7.168	-4.505			
U23	0.317	0.584	0.641	0.593	0.901	0.998	2.581	2.046	1.835	20.7	6.973	-1.818	7.282	0.909	-80.146			

Table 6 Chip data for when the magnet is placed 5 mm above the highlighted component.

Ref	X_mT	Y_mT	Z_mT	X_mT	Y_mT	Z_mT	X_mT	Y_mT	Z_mT	X_mT	Y_mT	Z_mT	X_mT	Y_mT	Z_mT	X_mT	Y_mT	Z_mT
U1	-0.276	0.032	-15.294	-6.356	-0.162	-9.969	-2.792	5.975	-9.157	5.731	3.231	-8.954	6.234	-2.2	-9.693	-0.438	-6.665	-9.611
U2	0.024	5.91	-10.366	0.211	-0.26	-15.724	-5.788	2.939	-8.865	-1.372	4.927	-2.719	0.804	5.187	-2.866	5.163	4.302	-6.868
U3	1.356	6.218	-9.571	5.95	3.669	-8.11	2.029	-0.698	-15.399	-4.643	4.246	-6.811	-1.851	5.187	-3.547	1.518	4.936	-2.703
U4	0.649	6.876	-8.621	1.705	5.544	-3.004	5.358	4.416	-6.648	-0.698	-0.016	-15.139	-5.163	3.458	-9.652	-1.997	5.341	-3.117
U5	-0.455	6.77	-8.645	-1.664	5.268	-3.044	1.145	5.179	-2.557	5.536	3.588	-8.727	2.143	0.722	-15.083	-5.666	3.312	-8.718
U6	-0.503	6.299	-9.701	-5.382	3.896	-8.101	-2.119	4.984	-2.995	1.826	5.065	-3.044	4.708	4.733	-6.494	1.826	-0.292	-15.716
U7	0.138	5.463	-3.823	0.146	5.926	-11.129	-3.418	4.846	-4.181	-0.544	2.679	-0.536	0.357	2.801	-0.528	2.744	4.367	-2.752
U8	0.325	5.634	-3.369	3.393	5.455	-4.522	-0.268	5.91	-11.332	-2.33	4.189	-1.932	-0.796	3.328	-0.568	0.641	3.247	-0.552
U9	0.211	5.471	-2.906	1.283	3.629	-1.007	3.556	5.423	-5.212	-3.296	5.382	-8.337	-2.492	4.067	-2.484	-0.39	2.792	-0.487
U10	0.016	5.617	-2.573	-0.081	3.093	-0.341	1.396	3.604	-0.828	3.288	5.788	-8.8	-2.046	6.023	-9.246	-1.9	3.945	-1.624
U11	-0.308	5.723	-3.288	-1.388	3.807	-1.258	-0.041	3.036	-0.495	2.273	4.505	-2.419	3.499	6.056	-7.728	-3.523	5.869	-7.963
U12	-0.373	5.926	-3.718	-3.409	5.35	-4.789	-1.25	3.547	-0.934	0.446	3.198	-0.625	1.891	4.53	-1.851	2.679	6.421	-10.772
U13	-0.114	3.612	-0.998	-0.081	6.291	-4.31	-1.867	3.823	-1.218	-0.357	1.64	0.081	0	1.753	0.146	1.007	3.19	-0.658
U14	0.146	3.572	-0.877	1.526	5.504	-2.955	-1.656	5.479	-3.304	-0.487	2.038	-0.008	-0.065	1.599	0.195	0.649	2.192	-0.057

U15	0.106	3.45	-0.787	1.331	3.929	-1.12	0.097	6.429	-4.668	-1.169	2.882	-0.511	-0.438	1.867	0.016	0.114	1.737	0.016
U16	0.122	3.466	-0.617	0.739	2.752	-0.235	1.607	5.414	-3.036	-1.794	4.294	-1.745	-0.852	2.435	-0.17	-0.138	1.672	0.041
U17	0.106	3.288	-0.471	0.398	2.062	0.057	1.494	3.702	-0.917	-1.104	5.877	-3.872	-1.266	3.418	-0.909	-0.276	1.778	0.049
U18	-0.016	3.271	-0.438	0.008	1.818	0.195	0.82	2.549	-0.106	0.674	6.178	-4.286	-1.599	4.927	-2.476	-0.649	2.159	-0.049
U19	-0.122	3.669	-0.317	-0.235	2.062	0.26	0.284	2.2	0.252	1.656	5.074	-2.119	-0.284	6.462	-3.896	-1.226	3.499	-0.495
U20	-0.244	3.596	-0.52	-0.479	2.151	-0.016	0.041	1.883	0.179	1.169	3.442	-0.763	1.323	5.788	-3.296	-1.851	4.765	-2.021
U21	-0.057	3.198	-0.739	-0.779	2.435	-0.455	-0.073	1.607	0.073	0.714	2.119	-0.219	1.567	3.921	-1.461	-0.836	6.096	-4.302
U22	-0.284	3.482	-0.804	-1.486	3.832	-1.185	-0.576	2.013	0.081	0.154	1.835	0.162	0.771	2.825	-0.227	0.998	6.51	-4.221
U23	-0.106	3.556	-0.925	-1.526	5.325	-2.947	-0.917	2.468	-0.244	0.008	1.542	0.162	0.414	2.029	0.073	1.713	4.781	-2.086
Ref	X_mT	Y_mT	Z_mT	X_mT	Y_mT	Z_mT	X_mT	Y_mT	Z_mT	X_mT	Y_mT	Z_mT	X_mT	Y_mT	Z_mT	X_mT	Y_mT	Z_mT
U1	-5.504	-0.382	-3.523	-3.312	4.392	-3.255	2.305	4.984	-2.939	5.65	1.031	-3.645	3.564	-4.465	-3.84	-2.119	-5.179	-3.612
U2	0.852	-5.983	-10.78	-6.299	-0.706	-5.341	-2.728	2.541	-1.031	-0.43	3.004	-0.593	2.046	3.052	-1.153	5.877	0.828	-4.327
U3	5.358	1.072	-3.288	4.108	-5.276	-9.636	-6.234	-1.445	-6.283	-3.539	2.825	-1.981	-0.373	3.166	-0.674	1.713	2.93	-0.747
U4	1.153	3.174	-0.544	4.083	2.476	-1.981	5.536	-4.083	-8.67	-5.374	-3.361	-9.644	-4.148	2.801	-2.297	-0.998	3.215	-0.544
U5	-1.404	2.995	-0.609	0.487	2.995	-0.422	3.491	2.679	-1.51	6.64	-1.25	-7.558	-4.091	-4.246	-10.569	-5.114	1.883	-3.004
U6	-5.593	1.031	-3.783	-2.167	2.801	-0.942	0.179	2.849	-0.463	2.63	3.166	-1.315	6.51	-0.17	-6.316	-1.104	-5.95	-11.162
U7	0.844	-0.52	-14.928	-5.423	2.419	-4.189	-1.234	1.624	-0.146	-0.162	1.469	0.106	0.998	1.802	-0.13	4.416	2.492	-2.695
U8	4.319	2.841	-2.736	2.305	-0.187	-14.441	-5.13	2.468	-3.491	-1.55	2.249	-0.195	-0.13	1.826	0.162	0.86	2.029	0.065
U9	1.104	1.908	0.032	4.181	2.744	-2.387	0.901	-0.966	-15.375	-5.414	2.581	-4.367	-1.185	1.924	-0.081	-0.016	1.55	0.26
U10	-0.097	1.721	0.317	0.925	1.981	0.179	4.635	2.703	-2.565	2.76	0.471	-15.196	-5.049	2.963	-3.945	-1.404	2.184	-0.057
U11	-1.299	2.184	-0.276	-0.154	1.826	0.049	0.844	2.127	-0.187	3.994	3.231	-2.663	1.632	0.682	-15.099	-5.358	2.744	-4.497
U12	-4.936	2.671	-3.75	-1.445	2.159	-0.292	-0.17	1.762	0.065	0.877	2.24	-0.106	4.473	3.296	-3.101	1.818	0.235	-15.545
U13	0.706	5.82	-10.975	-3.482	3.369	-2.013	-0.731	1.153	0.162	-0.179	0.99	0.252	0.39	1.274	0.235	2.257	2.963	-0.901
U14	4.221	4.651	-4.708	-3.767	5.114	-8.548	-1.437	1.81	-0.179	-0.219	1.136	0.276	0.179	1.096	0.308	1.055	1.697	0.146
U15	2.046	2.663	-0.771	2.792	5.764	-10.098	-3.645	3.336	-2.346	-0.909	1.542	0.057	-0.187	1.096	0.227	0.292	1.21	0.219
U16	0.787	1.705	0.122	3.734	4.059	-3.068	-3.953	5.285	-8.978	-2.029	2.533	-0.503	-0.487	1.234	0.227	-0.032	1.072	0.244
U17	0.406	1.153	0.308	1.64	2.232	-0.227	3.694	5.764	-10.253	-3.921	4.586	-3.677	-0.836	1.599	0.106	-0.138	0.958	0.284

U18	0.041	1.015	0.365	0.658	1.469	0.308	3.856	3.97	-2.776	-1.851	6.364	-10.285	-2.021	2.411	-0.495	-0.471	1.185	0.325
U19	-0.227	1.291	0.422	0.179	1.339	0.39	1.55	2.452	-0.097	4.075	6.064	-7.038	-3.848	4.781	-3.775	-1.096	1.989	0.195
U20	-0.56	1.396	0.268	-0.081	1.161	0.3	0.56	1.567	0.195	2.857	3.767	-1.615	-1.356	6.259	-9.977	-2.557	2.987	-0.909
U21	-0.974	1.632	-0.057	-0.114	0.901	0.162	0.26	0.974	0.162	1.258	1.867	-0.122	4.156	5.341	-6.843	-4.067	4.806	-5.731
U22	-2.63	2.898	-1.112	-0.666	1.437	0.235	-0.114	0.998	0.3	0.406	1.388	0.268	2.59	3.377	-1.396	0.219	6.137	-11.235
U23	-4.124	4.716	-5.869	-1.404	1.924	-0.146	-0.244	0.982	0.235	0.162	1.096	0.276	1.226	1.956	-0.032	4.465	5.025	-5.479
Ref	X_mT	Y_mT	Z_mT	X_mT	Y_mT	Z_mT	X_mT	Y_mT	Z_mT	X_mT	Y_mT	Z_mT	X_mT	Y_mT	Z_mT	X_mT	Y_mT	Z_mT
U1	-3.848	-0.308	-1.177	-3.02	1.591	-0.828	-1.632	3.32	-1.096	0.56	4.075	-1.185	2.33	2.801	-1.055	3.198	0.982	-0.812
U2	0.877	-6.389	-5.398	-3.791	-3.986	-3.312	-4.53	-0.406	-1.729	-2.922	1.412	-0.584	-1.323	1.705	-0.097	-0.471	1.656	0.081
U3	3.856	0.268	-1.201	4.384	-2.695	-2.5	1.461	-6.08	-5.26	-4.205	-4.343	-4.643	-4.489	-0.365	-1.908	-2.581	1.169	-0.455
U4	0.779	2.111	-0.008	1.591	1.729	-0.089	3.491	1.047	-0.958	5.098	-1.989	-3.166	2.086	-5.561	-5.179	-3.206	-4.343	-3.864
U5	-0.974	1.924	0.089	-0.17	1.77	0.122	0.593	1.964	0.146	1.721	1.981	-0.162	3.328	1.12	-0.796	4.392	-1.283	-2.094
U6	-4.278	0.114	-1.542	-2.322	1.218	-0.382	-1.12	1.77	-0.081	-0.235	1.948	0	0.584	1.883	-0.016	1.38	1.607	-0.089
U7	1.388	-5.812	-12.493	-6.137	-2.387	-6.031	-4.067	1.039	-1.372	-1.607	1.242	-0.073	-0.617	0.909	0.211	-0.17	0.698	0.219
U8	3.734	1.38	-1.242	5.983	-1.924	-5.617	-0.617	-5.09	-11.941	-6.389	-0.325	-5.017	-3.19	1.38	-0.682	-1.258	1.258	0.211
U9	0.885	1.177	0.252	1.843	1.283	-0.008	4.619	1.039	-2.086	5.877	-2.955	-9.79	-3.596	-4.603	-10.245	-5.033	-0.308	-2.654
U10	-0.057	1.145	0.43	0.235	1.08	0.365	0.934	1.364	0.308	2.484	1.583	-0.308	5.406	0.382	-3.036	4.448	-4.619	-9.303
U11	-1.072	1.477	0.114	-0.438	1.128	0.097	-0.073	1.258	0.227	0.333	1.388	0.195	1.088	1.542	0	2.5	1.477	-0.674
U12	-4.733	1.08	-2.167	-1.81	1.307	-0.146	-0.747	1.396	0.122	-0.26	1.348	0.195	0.106	1.291	0.17	0.528	1.315	0.227
U13	2.046	1.193	-15.505	-6.437	1.331	-6.518	-2.874	1.786	-0.666	-0.95	1.08	0.179	-0.463	0.779	0.235	-0.211	0.593	0.276
U14	5.666	2.573	-4.343	1.973	-0.244	-14.863	-5.958	1.964	-6.47	-2.541	1.721	-0.495	-0.804	0.998	0.235	-0.244	0.666	0.3
U15	1.973	1.753	-0.382	5.512	1.989	-4.335	1.339	1.356	-14.693	-5.902	2.435	-5.658	-2.533	1.64	-0.43	-0.934	0.966	0.211
U16	0.649	1.145	0.187	1.964	1.624	-0.26	5.593	2.403	-5	-0.203	1.591	-14.815	-5.845	2.167	-4.822	-2.354	1.51	-0.3
U17	0.349	0.836	0.341	0.706	0.99	0.284	2.2	1.68	-0.284	5.934	2.671	-5.561	0.016	1.161	-14.636	-5.634	1.713	-4.757
U18	0.041	0.658	0.365	0.187	0.739	0.365	0.796	1.12	0.341	2.525	1.981	-0.495	6.04	2.37	-6.137	-0.39	-0.114	-14.449
U19	-0.219	0.998	0.422	-0.057	0.836	0.373	0.195	1.096	0.455	0.852	1.526	0.349	2.468	2.119	-0.398	5.966	1.981	-5.561
U20	-0.471	0.99	0.341	-0.179	0.812	0.211	0	0.836	0.325	0.244	1.047	0.276	0.812	1.323	0.211	2.411	1.843	-0.552

U21	-0.893	1.12	0.114	-0.268	0.617	0.187	0.049	0.625	0.195	0.154	0.658	0.219	0.39	0.739	0.195	0.885	1.015	0.17
U22	-3.028	1.94	-0.682	-0.998	1.096	0.284	-0.406	0.869	0.308	-0.162	0.779	0.3	0.032	0.763	0.325	0.252	0.893	0.325
U23	-6.462	2.184	-7.006	-2.687	1.559	-0.568	-0.95	1.161	0.195	-0.382	0.852	0.252	-0.073	0.633	0.252	0.073	0.641	0.26
Ref	X_mT	Y_mT	Z_mT	X_mT	Y_mT	Z_mT	X_mT	Y_mT	Z_mT	X_mT	Y_mT	Z_mT	X_mT	Y_mT	Z_mT			
U1	3.669	-0.52	-0.958	2.817	-2.273	-1.023	0.796	-3.239	-0.877	-1.096	-3.231	-0.917	-2.947	-2.362	-1.063			
U2	0.13	1.81	0.041	0.869	1.778	-0.049	2.135	1.274	-0.333	3.872	0.073	-1.169	4.789	-3.247	-3.271			
U3	-1.591	1.648	-0.195	-0.658	1.745	0	0.252	1.51	0.057	0.958	1.469	0.073	2.086	1.291	-0.227			
U4	-4.871	-1.51	-2.541	-3.62	0.998	-0.958	-1.762	1.786	-0.17	-0.682	1.956	0.081	0.016	2.029	0.073			
U5	3.986	-4.692	-4.611	-0.998	-5.999	-5.382	-4.513	-2.176	-2.484	-3.661	0.609	-0.787	-2.257	1.615	-0.179			
U6	2.695	1.421	-0.503	4.27	0.106	-1.559	4.099	-3.953	-3.369	-0.349	-6.283	-4.676	-4.522	-3.572	-3.539			
U7	0.032	0.779	0.244	0.341	0.893	0.195	1.299	0.917	0.057	3.255	0.893	-0.836	6.478	-1.274	-5.147			
U8	-0.641	1.266	0.3	-0.276	1.128	0.292	0.13	0.998	0.325	0.528	1.185	0.365	1.421	1.421	0.13			
U9	-2.914	1.039	-0.584	-1.274	1.096	0.179	-0.349	0.909	0.284	0.032	0.844	0.357	0.382	0.95	0.349			
U10	-3.718	-5.041	-11.097	-5.975	-0.138	-3.97	-2.606	1.372	-0.235	-1.039	1.339	0.325	-0.438	1.234	0.406			
U11	5.431	0.674	-3.255	5.52	-3.702	-10.05	-5.114	-4.335	-8.938	-5.179	0.552	-2.565	-2.622	1.55	-0.373			
U12	1.193	1.55	0.146	2.654	1.737	-0.503	5.991	-0.43	-3.945	3.19	-5.666	-11.43	-6.048	-3.385	-8.946			
U13	-0.057	0.617	0.268	0.106	0.804	0.26	0.658	0.95	0.211	2.038	1.648	-0.211	5.837	2.476	-4.27			
U14	0	0.658	0.325	0.057	0.641	0.276	0.365	0.625	0.325	0.755	1.031	0.308	2.119	1.688	-0.138			
U15	-0.511	0.812	0.235	-0.268	0.674	0.227	0.016	0.584	0.187	0.114	0.706	0.252	0.576	1.055	0.227			
U16	-1.08	1.185	0.187	-0.52	0.844	0.268	-0.17	0.69	0.227	-0.016	0.625	0.26	0.146	0.844	0.3			
U17	-2.922	1.81	-0.731	-1.055	1.193	0.17	-0.317	0.787	0.26	-0.057	0.625	0.317	0.089	0.666	0.325			
U18	-6.405	1.964	-6.924	-3.206	1.786	-0.82	-0.917	1.023	0.244	-0.325	0.787	0.39	-0.138	0.698	0.382			
U19	2.265	1.21	-15.424	-6.437	2.33	-8.053	-2.857	2.046	-0.446	-0.974	1.437	0.365	-0.463	1.161	0.463			
U20	5.723	2.5	-4.457	2.914	1.25	-14.823	-6.656	1.802	-6.356	-2.882	1.956	-0.536	-1.104	1.331	0.203			
U21	2.176	1.55	-0.3	5.455	2.249	-3.832	1.729	-0.406	-16.349	-6.592	1.826	-7.062	-2.979	1.81	-0.82			
U22	0.666	1.169	0.373	1.867	1.786	-0.041	6.08	2.005	-4.554	1.851	-0.032	-16.528	-6.884	2.102	-7.639			
U23	0.308	0.787	0.325	0.698	1.047	0.3	2.135	1.51	-0.252	6.226	2.127	-4.684	2.508	0.617	-16.308			

Appendix D: Scan Repeatability Plots

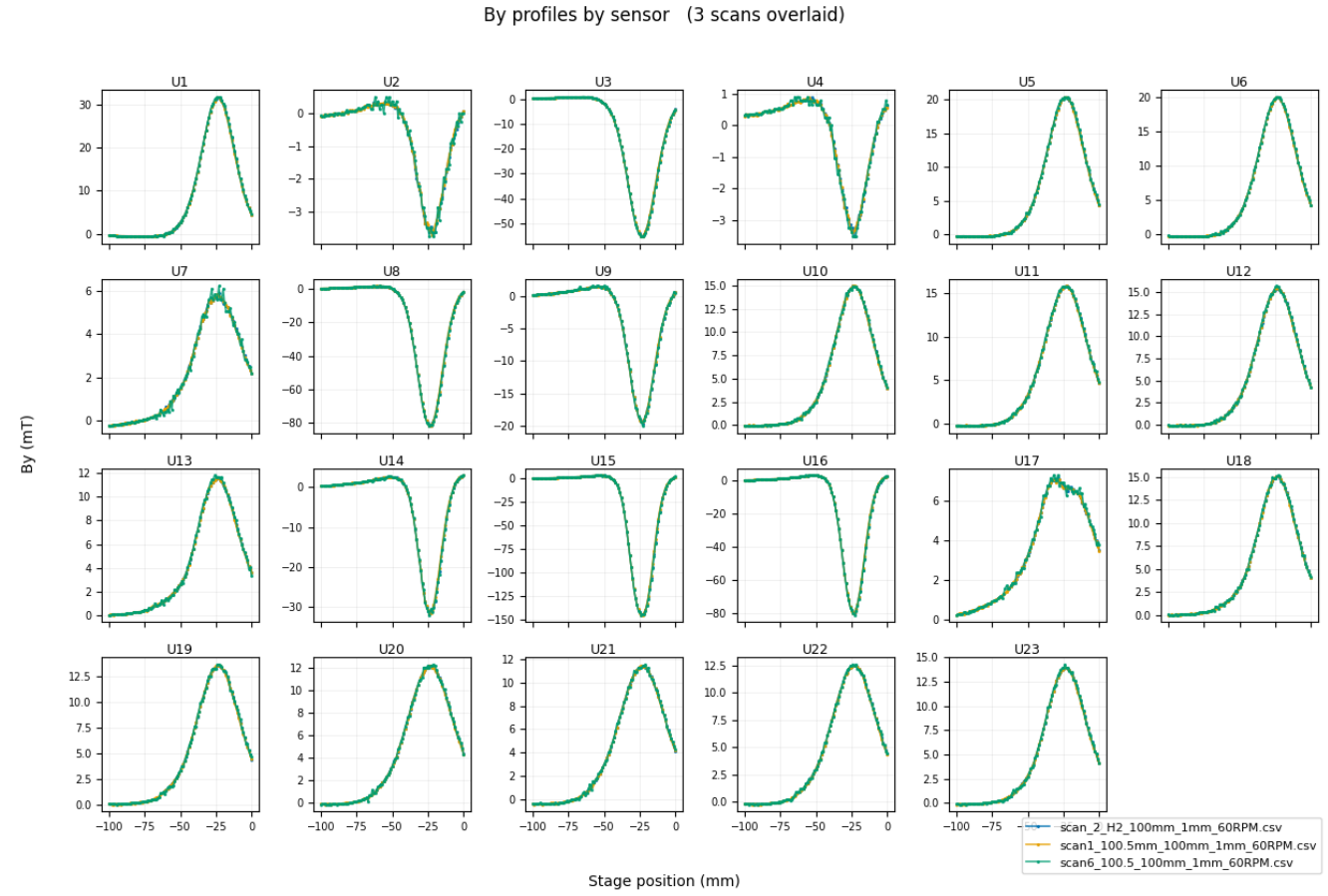

Figure 66: *By profiles by sensor, scans overlaid.*

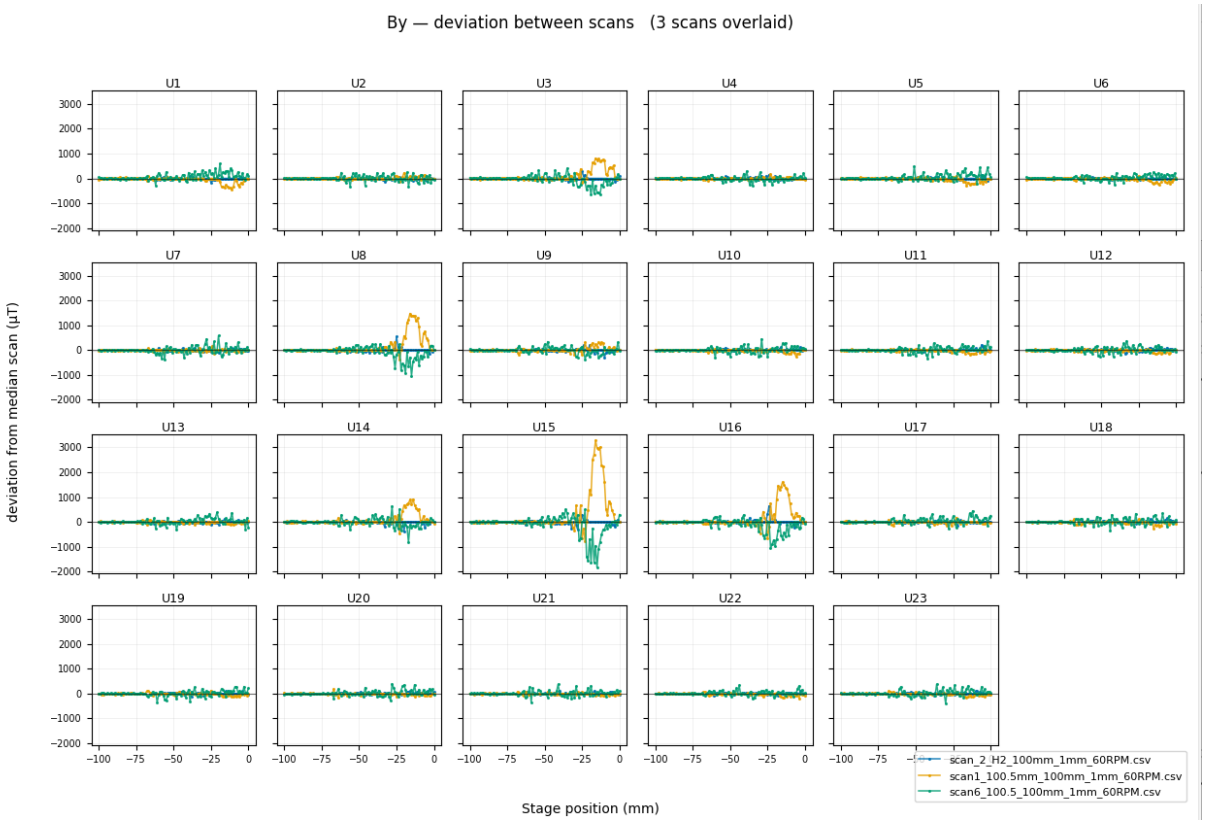

Figure 67: *By deviation between scans.*

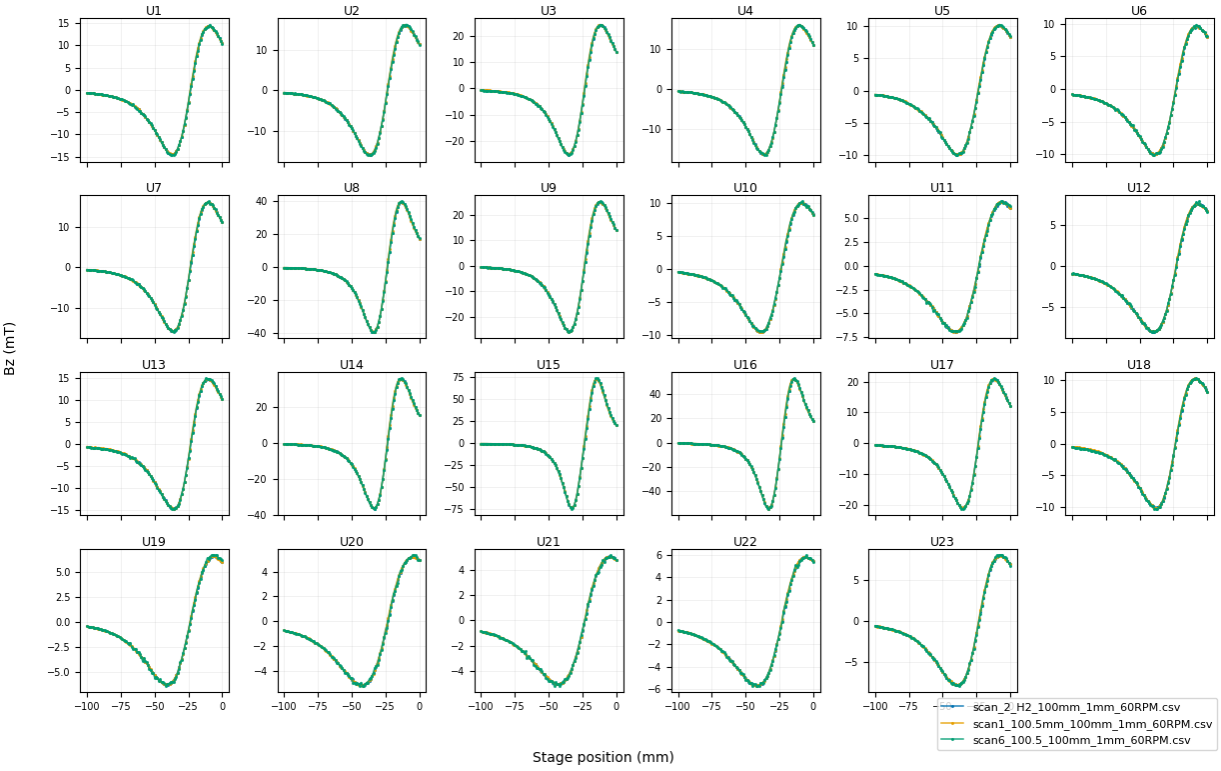

Figure 68: *Bz profiles by sensor, scans overlaid.*

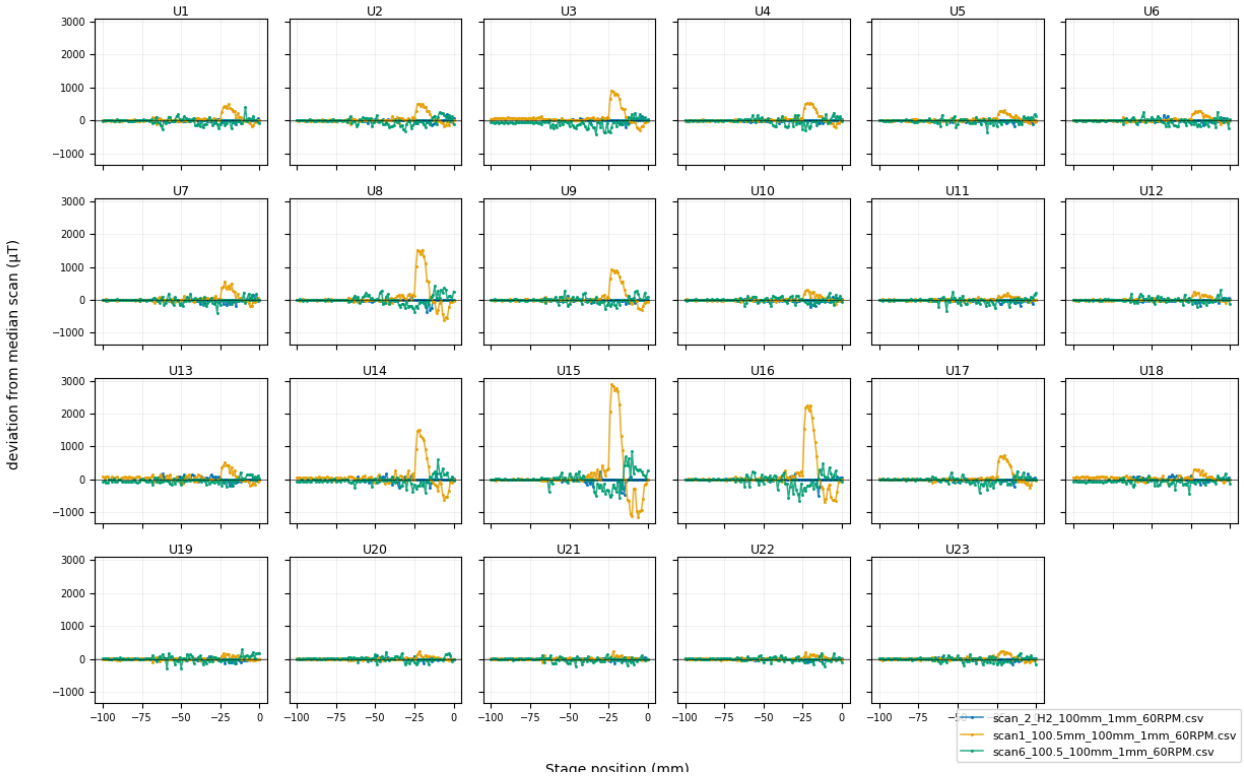

Figure 69: *Bz deviation between scans.*

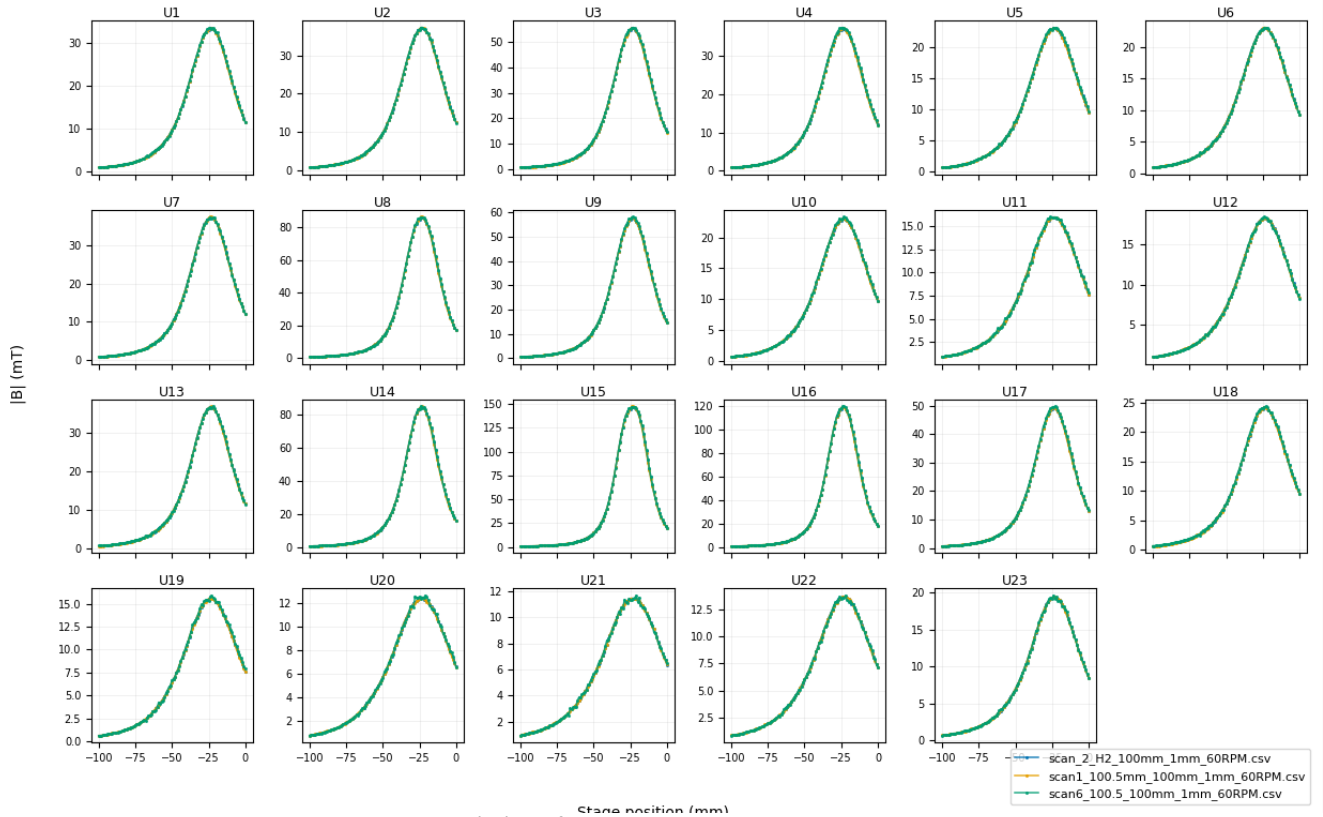

Figure 70: *|B| profiles by sensor, scans overlaid.*

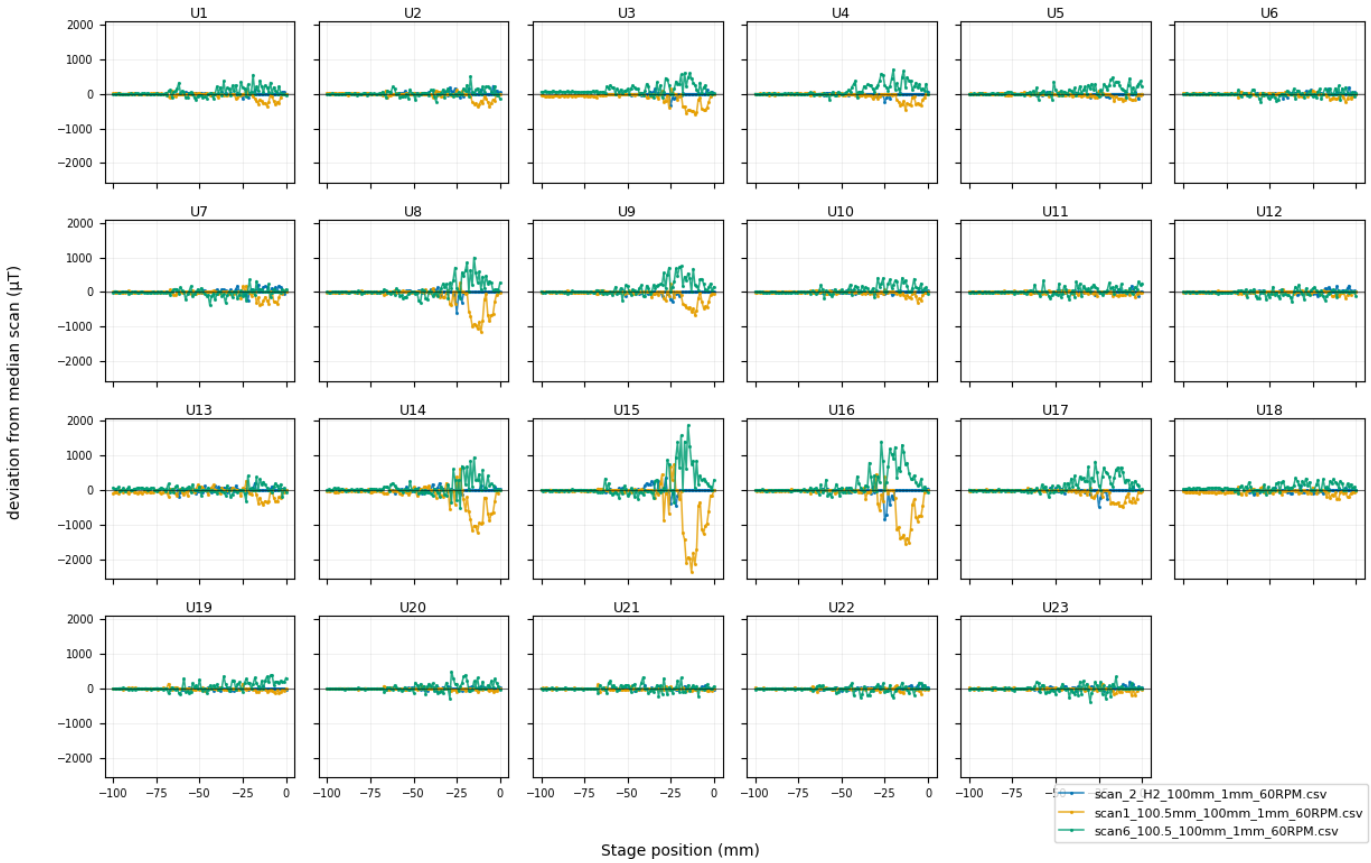

Figure 71: *|B| deviation between scans.*

Appendix E: Magnetic Field Map Reconstruction

The 3D map is built so that it obeys Maxwell's equations, rather than interpolating between chips. Inside the bore there are no sources, so:

$$\nabla \cdot \mathrm{B} = 0, \qquad \nabla \times \mathrm{B} = 0$$

A curl-free field can always be written as the gradient of a scalar potential, $B = -\nabla\Phi$. Substituting into $\nabla \cdot B = 0$ gives Laplace's equation:

$$\nabla^2 \Phi = 0$$

In cylindrical coordinates (r, ϕ, z):

$$\frac{1}{r}\frac{\partial}{\partial r}\left(r\frac{\partial \Phi}{\partial r}\right) + \frac{1}{r^2}\left(\frac{\partial^2 \Phi}{\partial \varphi^2}\right) + \frac{\partial^2 \Phi}{\partial z^2} = 0$$

This turns three unknown field components into one unknown function Φ, and Φ cannot take any shape: it must satisfy $\nabla^2\Phi = 0$ everywhere in the bore. That constraint is what lets discrete measurements define the whole volume.

Series: The potential is written as the generalized-gradient expansion, the interior cylindrical multipole solution of Laplace's equation (Venturini & Dragt, NIM A 427, 1999):

$\Phi(r, \phi, z) = \Sigma_{n=0}^{6} \Sigma_{s=0}^{3} a_{n,s}\, r^{n+2s} [C_n^{c(2s)}(z) \cos n\phi + C_n^{s(2s)}(z) \sin n\phi]$, $a_{n,s} = (-1)^s\, n! / (4^s\, s!\, (n+s)!)$

Here $C_n^c(z)$ and $C_n^s(z)$ are the on-axis gradients of multipole order n, and the superscript (2s) denotes the 2s-th derivative with respect to z.

Angle: a Fourier series in ϕ, n = 0 to 6, with independent cos and sin terms. Since sin 0ϕ = 0, this gives 7 + 6 = 13 channels. cos nϕ is the fixed shape around the circle; for example, n = 2 is the four-lobe quadrupole pattern.

This is equivalent to the modified-Bessel (I_n) solution of Laplace's equation, expanded as a power series in r. This form lets each on-axis gradient be fitted directly as a spline without evaluating Bessel functions.

Radius: a power series starting at r^n. Laplace's equation fixes them through the even z-derivatives of each C_n, with weights $a_{n,s}$.

Axis: each on-axis gradient $C_n(z)$ is a B-spline with 16 weights. It sets how strong each pattern is at each stage position.

Fit: the measured field determines the 13 × 16 = 208 spline weights by linear least squares (A c = b) on $B = -\nabla\Phi$ at every chip, axis and stage position. Everything is linear, so the whole scan is solved in one matrix operation.

No boundary values are imposed on the bore wall; the measurements alone determine the solution.

To evaluate the map at a point (x, y, z):

- Convert x and y to r and ϕ.
- Evaluate each $C_n(z)$ and its even derivatives up to $C_n^{(6)}(z)$ from the splines.
- For each channel, sum the radial series $a_{n,s}\, r^{n+2s}\, C_n^{(2s)}(z)$ over s = 0 to 3, and multiply by cos nϕ or sin nϕ.
- Add up the 13 channels to get Φ.
- Take $B = -\nabla\Phi$ (computed analytically).